

<http://researchcommons.waikato.ac.nz/>

Research Commons at the University of Waikato

Copyright Statement:

The digital copy of this thesis is protected by the Copyright Act 1994 (New Zealand).

The thesis may be consulted by you, provided you comply with the provisions of the Act and the following conditions of use:

- Any use you make of these documents or images must be for research or private study purposes only, and you may not make them available to any other person.
- Authors control the copyright of their thesis. You will recognise the author's right to be identified as the author of the thesis, and due acknowledgement will be made to the author where appropriate.
- You will obtain the author's permission before publishing any material from the thesis.

Capabilities and considerations for the implementation of a phycocyanin sensor to enhance cyanobacteria monitoring in lakes

A thesis
submitted partial fulfilment
of the requirements for the degree
of
Master of Science (Research) in Biological Science
at
The University of Waikato
by
Vanessa Cotterill



THE UNIVERSITY OF
WAIKATO
Te Whare Wānanga o Waikato

2017

Abstract

Bloom-forming cyanobacteria are problematic in recreational waters as humans may be exposed to their toxins via primary contact or ingestion. Cyanobacteria can be monitored using microscopy but this is time consuming, costly and requires taxonomic expertise. Phycocyanin (an accessory pigment specific to cyanobacteria) can be used as a proxy for cyanobacteria biomass. Phycocyanin sensors are thus increasingly being used to monitor cyanobacteria, even though many limitations to their use still exist. This research investigated the opportunities and challenges of using a phycocyanin sensor for cyanobacteria monitoring. It tested three hypotheses that: 1) there would be a strong relationship between phycocyanin and biovolumes in samples collected from the Te Arawa/Rotorua Lakes, North Island, New Zealand, 2) colony morphology and cell size affect phycocyanin readings, and 3) nutrient and light exposure would affect phycocyanin quotas independently of growth in *Microcystis aeruginosa*.

The relationship between phycocyanin and biovolume was investigated using data collected in the field from over two summers (2016 and 2017). A phycocyanin sensor was used to measure phycocyanin *in situ*, and biovolume was enumerated by microscopy. Eutrophic lakes with high biovolumes ($>1.8 \text{ mm}^3 \text{ L}^{-1}$) and single species dominance had stronger relationships with phycocyanin. Phycocyanin concentration $>40 \mu\text{g L}^{-1}$ derived from the sensor approximated a biovolume of $1.8 \text{ mm}^3 \text{ L}^{-1}$, which is the health warning level for potentially toxic cyanobacteria

species under the New Zealand guidelines for recreational monitoring of cyanobacteria in fresh waters.

The effect of colony morphology and cell size on phycocyanin detection was tested with serial dilutions of cultures of four cyanobacterial species. Large colonial *Microcystis wesenbergii* had the highest variability in phycocyanin readings from the sensor. Non-linear relationships in all four species resulted in low confidence for predicting low biovolumes $<1.8 \text{ mm}^3 \text{ L}^{-1}$ from phycocyanin.

The effects of nutrients and light intensity on growth and phycocyanin quota in *M. aeruginosa* were assessed by a laboratory experiment using a Central Composite design and Response Surface Methodology (RSM). RSM models tested for significant interactions and effects of 20 different combinations of nitrogen (26-84 mg L^{-1}), phosphorus (0.05-5.47 mg L^{-1}) and light intensity (10-400 $\mu\text{mol m}^{-2} \text{ s}^{-1}$) on the growth and phycocyanin quota. Phycocyanin from the sensor and cell concentrations from microscopy were measured over 26 days at five-day intervals. Phycocyanin quota was significantly ($P < 0.05$) higher in four of the 20 treatments at day 18 compared to the day 22. Importantly phycocyanin quotas at day 18 and 22 were affected differently by light and nutrients. RSM demonstrated that light and nutrient concentrations affected both growth rate and phycocyanin quota differently. This experiment suggests phycocyanin quota changes in cyanobacteria, and this may result in over or underestimates of biomass by a sensor. Regardless of the challenges of using phycocyanin sensors with changing species compositions, morphology, density and with the effects of nutrients and

light on phycocyanin and growth. Phycocyanin sensors offer an opportunity to increase current sampling capability and the prioritisation of high-risk samples for counting which may lead to improved protection of human health from the toxicity associated with cyanobacteria blooms.

Acknowledgements

I thank my supervisors for the positive feedback and training in the field of research. Susie Wood you have been inspirational and motivating at every step of this journey even prior to my Masters enrolment. You excited me about cyanobacteria and have carried this through to the completion of this thesis. David Hamilton's diverse knowledge and research have provided me with improved knowledge of the Te Arawa Lakes. Your positive feedback and critical review were fundamental to my development as a researcher and in the art of science communication.

Many thanks to the staff at Bay of Plenty Regional Council. The science team have supported this research as a way to explore new methods for enhancing the Algal Monitoring Programme. Alastair Suren's ideas, support and supervision for three summers have been fundamental to the collection of the data and your reviews of early drafts were appreciated. Paul Scholes always took time to offer additional support and encouragement in many parts of my research, particularly data analysis and my oral presentations. Joe Butterworth kept me safe during field work on the lakes and offered motivation to help me stay focused about my research. Andy Bruere is thanked for supporting and believing in this research. Rob Donald provided continued support in this research and in the three summers of employment as the Algal Monitoring Assistant while I was studying and completing this thesis.

I would like to thank the Cawthron Institute, particularly the Coastal and Freshwater group, for enabling me to carry out my experimental research with guidance. Jonathan Puddick provided expertise and encouragement in science, and knowledge of analytical chemistry which introduced me to an area that was very important for my research. I thank Jonathan for all the time and help with equations and theory of fluorescence techniques. Janet Adamson is thanked for providing knowledge and encouragement during the setup and running of the experiment and I could not have done the experiment without you. Veronica Beuzenberg gave support and shared current techniques in algal research. I valued your input and thank you for helping to keep me safe in the laboratory during my experiments.

I thank many University of Waikato students, staff, and academics who helped me complete this thesis. Ian Hawes is thanked for supporting the write up of this thesis and providing cyanobacteria expertise. Barry O'Brien is thanked for facilitating and guiding microscopy work. Grant Tempero helped with concentration conversions and supplied algal contracts. Chris McBride is thanked for guidance and knowledge on the use of phycocyanin sensors. I thank Kohji Muraoka for tasty lunch breaks during my studies. Jane Cope and Fenna Beets provided console during my write up. Caroline Hodges, your research was a guiding light to this research. It was an honor to accept the following funding and awards from the University; University of Waikato Masters Research Scholarship 2016 Award, the Hilary Jolly Memorial Scholarship 2016 and the Vivienne Cassie Cooper Outstanding Algal Person Award 2017.

To my husband, I could not have done this thesis without your support. You are an inspiration and thank you for your patience over this time. This thesis is dedicated to my mother and father-in-law, who passed away during my university studies.

Table of Contents

Abstract	iii
Acknowledgements	vii
Table of Contents	xi
List of Figures	xv
List of Tables	xvii
1 Chapter 1	1
Introduction	1
1.1 Background	1
1.2 Overview and objectives	12
1.3 References	14
2 Chapter 2	25
Opportunities and challenges for use of a phycocyanin sensor to monitor cyanobacteria	25
2.1 Abstract	25
2.2 Introduction	26
2.3 Methods	31
2.3.1 Phycocyanin sensor	31
2.3.2 Study sites	33
2.3.3 Field sampling	35
2.3.4 Species dilution experiments	36
2.3.5 Data analysis	39
2.4 Results	41
2.4.1 Field studies	41
2.4.2 Multivariate analysis of cyanobacteria composition	42
2.4.3 Phycocyanin relationships with biovolume	45

2.4.4	Relationships for phycocyanin to biovolume for different locations	45
2.4.5	Recreational monitoring threshold predictions for phycocyanin	47
2.4.6	Dilution series experiments for four species.....	50
2.5	Discussion	54
2.5.1	Relationship of phycocyanin to biovolume in the field.....	54
2.5.2	Three assessments of phycocyanin for the species dilution experiments.....	61
2.5.3	Recreational threshold setting for phycocyanin sensors	63
2.6	References	66
3	Chapter 3	77
	Effects of nutrients and light intensity on phycocyanin quota and growth rates in <i>Microcystis aeruginosa</i>	77
3.1	Abstract.....	77
3.2	Introduction	78
3.3	Methodology	82
3.3.1	Stock cyanobacteria culture	82
3.3.2	Nitrate and phosphate stock solutions and treatment preparation.	82
3.3.3	Sampling	83
3.3.4	Phycocyanin determination for sensor phycocyanin and extracted phycocyanin samples.....	86
3.3.5	Response variable calculations for maximum growth rates and phycocyanin quotas.....	87
3.3.6	Data analysis.....	88
3.3.7	Normalisation	90
3.4	Results.....	91
3.4.1	Comparison of phycocyanin determination from two methods (spectrophotometry and sensor) at experiment endpoint	92
3.4.2	Comparing Phycocyanin quota at day 18 and day 22	94

3.4.3	Effects of nutrients and light on phycocyanin quotas and maximum growth rate	96
3.5	Discussion	102
3.5.1	Comparison of phycocyanin measurements undertaken by sensor and spectrophotometry	102
3.5.2	Comparing phycocyanin quotas at day 18 to day 22	103
3.5.3	Effects of nutrients and light on phycocyanin quotas	103
3.5.4	Effects of nutrients and light intensity on growth rates	105
3.6	References	108
4	Chapter 4	117
	Conclusion	117
	Appendices	123

List of Figures

Chapter 2

- Figure 1. Location of 16 monitoring sites (black dots) in the Te Arawa lakes district of Rotorua, New Zealand (See Table 1 for site names)34
- Figure 2. Morphology of cyanobacteria used in the species dilution experiment: a) *Microcystis aeruginosa* (CAWBG617), b) *Microcystis wesenbergii* (CAWBG618), c) *Dolichospermum lemmermannii* (CAWBG564), and d) *Cuspidothrix issatschenkoi* (CAWBG595). Scale bar =10 μm . Photos: S. Wood.....38
- Figure 3. Proportion of biovolume for the dominant cyanobacteria species found across all locations in (a) 2016 and (b) 201743
- Figure 4. Non-metric Multidimensional Scaling (nMDS) plot of cyanobacterial communities on each sampling occasion at 16 sites in the five lakes and one river (Table 1) for (a) 2016 and (b) 2017. Solid square is the Lake Okaro site, solid circles are sites of Lake Rotoehu, stars are sites of Lake Rotoiti, open triangles are sites of Lake Rotorua, open squares are sites of Lake Tarawera, and the open circle is the Kaituna River site44
- Figure 5. Relationship between log (phycocyanin +1) and log (biovolume +1) for all sites sampled from January to April 2016, n= 121. Phycocyanin was measured in units of $\mu\text{g L}^{-1}$ (averages $\pm\text{SD}$, n=5) from the sensor and biovolume in $\text{mm}^3 \text{L}^{-1}$. The regression (solid line) and the 95% prediction intervals (dashed line) for the regression line are shown. Horizontal lines indicate, bottom up, the red action threshold in the New Zealand guidelines for recreational contact, with potentially toxic species $>1.8 \text{ mm}^3 \text{L}^{-1}$ and total cyanobacteria threshold $>10 \text{ mm}^3 \text{L}^{-1}$..46
- Figure 6 Relationship between log (phycocyanin +1) and log (biovolume +1) for sites sampled from January to March 2017, n= 63. Phycocyanin was measured in units of $\mu\text{g L}^{-1}$ (averages $\pm\text{SD}$, n=5) from the sensor and biovolume $\text{mm}^3 \text{L}^{-1}$. The regression (solid line) and the 95% prediction intervals (dashed lines) for the regression line are shown. Horizontal lines indicate, bottom up, the red action threshold in the New Zealand guidelines for recreational contact with potentially toxic species $>1.8 \text{ mm}^3 \text{L}^{-1}$ and total cyanobacteria threshold $>10 \text{ mm}^3 \text{L}^{-1}$ 47
- Figure 7. Log (biovolume +1) and log (phycocyanin +1) values for species dilutions. Phycocyanin was measured in $\mu\text{g L}^{-1}$ (averages $\pm\text{SD}$, n=7) from the sensor and biovolume in $\text{mm}^3 \text{L}^{-1}$. a) *Microcystis aeruginosa*, b) *Microcystis wesenbergii*, c) *Dolichospermum lemmermannii*, and d) *Cuspidothrix issatschenkoi*52

Figure 8. Breakpoint models for prediction of biovolume log (biovolume +1) from phycocyanin log (phycocyanin +1) using species dilutions for a) *Microcystis aeruginosa*, b) *Microcystis wesenbergii*, c) *Dolichospermum lemmermannii*, and d) *Cuspidothrix issatschenkoi*. Phycocyanin in units of $\mu\text{g L}^{-1}$ (averages $\pm\text{SD}$, $n=7$) from the sensor and biovolume in $\text{mm}^3 \text{L}^{-1}$. Dashed line is segmented regression breakpoint estimate for each species (see Table 6 for breakpoint estimate values). Numbers on graph are slopes ($\text{mm}^3 (\mu\text{g})^{-1}$) above and below the breakpoints. Solid line is biovolume $1.8 \text{ mm}^3 \text{L}^{-1}$ 53

Chapter 3

Figure 1. Phycocyanin (PC) measured by spectrophotometry (Spectro PC) and a sensor (Sensor PC) at day 22 93

Figure 2. Average phycocyanin ($n=3$) on day 22 for each treatment measured by spectrophotometry (black) and the sensor (grey). Error bars are \pm one standard deviation. See Table 1 for individual treatment nutrient concentrations and light intensity used in each treatment 94

Figure 3. Average ($n=3$) phycocyanin quota (pg cell^{-1}) (PC quota) for the 20 treatments on days 18 (black) and 22 (grey). Error bars show one standard deviation. See Table 1 for nutrients concentrations and light intensity used for each treatment 95

Figure 4. Contour plots (upper pane) and response surface plots (lower pane) showing phycocyanin quota (PC Quota) at day 18 in response to combinations of: (a) nitrogen (nitrate-N) and log-transformed phosphorus (phosphate-P) (b) square root-transformed light and nitrogen (nitrate-N) (c) square root-transformed light and log-transformed phosphorus (phosphate-P). Contour lines show phycocyanin quota values 99

Figure 5. Contour plots (upper pane) and response surface plots (lower pane) showing phycocyanin quota (PC Quota) at day 22 in response to combinations of: (a) nitrogen (nitrate-N) and log-transformed phosphorus (phosphate-P) (b) square root-transformed light and nitrogen (nitrate-N) (c) square root-transformed light and log-transformed phosphorus (phosphate-P). Contour lines show phycocyanin quota value 100

Figure 6. Contour plots (upper pane) and response surface plots (lower pane) showing maximum growth rates in response to combinations: (a) nitrogen (nitrate-N) and log-transformed phosphorus (phosphate-P) (b) square root-transformed light and nitrogen (nitrate-N) (c) square root-transformed light and log-transformed phosphorus (phosphate-P). Contour lines show maximum growth rates (day^{-1}) 101

List of Tables

Chapter 1

Table 1. Description of the fluorescence techniques available for quantifying cyanobacteria biomass and the applicability for use in recreational monitoring based on cost, field capabilities and simplicity in use	5
Table 2 Comparison of cyanobacteria monitoring thresholds for recreational contact and proposed phycocyanin thresholds from specific studies. (-) no data	10

Chapter 2

Table 1. New Zealand guidelines for cyanobacteria in recreational fresh waters (Wood et al. 2009). Alert level mode, biovolume thresholds and required monitoring and management	27
Table 2. Location, site name, trophic state, maximum depth and lake areas of the five lakes and one river, sampled over two summers (2016 and 2017), in the Te Arawa Rotorua lakes district, New Zealand. See Figure 1 for locations. *High/moderate cyanobacteria risk sites. NA = not available	34
Table 3. The concentration ranges of biovolume, phycocyanin, number of dilutions, and morphology of the species used in the dilution experiments	38
Table 4. Total cyanobacteria species and total biovolume for each lake or river in 2016 and 2017, sample size for each location (lake or river) and total sample size (n) and the average across all location (five lakes and one river) in 2016 (16 sites) and 2017 (10 sites).....	42
Table 5. Relationship between log (phycocyanin +1) and log (biovolume +1), the percentage of variation explained (R^2) value and significance value (P), sample size of for the sampling locations over two sampling years, combined years for each location and across all locations. Predicted phycocyanin ($\mu\text{g L}^{-1}$) calculated using the regression equations: a is the slope, x is the biovolume and b is the intercept at the three biovolume threshold values. Bold values are significant ($P < 0.05$). The Kaituna River and Lake Tarawera were data deficient in both years ($n < 10$) and Lake Rotorua was data deficient in 2017. NA; not applicable due to weak relationship	49
Table 6. Minimum phycocyanin detection limits ($\mu\text{g L}^{-1}$) (average \pm SD, $n=7$) and corresponding biovolume ($\text{mm}^3 \text{L}^{-1}$) using dilution series and species cell volumes (μm^3) from measured dimensions for the four-cultured	

species, *Microcystis wesenburgii*, *Microcystis aeruginosa*,
Dolichospermum lemmermannii, and *Cuspidothrix issatschenkoi*.....51

Table 7. Segmented regression model regression coefficients and significance values, log(phycocyanin+1), breakpoint estimates (standard error), breakpoint values for phycocyanin ($\mu\text{g L}^{-1}$) and pscore statistical test for significance of breakpoint 53

Table 8. Detection limits for phycocyanin (PC) from sensors, reported cell concentrations, calculated biovolumes from literature values or the source study, the sensor used and source of information. NA data not given in the study 64

Chapter 3

Table 1. Experimental design matrix for concentrations of nitrate-N (N), phosphate-P (P) and light intensity (I) for each treatment from the Central Composite design, ratios of nitrogen to phosphorus and average temperature for the 12 h light: 12 h dark periods 84

Table 2. Experimental results of the phycocyanin (PC) quota, (pg cell^{-1}) at day 18 and day 22 and the maximum growth rate and day interval for maximum growth rate calculation between days 6-22. Experimental results are averages (n=3). Bold values represent results of Students t-test ($P<0.05$ significance level) for PC quota between two growth phases, (*) could not conduct Students t-test due to reduced sample size 92

Table 3. Summary of relationship, significance values and ANOVA lack of fit values generated from the Response Surface Methodology analysis of maximum growth rates (day^{-1}) and phycocyanin quota (pg cell^{-1}) at day 18 and day 22. Variables are first order N: Nitrate-N, P: log-transformed phosphate-P, I: light, I²: light squared; and their interaction N&P, N&I, P&I. NS: not significant. There were no significant terms for N² and P² 97

Chapter 1

Introduction

1.1 Background

Cyanobacteria are a group of oxygenic photosynthetic bacteria that are found in a diverse array of ecosystems (Reynolds, 2006). They are microscopic and can be found amongst the plankton of lakes. Under favorable conditions, they can form dense blooms (Reynolds, 2006). These conditions may include thermal stratification, high nutrient availability, warm temperatures and suitable light climate (Oliver et al. 2012). Cyanobacteria compete strongly for light and nutrients, with some species having accessory pigments conferring resilience to high irradiance and/or being capable of nitrogen fixation (Stal, 2012). Some species are buoyant as they contain gas vacuoles and under calm conditions (e.g., during thermal stratification) they can float to the surface where light is more abundant (Havens, 2008). This enhances the probability of surface water bloom formation.

Cyanobacteria have different morphologies which can be a favorable strategy for optimal positioning within the water column (Oliver et al. 2012). Some species form large colonies as a response to growth limiting conditions (Ma et al. 2014). Although unicellular cyanobacteria can be small, from 0.5 μm for pico-cyanobacteria, colony aggregates and filamentous trichomes can be macroscopic and visible, with lengths or diameters up to 50 μm for large filamentous taxa or

colonial taxa, respectively (Baker & Fabbro, 2002). When cells/colonies aggregate and form blooms, the water becomes discoloured and surface scums can form.

An increasing number of bloom-forming cyanobacteria have been identified which produce toxins (collectively known as cyanotoxins) (Meriluoto et al. 2017). Cyanotoxins can be harmful to humans, animals and aquatic life (Chorus & Bartram, 1999). The most common toxins found in cyanobacteria are neurotoxins (e.g. anatoxins, saxitoxins) and hepatotoxins (e.g., microcystins) (Chorus & Bartram, 1999). The risk posed by toxin exposure requires regular monitoring and guidelines to protect human health in drinking and recreational waters (Newcombe et al. 2010).

The monitoring of recreational waters is undertaken in many ways, across a variety of countries (Ibelings et al. 2015). Recreational monitoring programs generally have guideline thresholds of cyanobacteria concentration for risk assessment, these are generally applied in a two or three-tier alert level framework. Threshold values commonly used are concentration (cells mL^{-1}), biovolume ($\text{mm}^3 \text{L}^{-1}$), microcystins ($\mu\text{g L}^{-1}$) and sometimes chlorophyll *a* ($\mu\text{g L}^{-1}$) (Ibelings et al. 2015). In New Zealand, the recreational monitoring programs for freshwater use a three-tier alert level framework that has biovolume thresholds for cyanobacteria biomass (Wood et al. 2009). Biovolumes $<0.5 \text{ mm}^3 \text{L}^{-1}$ are in the surveillance mode threshold, requiring weekly or fortnightly sampling and inspection. The first alert mode is at >0.5 to $<1.8 \text{ mm}^3 \text{L}^{-1}$ and red action mode is triggered when potentially toxic cyanobacteria dominate at $\geq 1.8 \text{ mm}^3 \text{L}^{-1}$ or $\geq 10 \text{ mm}^3 \text{L}^{-1}$ for all cyanobacteria (Wood et al. 2009). Because recreational monitoring for cyanobacteria in New

Zealand uses biovolume, it requires collecting grab samples for microscopic analysis of species and enumeration (Wood et al. 2008). This method is time-consuming, requires a high level of taxonomic expertise, and toxic and non-toxic species cannot always be differentiated under the microscope (Straile et al. 2015). The current sampling and monitoring technique is limited in efficiency and is unable to provide timely assessments of cyanobacteria blooms. Therefore, the response times for issuing health warnings have a delay which could be up to a week, depending on the organisation issuing the warning (National Institute of Water and Atmospheric Research, NIWA, 2017).

Several fluorescence-based technologies exist to increase the capacity to monitor cyanobacteria. These include; optical sensors, remote sensing, spectrophotometry, fluorometry, and flow cytometry. A brief comparison of the techniques, and the benefits and limitations of each is given in Table 1. The first two techniques, optical sensors, and remote sensing, are methods suitable for field assessments. Optical sensors can effectively function at the 'microscale' (cm^3 of water sample) and remote sensing at the 'macroscale' (up to many km^2 of water surface) (Gholizadeh et al. 2016). Optical sensors can read pigment wavelengths *in situ*, from within the water. This provides an estimate of the concentration of pigment *in vivo* which can be related to biomass (Zamyadi et al. 2012a). Remote sensing with satellites allows whole lakes to be analysed for various wavelengths of the light spectrum (Vincent et al. 2004). Remote sensing images can be gained from satellites with relevant sensing spectral bands and can be processed with algorithms to calculate the concentration of cyanobacterial pigments in surface

waters (Trescott & Park, 2012; Dörnhöfer & Oppelt, 2016). Quantitative analysis of cyanobacteria pigments can be obtained using spectrophotometry or fluorometry, and flow cytometry in the laboratory. These techniques all operate by quantifying the spectral fluorescence characteristics related to absorbance and emission of cyanobacteria pigments (Richardson et al. 2010; Dennis et al. 2011; Kasinak et al. 2014; Silva et al. 2016).

Spectrophotometry and fluorometry require pigment extractions from water samples, which are then analysed for absorbance at a specific wavelength in a benchtop instrument (Kasinak et al. 2014). Fluorescence may also be analysed similarly or directly from raw water samples using flow cytometry (Cellamare et al. 2010). A 'flow cam' is a particle analyser that can produce species assessments and fluorescence readings for raw water samples (FlowCam® Fluid Imaging Technologies., 2017). These laboratory techniques for analysing fluorescence have moderate instrument costs, take a few hours of time and require expertise to process samples accurately and efficiently. Remote sensing techniques for whole lake assessments of cyanobacteria biomass are reliant on clear skies and satellite overpass times, and some satellites have limited spectral bands to support cyanobacterial pigment analysis (Srivastava et al. 2013). Optical sensors are a viable technique to reduce costs, reduce processing time, and they can be used in the field for recreational monitoring purposes.

Table 1. Description of the fluorescence techniques available for quantifying cyanobacteria biomass and the applicability for use in recreational monitoring based on cost, field capabilities and simplicity in use.

Method of quantification	Source/ reference	Description	Advantages	Disadvantages
Microscopic enumeration	(Hötzel & Croome, 1999; Lawton et al. 1999)	Counting cells and identifying species at high magnification using an inverted microscope	<ul style="list-style-type: none"> • Accurate • Species composition • Trusted and tried • Used in monitoring as thresholds for risk assessments 	<ul style="list-style-type: none"> • Time consuming • Labour intensive • Requires taxonomic expertise • Slow sample turnaround times for health warnings
Flow cytometry with flow cam application	(Cellamare et al. 2010; Dennis et al. 2011; FlowCam [®] Fluid Imaging Technologies., 2017)	Samples are assessed in a flow cell, fluorescence gives the relative group abundance for taxa and Flow Cam application can classify cells on both size and morphology while providing images for species level assessments	<ul style="list-style-type: none"> • Time efficient • Large volumes of samples • Accurate automated analysis • Gives particle size distributions • Flow cam can hold a species database • Algal group distributions 	<ul style="list-style-type: none"> • Particle size restrictions in some models • Equipment costs and technician required • Extensive species calibration needed to obtain full benefits of FlowCam application
Remote sensing from satellite and Unmanned aerial vehicle (UAV)	(Zarco-Tejada et al. 2012; Olmanson et al. 2013; Srivastava et al. 2013; Dörnhöfer & Oppelt, 2016)	Imagery from satellite sensors collects reflectance from the water surface. Narrow-band sensors can give an approximation of phycocyanin concentrations. Unmanned aerial vehicle (UAV) can be used onsite to collect images with the spectral bands of choice	<ul style="list-style-type: none"> • High spatial coverage • Whole lake analysis over time • Historical trend analysis • Free images • UAV allow local-scale assessments and can be used anytime 	<ul style="list-style-type: none"> • Low accuracy in image analysis • Temporally restricted to quality overpasses - cloud cover restricts use • Costs for high-resolution images • Chlorophyll interferences due to limited spectral bands • Expensive to use UAV

Optical sensors	(Bastien et al. 2011; Brient et al. 2008; Zamyadi, 2011; Zamyadi et al., 2016)	Measures the <i>In situ</i> fluorescence of the cell pigment phycocyanin from water bodies can be deployed or handheld	<ul style="list-style-type: none"> • Low cost • Cyanobacteria-specific • Portable • <i>In situ</i> sampling • Highly correlated to biovolume • Instantaneous results • Online reporting applications 	<ul style="list-style-type: none"> • Optical interferences include turbidity, chlorophyll <i>a</i>. incidence light • Only site-specific phycocyanin thresholds have been developed for field monitoring • Instrument range and calibrations differ with brands
Spectrophotometry and Fluorometry	(Hagerthey et al. 2006; Kasinak et al. 2014)	Laboratory quantification of phycocyanin uses the absorption and emission at any wavelength specified to calculate corresponding pigment concentrations	<ul style="list-style-type: none"> • Some field models • Low cost if laboratory instruments already exist • Well-developed and repeatable methods available 	<ul style="list-style-type: none"> • Some models have field capacity but are bulky and require solutions and specialised sample cuvettes in the field • Requires preparing solutions and specialised sample cuvettes for the instrument under light and temperature controlled conditions • Pigment must be extracted efficiently

Freshwater cyanobacteria have two photosystems in their photosynthetic apparatus which function like those of higher plants, using water as an electron donor and creating oxygen (Stal, 2012). The two photosystems of cyanobacteria contain chlorophyll *a* and phycobiliproteins. Phycobiliproteins are light harvesting pigments situated on structures called phycobilisomes (Falkowski & Raven, 2007). The pigment molecules of phycocyanin are stacked out from the core of the phycobilisomes structure and the core contains the pigment allophycocyanin. These two pigments are always present in cyanobacteria and have a blue chromophore. Some cyanobacteria contain a third pigment phycoerythrin (Glazer, 1976). These pigments give cyanobacteria the ability to photoacclimate. Photoacclimation offers resistance to high irradiance and protects the chlorophyll photosystem from becoming damaged from high energy transfer (Ibelings et al. 1994; Campbell et al. 1998). The evolution of these pigments allows for chromatic adaptation to spectral changes in light (Dubinsky & Stambler, 2009) and allows cyanobacteria to optimally harvest light at different wavelengths, corresponding to different spectral quality across waterbodies or within the water column (Bermejo, 2014).

Fluorescence theory is based on the molecular absorption of light energy at one wavelength and the emission of light at a longer wavelength (Valeur & Berberan-Santos, 2012). A fluorescent compound has two wavelengths which can be used to measure and calculate the quantity of the compound within a substance (Valeur & Berberan-Santos, 2012). Phycocyanin has bright reflectance properties

(Campbell et al. 1998) and can, therefore, be used to quantify cyanobacteria biomass. Phycocyanin can be detected by excitation of fluorescence signals at wavelengths between 610 and 630 nm. Although each species can have a specific absorbance maxima within this range (Gregor et al. 2007; Chang et al. 2012; Rastogi et al. 2015), the peak is generally around 620 nm. The phycocyanin peak can be of varying strengths for different species (Silva et al. 2016). The allophycocyanin fluorescence absorbance maximum is between 650–655 nm which is the phycocyanin emission wavelength (Bennett & Bogorad, 1973). Phycocyanin sensors can be used to measure the phycocyanin pigment of cyanobacteria (Zamyadi et al. 2012b).

Phycocyanin sensors are becoming increasingly popular as they offer the ability to monitor cyanobacteria biomass at high frequency. Sensors can be used *in situ*, either on platforms or as handheld devices. Phycocyanin sensors also allow for early detection of cyanobacteria in drinking water plants and can detect changes in abundance at high frequency (Izydorczyk et al. 2009). This is of particular importance for species that have regular surface migrations due to buoyancy by gas vacuoles. Species such as *Microcystis aeruginosa* can optimise their position in the water column to take advantage of light in the surface waters. This increases their spatial and temporal variability. For this reason, phycocyanin sensors offer a cost-effective monitoring tool for monitoring changes in cyanobacteria in real time or for frequent discrete sampling (Zamyadi et al. 2016).

Phycocyanin sensors can be set up with online reporting applications to provide real-time cyanobacteria assessments. This technique has been implemented to monitor cyanobacteria in drinking water reservoirs (Zamyadi et al. 2012b). Monitoring cyanobacteria using in-line, flow-through sensors and sensors on monitoring platform units in lakes can inform management for early warning actions. This can be used to inform management actions which reduce the risk of cyanobacteria contamination in water treatment plant intakes (Zamyadi et al. 2013). Research applications can include long-term trend analysis for model validation (Ribeiro & Torgo, 2008; Hamilton et al. 2015; Branco et al. 2016) or spatial assessments of cyanobacteria community and biomass for large water bodies such as the Baltic Sea (Seppälä et al. 2007).

Several studies have investigated the relationship between phycocyanin measured with the sensors and cyanobacteria cell concentrations or biovolume (Bastien et al. 2011; Kong et al. 2014; Bowling et al. 2016). Kong et al. (2014) found relationships of phycocyanin to cell concentrations ($R^2=0.77$), and biovolumes ($R^2=0.99$). Bastien et al. (2011), found strong relationships of phycocyanin to biovolume ($R^2=0.83$), but not to cell concentrations ($R^2=0.46$). Bowling et al., (2016) found stronger relationships of phycocyanin to biovolume for larger cyanobacteria species ($R^2=0.77$) compared to pico-cyanobacteria ($R^2=0.19$).

Currently, there are no international alert level framework thresholds for using phycocyanin concentrations for risk management of cyanobacteria in recreational waters (Zamyadi et al. 2016). Despite this, there have been attempts to use

phycocyanin threshold values for recreational monitoring in Korea (Ahn et al. 2007) and for drinking waters in Quebec (Table 2) (Izydorczyk et al. 2009). The Korean cyanobacteria alert level system for recreational bathing is based on chlorophyll *a*. Ahn et al. (2007) validated phycocyanin to chlorophyll *a* and set out to implement it in their thresholds framework. Ahn et al. (2007) suggested if monitoring was carried out using a PerkinElmer 45 sensor, that current chlorophyll *a* thresholds of 3, 30, and 100 µg L⁻¹ could be replaced by phycocyanin thresholds of 0.1, 5, and 40 µg L⁻¹. In Quebec, Izydorczyk et al. (2009) developed drinking water thresholds using phycocyanin. They used a multi-wavelength approach for detecting four different algal groups using the Algae Online Analyser (AOA, bbe Moldaenke, Kiel, Germany). Their phycocyanin threshold values for a three-tier alert level framework were 1.9, 4.9 and 49.4 µg L⁻¹.

Table 2. Comparison of cyanobacteria monitoring thresholds for recreational contact and proposed phycocyanin thresholds from specific studies. (-) no data.

Source	Cell concentration threshold (cells mL ⁻¹)	Chlorophyll <i>a</i> concentration threshold (µg L ⁻¹)	Biovolume threshold (mm ³ L ⁻¹)	Phycocyanin threshold (µg L ⁻¹)
(Chorus & Bartram, 1999):				
Alert level 1	2000	1	0.2	-
Alert level 2	1,000,000	50	10	-
(Ahn et al., 2007):				
Caution	500	15	-	0.1
Warning	5000	25	-	5
Outbreak	1,000,000	100	-	40
(Izydorczyk et al., 2009):				
Alert level 1	2000	-	0.2	1.9
Alert level 2	5000	-	-	4.9
Alert level 3	50,000	-	5-10	49.4

Several limitations for the use of phycocyanin sensors in recreational monitoring exist. Phycocyanin sensors rely on the excitation and emission of fluorescence from phycocyanin. Anything that is not phycocyanin that passes through the light path when readings are taken could cause interference in the sensor detector and

thus introduce errors in sensor readings (Zamyadi et al. 2016). Interferences occur when there are large colonies of cyanobacteria (Chang et al. 2012) or high densities of phytoplankton containing different pigment ratios (Beutler et al. 2002). It is suggested that the fluorescence inside large dense colonies is not able to be detected by sensors (Chang et al. 2012). Hodges, (2016) and Chang et al. (2012) both found that when large *Microcystis* colonies were disaggregated, the phycocyanin fluorescence detected by sensors increased. It has also been noted that the physiological state of cyanobacteria cells also influences phycocyanin fluorescence (Loftus & Seliger, 1975). As the cells age the phycocyanin fluorescence has been reported to decrease (Chang et al. 2012). This can affect the relationship between the phycocyanin sensor and biovolumes.

Physical structure of the water layers in lakes is subject to seasonal and weather-driven changes. Mixing and stratification are important parameters because they alter light intensity which affects growth and may, therefore, affect phycocyanin quotas in cyanobacteria (Reynolds & Walsby, 1975). Cyanobacteria have different physiological traits to aid in light adaptation (Carey et al. 2012). Photoacclimation is used to transfer energy from photosystems without damaging pigment proteins, therefore allowing survival under high light intensities (Bennett & Bogorad, 1973; Ibelings et al. 1994). However, the effect on fluorescence is that it becomes reduced as energy transfer switches to heat emission (Dubinsky & Stambler, 2009). The exposure of cyanobacteria cells to ultraviolet (UV) light can affect the pigment proteins and photosystem reaction centers. Donkor & Häder, (1996) investigated the pigments in several cyanobacteria species and found bleaching and reduced

fluorescence under continuous exposure to UV light. Laboratory tests with several cyanobacteria species by Brient et al. (2008) showed that fluorescence determined by a sensor increased with artificial light intensity. In contrast, Raps et al. (1983) reported a decrease in phycocyanin with increasing light intensity. Because the photosynthetically available light in the water column of lakes can change with weather patterns, cloud cover and depth, pigment ratios are altered and fluorescence can vary (Ibelings et al. 1994). In phycocyanin yield experiments, nitrogen and sucrose were used to supplement the nutrition of *Dolichospermum/Anabaena fertilissima*. This resulted in higher phycocyanin quotas (Khattar et al. 2015). Similarly, the phycocyanin quota of *Phormidium ceylanicum* was enhanced using high concentrations of nitrogen (285 mg L⁻¹) (Singh et al. 2009). Cyanobacteria have a range of growth adaptations to changing environmental factors and this can directly affect phycocyanin quotas. The effects of nutrients and light intensity on phycocyanin content has not previously been investigated using phycocyanin sensors.

1.2 Overview and objectives

This thesis describes a study of the evaluation of a phycocyanin sensor for monitoring purposes. The aims of the study were to 1) evaluate the use of phycocyanin detected by a sensor in field samples and laboratory cultures for potential use in a cyanobacteria monitoring program, and 2) investigate the effects of environmental factors (nutrients and light) on the growth rate and phycocyanin quota (determined by a phycocyanin sensor) in the bloom-forming cyanobacteria species *M. aeruginosa*.

Chapter 2 describes an investigation of the relationship between *in situ* phycocyanin sensor measurements and biovolumes from five lakes and one river over two summers (2016 and 2017) in the Te Arawa lakes of the Rotorua district, North Island, New Zealand. It examines the variability in phycocyanin, the minimum phycocyanin detection limits, and non-linear relationships in phycocyanin and biovolume, four cyanobacteria species which are common in these lakes that have varying morphology and cell sizes.

Chapter 3 describes an investigation into the effect of nutrients and light intensity on the growth rates and phycocyanin quotas in *M. aeruginosa*. The aim of this chapter is to evaluate if changes in phycocyanin quotas over the growth cycle can be detected by a phycocyanin sensor and to examine the combination of nutrients and light intensity that optimise growth rate or phycocyanin quota.

Chapter 4 summarises the significance of this research and suggests future research directions related to the implementation of phycocyanin sensors.

The two research chapters (2 and 3) are intended to be published as journal articles. Therefore, there may be some repetition of literature and methods since each chapter is written as a self-contained paper.

1.3 References

- Ahn, C., Joung, S., Yoon, S., & Oh, H. (2007). Alternative alert system for cyanobacterial bloom, using phycocyanin as a level determinant. *Journal of Microbiology (Seoul, Korea)*, 45(2), 98–104.
- Baker, P. D., & Fabbro, L. D. (2002). *A guide to the identification of common blue-green algae (Cyanoprokaryotes) in Australian freshwaters*. Thruagoona, NSW: Cooperative Research Centre for Freshwater Ecology.
- Bastien, C., Cardin, R., Veilleux, E., Deblois, C., Warren, A., & Laurion, I. (2011). Performance evaluation of phycocyanin probes for the monitoring of cyanobacteria. *Journal of Environmental Monitoring*, 13, 110–118. <https://doi.org/10.1039/c0em00366b>.
- Bennett, A., & Bogorad, L. (1973). Complementary chromatic adaption in a filamentous blue-green alga. *The Journal of Cell Biology*, 58, 419–435. <https://doi.org/10.1083/jcb.58.2.419>.
- Bermejo, R. (2014). Phycocyanins. In *Cyanobacteria: An economic perspective* (pp. 209–225). Hoboken: John Wiley & Sons, Ltd. <https://doi.org/10.1017/CBO9781107415324.004>.
- Beutler, M., Wiltshire, K. H., Meyer, B., Moldaenke, C., Lüring, C., Meyerhöfer, M., Hansen, U. P., & Dau, H. (2002). A fluorometric method for the differentiation of algal populations *in vivo* and *in situ*. *Photosynthesis Research*, 72(1), 39–53. <https://doi.org/10.1023/A:1016026607048>.
- Bowling, L. C., Zamyadi, A., & Henderson, R. K. (2016). Assessment of *in situ* fluorometry to measure cyanobacterial presence in water bodies with diverse cyanobacterial populations. *Water Research*, 105, 22–33.

<https://doi.org/10.1016/j.watres.2016.08.051>.

Branco, P., Torgo, L., & Ribeiro, R. P. (2016). A survey of predictive modeling on imbalanced domains. *ACM Computing Surveys*, 49(2), 1–50.

<https://doi.org/10.1145/2907070>.

Brient, L., Lengronne, M., Bertrand, E., Rolland, D., Sipel, A., Steinmann, D., Baudin, I., Legeas, M., Le Rouzic, B., & Bormans, M. (2008). A phycocyanin probe as a tool for monitoring cyanobacteria in freshwater bodies. *Journal of Environmental Monitoring*, 10(2), 248–255.

<https://doi.org/10.1039/B714238B>.

Campbell, D. A., Hurry, V., Clarke, K., Gustafsson, P., & Oquist, G. (1998). Chlorophyll fluorescence analysis of cyanobacterial photosynthesis and acclimation. *Microbiology and Molecular Biology Reviews : MMBR*, 62(3), 667–683. <https://doi.org/10.1093/mmb/62.3.667>.

Carey, C. C., Ibelings, B. W., Hoffmann, E. P., Hamilton, D. P., & Brookes, J. D. (2012). Eco-physiological adaptations that favour freshwater cyanobacteria in a changing climate. *Water Research*, 46(5), 1394–1407. <https://doi.org/10.1016/j.watres.2011.12.016>.

Cellamare, M., Rolland, A., & Jacquet, S. (2010). Flow cytometry sorting of freshwater phytoplankton. *Journal of Applied Phycology*, 22(1), 87–100. <https://doi.org/10.1007/s10811-009-9439-4>.

Chang, D. W., Hobson, P., Burch, M., & Lin, T. F. (2012). Measurement of cyanobacteria using *in-vivo* fluoroscopy - Effect of cyanobacterial species, pigments, and colonies. *Water Research*, 46(16), 5037–5048. <https://doi.org/10.1016/j.watres.2012.06.050>.

- Chorus, I., & Bartram, J. (Eds.). (1999). Toxic Cyanobacteria in Water: A Guide to their Public Health Consequences, Monitoring and Management. London, U.K.: Taylor & Francis.
- Dennis, M. A., Landman, M., Wood, S. A., & Hamilton, D. (2011). Application of flow cytometry for examining phytoplankton succession in two eutrophic lakes. *Water Science and Technology*, 64(4), 999–1008. <https://doi.org/10.2166/wst.2011.099>.
- Donkor, V. A., & Häder, D. P. (1996). Effects of ultraviolet irradiation on photosynthetic pigments in some filamentous cyanobacteria. *Aquatic Microbial Ecology*, 11(2), 143–149. <https://doi.org/10.3354/ame011143>.
- Dörnhöfer, K., & Oppelt, N. (2016). Remote sensing for lake research and monitoring - Recent advances. *Ecological Indicators*, 64, 105–122. <https://doi.org/10.1016/j.ecolind.2015.12.009>.
- Dubinsky, Z., & Stambler, N. (2009). Photoacclimation processes in phytoplankton: Mechanisms, consequences, and applications. *Aquatic Microbial Ecology*, 56(2–3), 163–176. <https://doi.org/10.3354/ame01345>.
- Falkowski, P. G., & Raven, J. A. (2007). An introduction to photosynthesis in aquatic systems. In *Aquatic Photosynthesis* (2nd ed., pp. 1–44). Ney Jesery, USA: Princeton University Press. <https://doi.org/10.1017/CBO9781107415324.004>.
- Fluid Imaging Technologies. (2017). *Imaging Particle Analysis Solutions for Water Treatment* [Brochure]. Retrieved April, 5 2017, from <http://info.fluidimaging.com/hubfs/Brochures/FlowCam%20Water%20Tre>

atment%20Brochure%20-%202017.pdf?hsCtaTracking=c2b62ff8-4c6a-4358-be1a-c65030c3fce7%7C168f5e18-6b80-4a9e-8ace-111d204493fd.

Gholizadeh, M. H., Melesse, A. M., & Reddi, L. (2016). A comprehensive review on water quality parameters estimation using remote sensing techniques. *Sensors (Basel, Switzerland)*, 16(8), 1298. <https://doi.org/10.3390/s16081298>.

Glazer, A. N. (1976). Phycocyanins : Structure and Function. In *In photochemical and photobiological reviews* (pp. 71–115). US: Springer International Publishing.

Gregor, J., Maršálek, B., & Šípková, H. (2007). Detection and estimation of potentially toxic cyanobacteria in raw water at the drinking water treatment plant by *in vivo* fluorescence method. *Water Research*, 41(1), 228–234. <https://doi.org/10.1016/j.watres.2006.08.011>.

Hagerthey, S. E., William Louda, J., & Mongkronsri, P. (2006). Evaluation of pigment extraction methods and a recommended protocol for periphyton chlorophyll *a* determination and chemotaxonomic assessment. *Journal of Phycology*, 42(5), 1125–1136. <https://doi.org/10.1111/j.1529-8817.2006.00257.x>.

Hamilton, D. P., Carey, C. C., Arvola, L., Arzberger, P., Brewer, C., Cole, J. J., Gaiser, E., Hanson, P. C., Ibelings, B. W., Jennings, E., Kratz, T K., Lin, F. P., McBride, C. G., de Motta Marques, D., Muraoka, K., Nishri, A., Qin, B., Read, J. S., Rose, K. C., Ryder, E., Weathers, K. C., Zhu, G., Trolle, D., & Brookes, J. D. (2015). A Global lake ecological observatory network (GLEON) for synthesising high-

- frequency sensor data for validation of deterministic ecological models. *Inland Waters*, 5(1), 49–56. <https://doi.org/10.5268/IW-5.1.566>.
- Havens, K. E. (2008). Cyanobacteria blooms: Effects on aquatic ecosystems. In H. K. Hudnell (Ed.), *Cyanobacterial Harmful Algal Blooms: State of the Science and Research Needs* (Vol. 619, pp. 733-747). New York, NY: Springer.
- Hodges, C. (2016). *A validation study of phycocyanin sensors for monitoring cyanobacteria in cultures and field samples*. University of Waikato, Hamilton.
- Hötzel, G., & Croome, R. (1999). *A phytoplankton methods manual for Australian freshwaters*. Occasional Paper 22/99. Land and Water Resources Research and Development Corporation, Wodonga, Victoria, Australia. <http://npsi.gov.au/files/products/national-river-health-program/pr990300/pr990300.pdf>.
- Ibelings, B. W., Backer, L. C., Kardinaal, W. E. A., & Chorus, I. (2015). Current approaches to cyanotoxin risk assessment and risk management around the globe. *Harmful Algae*, 49, 63–74. <https://doi.org/10.1016/j.hal.2014.10.002>.
- Ibelings, B. W., Kroon, B. M. a., & Mur, L. R. (1994). Acclimation of photosystem II in a cyanobacterium and a eukaryotic green alga to high and fluctuating photosynthetic photon flux densities, simulating light regimes induced by mixing in lakes. *New Phytologist*, 128(3), 407–424. <https://doi.org/10.1111/j.1469-8137.1994.tb02987.x>.
- Izydorczyk, K., Carpentier, C., Mrówczyński, J., Wagenvoort, A., Jurczak, T., & Tarczyńska, M. (2009). Establishment of an Alert Level Framework for cyanobacteria in drinking water resources by using the Algae Online Analyser for monitoring cyanobacterial chlorophyll *a*. *Water Research*, 43(4), 989–996.

<https://doi.org/10.1016/j.watres.2008.11.048>.

- Kasinak, J. M. E., Holt, B. M., Chislock, M. F., & Wilson, A. E. (2014). Benchtop fluorometry of phycocyanin as a rapid approach for estimating cyanobacterial biovolume. *Journal of Plankton Research*, 37(1), 248–257. <https://doi.org/10.1093/plankt/fbu096>.
- Khattar, J. I. S., Kaur, S., Kaushal, S., Singh, Y., Singh, D. P., Rana, S., & Gulati, A. (2015). Hyperproduction of phycobiliproteins by the cyanobacterium *Anabaena fertilissima* PUPCCC 410.5 under optimized culture conditions. *Algal Research*, 12, 463–469. <https://doi.org/10.1016/j.algal.2015.10.007>.
- Kong, Y., Lou, I., Zhang, Y., Lou, C. U., & Mok, K. M. (2014). Using an online phycocyanin fluorescence probe for rapid monitoring of cyanobacteria in Macau freshwater reservoir. *Hydrobiologia*, 741(1), 33–49. <https://doi.org/10.1007/s10750-013-1759-3>.
- Lawton, L., Marsalek, B., Padisák, J., & Chorus, I. (1999). Determination of cyanobacteria in the laboratory. In I. Chorus & J. Bartram (Eds.), *Toxic Cyanobacteria in Water: A Guide to their Public Health Consequences, Monitoring and Management* (pp. 203-216). London, U.K.: Taylor & Francis.
- Loftus, M. E., & Seliger, H. H. (1975). Some limitations of the *in vivo* fluorescence technique. *Chesapeake Science*, 16(2), 79–92.
- Ma, J., Brookes, J. D., Qin, B., Paerl, H. W., Gao, G., Wu, P., Zhang, W., Deng, J., Zhu, G., Zhang, Y., Xu, H., & Niu, H. (2014). Environmental factors controlling colony formation in blooms of the cyanobacteria *Microcystis* spp. in Lake Taihu, China. *Harmful Algae*, 31, 136–142. <https://doi.org/10.1016/j.hal.2013.10.016>.

- Meriluoto, J., Blaha, L., Bojadzija, G., Bormans, M., Brient, L., Codd, G. A., Drobač, D., Faassen, E. J., Fastner, J., Hiskia, A., Ibelings, B. W., Kaloudis, T., Kokocinski, M., Kurmayer, R., Pantelić, D., Quesada, A., Salmaso, N., Tokodi, N., Triantis, T. M., Visser, P. M., & Svirčev, Z. (2017). Toxic cyanobacteria and cyanotoxins in European waters – recent progress achieved through the CYANOCOST Action and challenges for further research. *Advances in Oceanography and Limnology*, 8(1).
<https://doi.org/10.4081/aiol.2017.6429>.
- Newcombe, G., House, J., Ho, L., Baker, P., & Burch, M. D. (2010). *Management strategies for Cyanobacteria: a guide for water utilities*, Research Report 74. Water Quality Research Australia, Adelaide, South Australia.
- NIWA. (nd). Algal monitoring service. NIWA (National Institute of Water and Atmospheric Research, New Zealand. Retrieved January 25, 2017, from www.niwa.co.nz/our-science/freshwater/our-services/specialist-analytical-services/algal-monitoring-service.
- Oliver, R. L., Hamilton, D. P., Brookes, J. D., & Ganf, G. G. (2012). Physiology, blooms and prediction of planktonic cyanobacteria. In B.A. Whitton (Ed.), *Ecology of Cyanobacteria II: their Diversity in Space and Time*. (pp. 155-194). Netherlands: Springer-Verlag.
- Olmanson, L. G., Brezonik, P. L., & Bauer, M. E. (2013). Airborne hyperspectral remote sensing to assess spatial distribution of water quality characteristics in large rivers: The Mississippi River and its tributaries in Minnesota. *Remote Sensing of Environment*, 130, 254–265.
<https://doi.org/10.1016/j.rse.2012.11.023>.

- Raps, S., Wyman, K., Siegelman, H. W., & Falkowski, P. G. (1983). Adaptation of the cyanobacterium *Microcystis aeruginosa* to light intensity. *Plant Physiology*, 72(3), 829–832. <https://doi.org/10.1104/pp.72.3.829>.
- Rastogi, R. P., Sonani, R. R., & Madamwar, D. (2015). Physico-chemical factors affecting the *in vitro* stability of phycobiliproteins from *Phormidium rubidum* A09DM. *Bioresource Technology*, 190, 219–226. <https://doi.org/10.1016/j.biortech.2015.04.090>.
- Reynolds, C. S., & Walsby, A. E. (1975). Water-Blooms. *Biological Reviews*, 50(4), 437–481. <https://doi.org/10.1111/j.1469-185X.1975.tb01060.x>.
- Reynolds, C. S. (2006). *The Ecology of Phytoplankton*. Cambridge, UK: Cambridge University Press. 551p. <https://doi.org/10.1177/0309133310367548>.
- Ribeiro, R., & Torgo, L. (2008). A comparative study on predicting algae blooms in Douro River, Portugal. *Ecological Modelling*. <https://doi.org/10.1016/j.ecolmodel.2007.10.018>.
- Richardson, T. L., Lawrenz, E., Pinckney, J. L., Guajardo, R. C., Walker, E. A., Paerl, H. W., & MacIntyre, H. L. (2010). Spectral fluorometric characterization of phytoplankton community composition using the Algae Online Analyser. *Water Research*, 44(8), 2461–2472. <https://doi.org/10.1016/j.watres.2010.01.012>.
- Seppälä, J., Ylöstalo, P., Kaitala, S., Hällfors, S., Raateoja, M., & Maunula, P. (2007). Ship-of-opportunity based phycocyanin fluorescence monitoring of the filamentous cyanobacteria bloom dynamics in the Baltic Sea. *Estuarine*,

Coastal and Shelf Science, 73(3–4), 489–500.

<https://doi.org/10.1016/j.ecss.2007.02.01>.

Silva, T., Giani, A., Figueredo, C., Viana, P., Khac, V. T., Lemaire, B. J., Tassin, B., Nascimento, N., & Vinçon-Leite, B. (2016). Comparison of cyanobacteria monitoring methods in a tropical reservoir by in vivo and in situ spectrofluorometry. *Ecological Engineering*, 97, 79–87.

<https://doi.org/10.1016/j.ecoleng.2016.06.037>.

Singh, N. K., Parmar, A., & Madamwar, D. (2009). Optimization of medium components for increased production of C-phyococyanin from *Phormidium ceylanicum* and its purification by single step process. *Bioresource Technology*, 100(4), 1663–1669.

<https://doi.org/10.1016/j.biortech.2008.09.021>.

Srivastava, A., Singh, S., Ahn, C. Y., Oh, H. M., & Asthana, R. K. (2013). Monitoring approaches for a toxic cyanobacterial bloom. *Environmental Science and Technology*, 47(16), 8999–9013. <https://doi.org/10.1021/es401245k>.

Stal, L. J. (2012). Environmental factors regulating nitrogen fixation in heterocystous and non- heterocystous cyanobacteria. In *Stress Biology of Cyanobacteria : Molecular Mechanisms to Cellular Responses*, (p.291-306).

Boca Raton: Taylor & Francis.

Straile, D., Jochimsen, M. C., & Kümmerlin, R. (2015). Taxonomic aggregation does not alleviate the lack of consistency in analysing diversity in long-term phytoplankton monitoring data: A rejoinder to Pomati et al. (2015).

Freshwater Biology, 60(5), 1060–1067. <https://doi.org/10.1111/fwb.1255>.

Trescott, A., & Park, D. M.-H. (2012). Remote Sensing Models of Algal Blooms and

- Cyanobacteria in Lake Champlain. *Environmental & Water Resources Engineering Masters Projects* (48), 95.
- Valeur, B., & Berberan-Santos, M. N. (2012). Introduction. In *Molecular fluorescence: principles and applications* (pp. 1–12). John Wiley & Sons. <https://doi.org/10.1007/978-0-387-93837-0>.
- Vincent, R. K., Qin, X., McKay, R. M. L., Miner, J., Czajkowski, K., Savino, J., & Bridgeman, T. (2004). Phycocyanin detection from LANDSAT TM data for mapping cyanobacterial blooms in Lake Erie. *Remote Sensing of Environment*, 89(3), 381–392. <https://doi.org/10.1016/j.rse.2003.10.014>.
- Wood, S. A., Hamilton, D. P., Paul, W. J., Safi, K. A., & Williamson, W. M. (2009). *New Zealand Guidelines for Cyanobacteria in Recreational Fresh Waters – Interim Guidelines*. Publication number ME 981, prepared for the Ministry for the Environment and the Ministry of Health. Ministry for the Environment, Wellington, New Zealand. 88p. <http://www.mfe.govt.nz/sites/default/files/nz-guidelines-cyanobacteria-recreational-fresh-waters.pdf>.
- Wood, S. A., Paul, W. J., & Hamilton, D. P. (2008). *Cyanobacterial Biovolumes for the Rotorua Lakes*. Cawthron Report No. 1504, prepared for Environment Bay of Plenty. 27p. <https://www.boprc.govt.nz/media/32233/Cawthron-090803-CyanobacterialbiovolumesforRotorualakes.pdf>.
- Zamyadi, A. (2011). *The value of in vivo monitoring and chlorination for the control of toxic cyanobacteria in drinking water production*. Retrieved from <http://publications.polymtl.ca/618>.
- Zamyadi, A., Choo, F., Newcombe, G., Stuetz, R., & Henderson, R. K. (2016). A

- review of monitoring technologies for real-time management of cyanobacteria: Recent advances and future direction. *TrAC - Trends in Analytical Chemistry*, 85, 83–96. <https://doi.org/10.1016/j.trac.2016.06.023>.
- Zamyadi, A., Dorner, S., Sauvé, S., Ellis, D., Bolduc, A., Bastien, C., & Prévost, M. (2013). Species-dependence of cyanobacteria removal efficiency by different drinking water treatment processes. *Water Research*, 47(8), 2689–2700. <https://doi.org/10.1016/j.watres.2013.02.040>.
- Zamyadi, A., MacLeod, S., Fan, Y., McQuaid, N., Dorner, S., Sauvé, S., & Prévost, M. (2012b). Toxic cyanobacterial breakthrough and accumulation in a drinking water plant: A monitoring and treatment challenge. *Water Research*, 46(5), 1511–1523. <https://doi.org/10.1016/j.watres.2011.11.01>.
- Zamyadi, A., McQuaid, N., Dorner, S., Bird, D. F., Burch, M., Baker, P., Hobson, P., & Prévost, M. (2012a). Cyanobacterial detection using *in vivo* fluorescence probes: Managing interferences for improved decision-making. *Journal - American Water Works Association*. <https://doi.org/10.5942/jawwa.2012.104.0114>.
- Zarco-Tejada, P. J., González-Dugo, V., & Berni, J. A. J. (2012). Fluorescence, temperature and narrow-band indices acquired from a UAV platform for water stress detection using a micro-hyperspectral imager and a thermal camera. *Remote Sensing of Environment*, 117, 322–337. <https://doi.org/10.1016/j.rse.2011.10.007>.

Chapter 2

Opportunities and challenges for use of a phycocyanin sensor to monitor cyanobacteria

2.1 Abstract

To protect human users, many lake monitoring programs assess cyanobacterial biomass using biovolume. This is commonly undertaken using microscopy, but this method is time-consuming and costly. Phycocyanin (a pigment specific to cyanobacteria) fluoresces at 620 nm. Phycocyanin sensors are increasingly used to aid in the rapid assessment of cyanobacteria biomass. In this study, a phycocyanin sensor was used to assess cyanobacteria biomass in parallel with microscopically determined biovolumes. Samples were collected from five lakes and one river in the Te Arawa Rotorua lakes district (North Island, New Zealand), over summer, in both 2016 (n= 121) and 2017 (n=63). In the field data, it was hypothesised that *in situ* sensor measurements of phycocyanin will be strongly correlated with biovolumes collected from a range of lakes. In the laboratory, phycocyanin relationships to biovolume were tested for four species with varying colony shape and cell size. It was hypothesised that each species would have different phycocyanin variability, different minimum phycocyanin detection limits, and may also exhibit non-linear relationships in phycocyanin at low biovolume. The field study results for relationships between phycocyanin and biovolume gave ($R^2=0.43$) for 2016 and ($R^2=0.66$) for 2017. For these relationships, high biovolume ($>10 \text{ mm}^3 \text{ L}^{-1}$) and/or dominance of large-celled cyanobacteria species improved the

relationship. Results for the predicted phycocyanin thresholds in comparison to the biovolume thresholds for recreational monitoring were different across lakes and between years. The predicted phycocyanin threshold of $>40 \mu\text{g L}^{-1}$ was found to be equal to biovolume threshold of $1.8 \text{ mm}^3 \text{ L}^{-1}$. Dilution experiments showed that phycocyanin varied between species. The large colonial cyanobacterium *Microcystis wesenbergii* had the largest variability in phycocyanin readings. Minimum phycocyanin detection limits from the dilutions were unsuitable in the recreational biovolume threshold ($<0.5 \text{ mm}^3 \text{ L}^{-1}$) due to variability between species. The non-linear response in phycocyanin to biovolume relationships was significant for three colonial species. While two species could be predicted at the biovolume threshold of $1.8 \text{ mm}^3 \text{ L}^{-1}$ two could not, this was due to breakpoint position in the dilution. Caution is recommended when using the phycocyanin values from a sensor as they provide only semi-quantitative estimates of biomass. Factors such as changes in species composition, morphology, density and prior light exposure contribute to some of this variation.

2.2 Introduction

Toxic cyanobacterial blooms are increasing globally, and this heightens the risk of toxin exposure for humans (Paerl et al. 2016). The toxins from cyanobacterial blooms can cause skin irritation (dermatotoxin), affect the nervous system (neurotoxins), as well as cause respiratory, gastrological and liver (hepatotoxic) problems in people who come into contact with, or ingest, contaminated water (Chorus & Bartram, 1999). Cyanobacterial blooms are more frequent in summer and this is when there is greater recreational use of lakes. Cyanobacterial blooms

can also create water quality issues including reduced dissolved oxygen and increased ammonia production when they decay (Reynolds, 2006). One of the most common bloom-forming cyanobacterial genera is *Microcystis*, with blooms reported in over 100 countries (Harke et al. 2016).

Cyanobacterial monitoring in the freshwater lakes of New Zealand is undertaken by regional authorities. They generally follow the New Zealand guidelines for cyanobacteria in recreational fresh waters (Wood et al. 2009; Table 1). New Zealand guidelines advise on using cyanobacterial biovolumes in a three-tier alert system to report 1) total cyanobacteria biovolume, or 2) potentially toxic cyanobacteria species (Wood et al. 2009). The first tier of the biovolume thresholds is the green surveillance mode threshold of biovolume $<0.5 \text{ mm}^3 \text{ L}^{-1}$ when weekly or fortnightly sampling and inspection is undertaken (Table 1). The next tier is amber alert mode (>0.5 to $<1.8 \text{ mm}^3 \text{ L}^{-1}$), and red action mode is triggered when potentially toxic cyanobacteria are elevated ($\geq 1.8 \text{ mm}^3 \text{ L}^{-1}$) or when the total cyanobacteria biovolume is $\geq 10 \text{ mm}^3 \text{ L}^{-1}$ (Wood et al. 2009).

Table 1. New Zealand guidelines for cyanobacteria in recreational fresh waters (Wood et al. 2009). Alert level mode, biovolume thresholds, and required monitoring and management.

Alert level	Biovolume threshold ($\text{mm}^3 \text{ L}^{-1}$)	Requirements
Green surveillance mode	<0.5	Weekly or fortnightly sampling
Amber alert level	>0.5 and <1.8	Weekly sampling
Red action mode	≥ 1.8 for potentially toxic or ≥ 10 for total cyanobacteria	Health warning in place of contamination

The Bay of Plenty Regional Council set up the Rotorua lakes' algal monitoring program in the early 1990s when local communities became concerned about

frequent cyanobacterial blooms in several of the lakes (Burns et al. 2005). The increased occurrence of blooms in different lakes was related to increased anthropogenic sources of nitrogen and phosphorus (Smith et al. 2016). The algal monitoring program provides additional information on other lake monitoring components (Lake Trophic Level Index) because cyanobacteria are an indicator of lake water quality and their composition changes with nutrient loads to the lakes (Özkundakci et al. 2010; Paul et al. 2012).

The Rotorua lakes are highly valued for recreational tourism activities and for their traditional Māori cultural purposes (Kusabs & Quinn, 2009). The presence of surface scums can affect the public perception of water quality (Burns et al. 2005). Timely reporting of these events can help to ensure people can safely recreate in the lakes without harm. Biovolume sampling requires collecting grab samples for microscopic identification and enumeration (Wood et al. 2008). Measurements of biovolume, however, are time-consuming, have substantial costs, and require an expert to accurately identify taxa. Current methods in the cyanobacterial monitoring program may be enhanced by phycocyanin sensors, by providing on-site health warnings for public protection as well as increased frequency of monitoring.

Phycocyanin sensors may offer an efficient way to assess cyanobacterial biomass *in situ* (Brient et al. 2008; Izydorczyk et al. 2009). For example, Izydorczyk et al. (2009) set threshold levels for cyanobacteria based on phycocyanin measured by a sensor in a drinking water reservoir. Brient et al. (2008) considered that sensors

can be used to complement enumeration methods to aid in risk assessment for cyanobacteria. Phycocyanin sensors detect discrete wavelengths of light emission corresponding to the peak emission wavelength from phycocyanin. Phycocyanin is an accessory pigment of cyanobacteria that is highly fluorescent (Glazer, 1976). Its maximum excitation absorption is about 620 nm and its emission wavelength is about 650 nm (Bermejo, 2014). Phycocyanin sensors can be used as handheld sensors or be deployed *in situ*, and therefore offer opportunities to monitor cyanobacteria at high frequency and in real time.

Phycocyanin sensors are currently used in water quality monitoring for drinking water reservoirs (Zamyadi et al. 2012) and natural lakes and rivers. They have also been used to provide data for recreational health assessments (Ahn et al. 2007) and water quality modelling (Ribeiro & Torgo, 2008; Hamilton et al. 2015). Sensor validation studies have been undertaken to assess the relationship between Raw Fluorescence Units (RFU) from a phycocyanin sensor, phycocyanin concentrations, and cyanobacteria cell concentrations or biovolume. Strong relationships have been found between phycocyanin and biovolumes when cyanobacteria are present in high density in field samples and dominated by a single species (Kong et al. 2014). There are few studies which have undertaken assessment when biovolumes are $<10 \text{ mm}^3 \text{ L}^{-1}$ (McQuaid et al. 2011). This represents a potential limitation to the development of a phycocyanin threshold in an alert level framework for recreational monitoring (Zamyadi et al. 2016). This may pose difficulty in context to the New Zealand alert level framework (Table 1) as the red action mode for potentially toxic species is $1.8 \text{ mm}^3 \text{ L}^{-1}$.

Phycocyanin sensors have known interferences at low biovolumes (Zamyadi et al. 2016). Sensor readings vary amongst model types and manufacturers (Hodges, 2016), and detection thresholds may not necessarily be sufficiently sensitive for recreational monitoring purposes (Zamyadi et al. 2016). Furthermore, sensor outputs can be in different units and calibrated differently with different manufacturer guidelines (Bastien et al. 2011). For example, Bastien et al. (2011) used a YSI 6600 sensor (YSI Inc., Yellow Springs, OH, USA) and performed a two-point calibration of phycocyanin from cell concentrations, as recommended by the manufacturer. The manufacturer gives information to indicate that the sensor is sensitive to phycocyanin as low as 5,000 cells mL⁻¹, with a degree of linearity from 5,000 cells mL⁻¹ down to zero. Bastien et al. (2011) found that for <310 cells mL⁻¹, the sensor may begin to give negative readings. This imposes difficulty in setting recreational thresholds for phycocyanin concentrations as a proxy for cyanobacterial biomass.

The Rotorua Lakes have a diverse cyanobacteria species composition and at many times of the year density and biovolumes are low. Pico-cyanobacteria have become common with recent improvements in water quality (Paul et al. 2012). Some lakes, however, are still subject to cyanobacterial blooms, with occurrences of potentially toxic species, such as *Microcystis wesenbergii*, which can form large colonies. Other cyanobacteria species have different morphologies and can range from globular to coiled or filamentous bunches. These morphologies may reduce fluorescence of cells in colonies or filaments (Chang et al. 2012), which would result in underestimation of phycocyanin. The presence of mixed species

assemblages with contrasting morphologies and phycocyanin content (Hemlata, 2009), may also affect the interpretation of phycocyanin sensor measurements.

The aim of this study is to investigate the use of a phycocyanin sensor as a monitoring tool in the Rotorua Lakes' cyanobacteria monitoring program. The program involves sampling a variety of lakes and algal communities and uses biovolume thresholds to monitor health risk. Two hypotheses were tested, 1) that *in situ* sensor measurements of phycocyanin will be strongly correlated with biovolumes collected from a range of lakes, and 2) that the phycocyanin of four species will have different phycocyanin variability, different minimum phycocyanin detection limits, and that relationships in phycocyanin concentration and low biovolumes may differ because of varying colony shape and cell size.

2.3 Methods

2.3.1 Phycocyanin sensor

A phycocyanin sensor (Cyclops-7, Turner Designs, USA) was used to measure phycocyanin, with the output measured by a voltmeter using adjustable gains to alter range and sensitivity. The sensor was cleaned regularly and thoroughly with Milli-Q water and Kimwipes (Kimberly-Clark, USA) between sampling sites and experiments. Sensor readings were conducted in a 'blackened out' (black neoprene sleeve) 1 L beaker with no temperature control during field sampling and under low light conditions (ca. $5 \mu\text{mol m}^{-2} \text{s}^{-1}$) and constant temperature ($18 \pm 1^\circ\text{C}$) in the laboratory experiments. All sample measurements were obtained at least 1 cm

below the water surface and were the average of five (field samples) or seven (species dilutions experiments) replicates.

Calibration

The phycocyanin standard consisted of *Spirulina* (10 mg; P2172, Sigma-Aldrich, USA) dissolved in sodium phosphate buffer (30 mL; 50 mM, pH 7) and diluted to 300 mL⁻¹ with Milli-Q water. The phycocyanin standard concentration was determined with spectrophotometry (Bennett & Bogorad, 1973):

$$\text{Phycocyanin } (\mu\text{g L}^{-1}) = \left[\frac{A_{615} - (0.474 \times A_{652})}{5.34} \right] \times 1,000,000 \quad (2-1)$$

where A_{615} is the maximum absorbance of phycocyanin and A_{652} is the maximum absorbance of phycocyanin emission (allophycocyanin) for a cuvette path length of 1 cm, and 1,000,000 is used to convert the data from mg mL⁻¹ to $\mu\text{g L}^{-1}$.

Sensor readings (V) were converted to phycocyanin ($\mu\text{g L}^{-1}$) using the phycocyanin –sensor calibration curve. The calibration curve was an eleven-point (0.5-1,000 $\mu\text{g L}^{-1}$) linear regression of sensor volts to phycocyanin concentration measured with the spectrophotometer. Background noise (determined by taking five replicate measurements in Milli-Q water before measuring the standards) was subtracted prior to linear regression. The sensor had an acceptable linear fit ($R^2 = 0.99$), with a slope of 0.00202 volts ($\mu\text{g L}^{-1}$)⁻¹ all sensor volts were converted using:

$$\text{Sensor phycocyanin } (\mu\text{g L}^{-1}) = \text{volts}/0.00202 \quad (2-2)$$

2.3.2 Study sites

Five lakes and one river in the Te Arawa lakes of the Rotorua district, New Zealand, were chosen for the study during summer 2016 and 2017; Lake Tarawera, Lake Okaro, Lake Rotorua, Lake Rotoiti, Lake Rotoehu and the Kaituna River (Table 2, Figure 2). The lakes vary in size, depth and water quality (Table 2). Lake Tarawera is usually considered oligotrophic (Scholes & Hamill, 2016) and Rotoiti is mesotrophic. These two lakes are deep (mean depth = 50 m and 31 m, respectively) with similar areas (41.2 km² and 33.7 km², respectively) (Paul et al. 2012). Lake Tarawera occasionally has cyanobacterial blooms in bays and near geothermal inputs (Scholes & Hamill, 2016). Lake Rotoiti has four sheltered embayments that can have high concentrations of cyanobacteria (Von Westernhagen et al. 2010). Lake Rotorua is a large (80.8 km²) eutrophic lake with one deep basin (45 m) and geothermal inputs. Cyanobacterial blooms sometimes form along shorelines exposed to light winds (Scholes, 2011). Lake Rotorua and Lake Rotoiti feed into the Kaituna River. Cyanobacteria in the Kaituna River generally represents a mixture of those from the two lakes (i.e., Rotorua and Rotoiti) but are generally present only at low densities (Wood et al. 2014). Lake Okaro and Lake Rotoehu are eutrophic and regularly experience cyanobacterial blooms in summer, when they are thermally stratified (Wood et al. 2014). Lake Okaro is a small (0.3 km²), shallow (18 m) lake and has a soft sediment bottom which can act as a source of phosphorus when the hypolimnion is depleted of oxygen (Özkundakci et al. 2014). Lake Rotoehu has geothermal inputs into the main basin and is polymictic, shallow (mean depth 8 m) and moderate area (7.9 km²).

Table 2. Location, site name, trophic state, maximum depth and lake areas of the five lakes and one river, sampled over two summers (2016 and 2017), in the Te Arawa Rotorua lakes district, New Zealand. See Figure 1 for locations. *High/moderate cyanobacteria risk sites. NA = not available.

Location	Site name	Trophic status	Maximum depth (m)	Lake area (ha)
Kaituna River	Trout Pool*	NA	NA	NA
Lake Okaro	Boat ramp*	Eutrophic	18	30
Lake Rotoehu	Otautu Bay* and Kennedy Bay*	Eutrophic	13.5	790
Lake Rotoiti	Hinehopu, Okawa Bay*, Otara Marae, Te Weta, Okere Arm*	Mesotrophic	126	3,369
Lake Rotorua	Holdens Bay*, Ohau Channel*, Hamurana, Ngongotaha	Eutrophic	45	8,048
Lake Tarawera	Hot Water Beach*, Boatshed Bay, Stoney point*	Oligotrophic/ mesotrophic	87.5	4,115

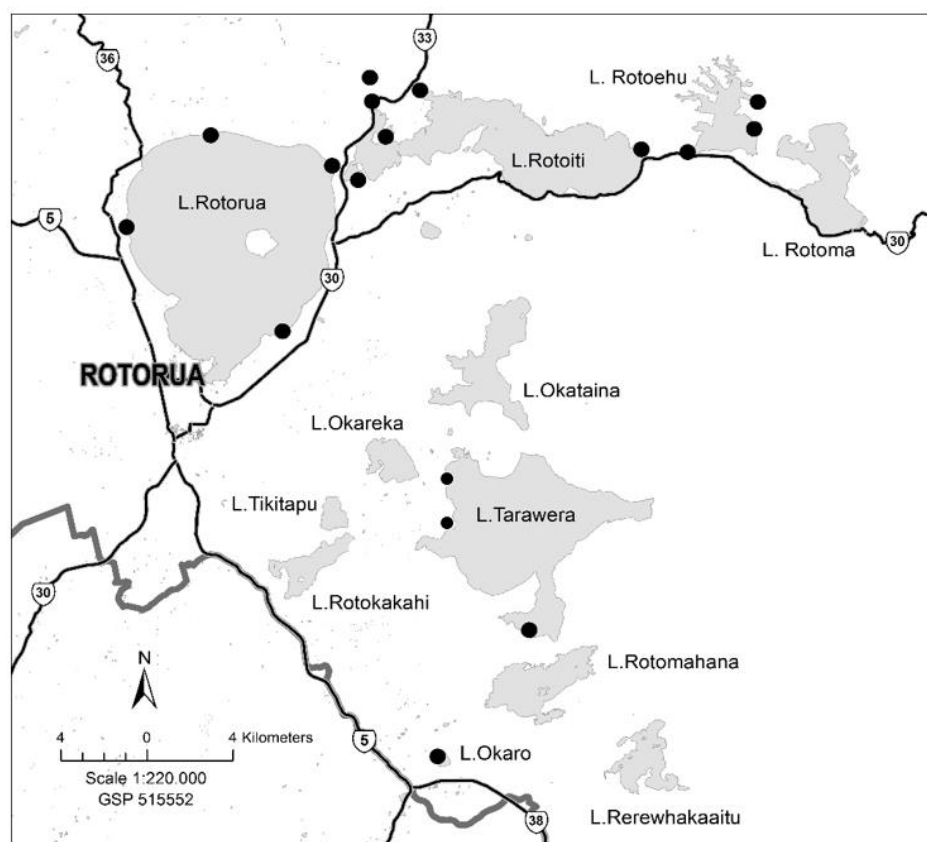


Figure 1. Location of 16 monitoring sites (black dots) in the Te Arawa lakes district of Rotorua, New Zealand (See Table 1 for site names).

2.3.3 Field sampling

Field sampling took place weekly or fortnightly over two consecutive summer-autumn periods from January to April in 2016 and January to March in 2017. Sixteen sites were selected from the five lakes and one river site. All sites were sampled in 2016 but only ten of the 16 sites were at moderate to high risk of experiencing cyanobacterial blooms and therefore monitoring was confined to these sites in 2017 (Table 2).

At each sampling site, a surface water sample (5 L) was collected using an integrated tube sampler (0.5 m). Phycocyanin levels in the samples were measured by five replicate readings after which time a sub-sample (100 mL) was preserved in Lugol's iodine for later biovolume analysis. Prior to each measurement a sample of Reverse Osmosis (RO) water was measured in triplicate (n=3) and considered indicative of background noise of the sensor. An alteration to the method described above was made for phycocyanin measurement for field samples in 2017. To reduce the effect of light when samples were collected at midday, all field samples were kept in the dark following sample collection and sensor readings were undertaken back at the laboratory. This also allowed the optical face of the sensor to be checked for bubbles, which were removed prior to measurement.

Cyanobacteria enumeration

Cyanobacteria were identified using taxonomic keys (Baker & Fabbro, 2002; Komárek & Komárková, 2002) and enumerated on a Zeiss Axiovert 100 using the

Utermöhl method (Utermöhl, 1958). Dominant species were counted up to 100 units (cells, colonies, trichomes) for dense samples and using the average cell count of the first 20 colonies counted to calculate total cell concentration. In low and moderate density samples, the entire plate or a single transect were counted. Cell concentrations for each species were converted to biovolume using the Rotorua cyanobacterial biovolume database (Wood et al. 2008). These methods provide a cell concentration with approximately $\pm 20\%$ error (Hötzel & Croome, 1999).

2.3.4 Species dilution experiments

A species dilution experiment was set up to, 1) study the variability in phycocyanin readings at a known biovolume for each species, 2) investigate the minimum phycocyanin detectable by a sensor for each species, and 3) investigate non-linear relationships between phycocyanin and biovolume. The four cyanobacteria used in the experiment are commonly found in the Rotorua lakes. Cultures were sourced from the Cawthron Institute Culture Collection of Micro-algae (www.cultures.cawthron.org.nz; Rhodes et al., 2016) where they were maintained in MLA medium (Bolch & Blackburn, 1996) under a light regime of $90 \mu\text{mol m}^{-2} \text{s}^{-1}$ with a 12 h: 12 h, light: dark cycle at 18°C ($\pm 1^\circ\text{C}$).

The four species have wide variations in morphology and cell size (Figure 2, Table 3). They included *Dolichospermum lemmermannii* (CAWBG564; tangled coiled filaments), *Cuspidothrix issatschenkoi* (CAWBG595; bunches of straight filaments), *Microcystis aeruginosa* (CAWBG617; single cell and small colonies), and

Microcystis wesenbergii (CAWBG618; large cell, globular colonies). Colony sizes for both *M. wesenbergii* and *D. lemmermannii* varied from 20 μm to 200 μm in diameter.

Experimental design

The dilution experiment was carried out using 10-16-point dilutions depending on the species (Table 3). Blank MLA media readings (n=7) were taken with the sensor prior to the commencement of each species dilution sequence. The average MLA media blank was used to provide a background noise measurement for each culture. Phycocyanin was measured seven times at each dilution and the readings averaged and a standard deviation calculated.

A subsample (1 mL) was taken from the culture at each dilution and preserved with Lugol's iodine and stored in the dark until enumeration. These samples were then pipetted into 12-well plates (Costar, Corning, NY, USA), and allowed to settle for a least 72 h. Cells were enumerated by scanning 1-2 transects or 10 fields at 400-800X magnification using an inverted microscope (Olympus, CKX41). For each species, cell size was measured and converted to cell volume, and the biovolume was calculated for the highest cell concentration and biovolumes for the diluted samples calculated from each dilution factor. Each culture was diluted in sequence from the highest to the lowest concentration until the readings from the sensor no longer decreased linearly (Table 3).

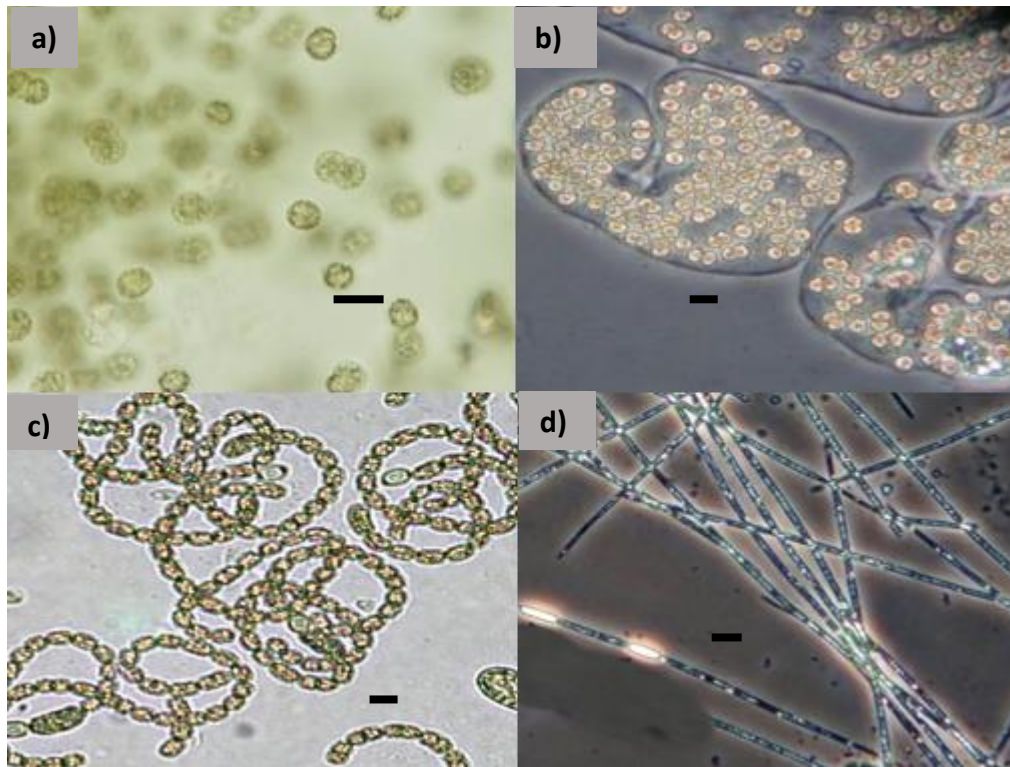


Figure 2. Morphology of cyanobacteria used in the species dilution experiment: a) *Microcystis aeruginosa* (CAWBG617), b) *Microcystis wesenbergii* (CAWBG618), c) *Dolichospermum lemmermannii* (CAWBG564), and d) *Cuspidothrix issatschenkoi* (CAWBG595). Scale bar =10 µm. Photos: S. Wood.

Table 3. The concentration ranges of biovolume, phycocyanin, number of dilutions, and morphology of the species used in the dilution experiments.

Species	Biovolume range (mm ³ L ⁻¹)	Phycocyanin range (µg L ⁻¹)	Number of dilutions	Morphology (shape)
<i>Microcystis aeruginosa</i>	0.3-85	38-524	10	Single cell, small colonies
<i>Microcystis wesenbergii</i>	0.2-60	90-1646	12	Large cells, globous colonies
<i>Dolichospermum lemmermannii</i>	0.2-18	33-371	16	Tangled, coiled filaments
<i>Cuspidothrix issatschenkoi</i>	0.5-48	30-295	10	Straight filaments, bunches

2.3.5 Data analysis

Field studies

Total biovolumes and total cyanobacteria species were calculated for all samples collected from each location and for both years. Dominant taxa were defined as species that had a total biovolume $>0.5 \text{ mm}^3 \text{ L}^{-1}$ from all samples for that location and were present across two or more locations.

Non-metric Multidimensional Scaling (nMDS) and Analysis of Similarity (ANOSIM) (PRIMER v.7, Primer-E Ltd, 2009) were used to assess changes in community composition in the lake and river samples for each year. Cyanobacterial species that occurred more than two times across all samples and had concentrations of $>2 \text{ cells mL}^{-1}$ were included in the analysis. Cell concentrations were $\log_{10}(x+1)$ transformed prior to the analysis. The nMDS analysis was conducted using a Bray-Curtis similarity matrix. The 2-dimensional representation plots for samples for each year show the similarity of sites to each other. The goodness of fit of the plot to the similarity matrix is specified by the stress value. A stress value of zero indicates a perfect fit.

An ANOSIM was conducted (999 permutations) on the Bray-Curtis similarity matrix for each location (lake or river) and for each year, to test if locations and years had community compositions that were significantly different from each other. This produced P-values (significance percentage level 0-100) and R values (0-1). An R-value near zero indicates the complete separation of species composition between locations and P indicates the level of significance of the separation.

Biovolume and phycocyanin values from 2016 (n=121) and 2017 (n=63) were $\log_{10}(x+1)$ transformed to improve normality and homogeneity. The relationship between $\log(\text{biovolume} + 1)$ and $\log(\text{phycocyanin} + 1)$ from the field data was analysed using linear regression with prediction intervals in the Statistica program (Version 13, Dell, Oklahoma, USA). Regressions were performed for each location in both years when sufficient data were available. Regression equations were used to calculate the predicted phycocyanin thresholds equal to the recreational biovolume thresholds of 0.5, 1.8, and 10 $\text{mm}^3 \text{L}^{-1}$.

Species dilution experiments

All data from the species dilution experiments for both biovolume (n=1) and phycocyanin were transformed using $\log(x+1)$. Averages and standard deviations were calculated for the phycocyanin (n=7) from each dilution for each species (Microsoft, Excel, 2016). At low concentrations in the dilution series, the phycocyanin values either remained constant or did not decrease linearly. The last dilutions of each series were determined to be the minimum values for detecting phycocyanin using the sensor (i.e., the minimum phycocyanin detection limit) and the associated biovolumes. Non-linear responses were investigated using the segmented regression and breakpoint analysis in the segmented package in R (Muggeo, 2008, 2017; R Development Core Team, 2016). Segmented regression is a regression model technique that estimates any segmented relationships, where the segment divide is the breakpoint, i.e., where the regression slope changes. Breakpoints in phycocyanin response were tested for statistical significance using the (pseudo) Score statistic test (Muggeo, 2016). Significance tests for the

breakpoint were carried out at 95% levels of confidence and were two-tailed. The null hypothesis (H_0) was tested where there is no difference in the segmented slopes and therefore no significant breakpoint in relationships in the linear model.

2.4 Results

2.4.1 Field studies

Cyanobacteria biovolumes and species in the lakes

Total biovolumes and total cyanobacterial species for each location (five lakes and one river) over each study period were used to compare cyanobacteria across years and location (Table 4). In 2016, an average of 17 cyanobacterial species were identified across all locations (five lakes and one river) with an average total biovolume of $24.1 \text{ mm}^3 \text{ L}^{-1}$ (Table 4). In 2016, Lake Rotoehu had the highest total biovolume of $77.7 \text{ mm}^3 \text{ L}^{-1}$ with 23 different species detected across the study period (Table 4). Lake Tarawera had the lowest total biovolume in 2016 ($0.3 \text{ mm}^3 \text{ L}^{-1}$) and only six cyanobacteria species were identified (Table 4). In 2016, the dominant species varied between lakes (Figure 3a). *Dolichospermum* spp. were dominant in lakes Rotoehu (40%), Okaro (80%) and Tarawera (90%), *Synechococcus* sp. in Lake Rotoiti (45%) and the Kaituna River (65%), and *M. wesenbergii* in lakes Rotorua (40%) and Rotoehu (40%) (Figure 3a).

In 2017, an average of 14 cyanobacterial species were identified across all locations with an average total biovolume of $66.2 \text{ mm}^3 \text{ L}^{-1}$ (Table 4). The total biovolume for each location (five lakes and one river) in 2017 showed that three of the six lakes had higher total biovolumes than in 2016 (Table 4). Average biovolumes in lakes Okaro and Rotoehu were three to four times higher than in

2016, respectively (Table 4). *Microcystis aeruginosa* was dominant (70%) in both Lake Rotoehu and Okaro (Figure 3b). Total biovolume for Lake Tarawera was approximately ninety-fold higher in 2017 than 2016 (Table 4), due to a large contribution of *Dolichospermum* spp. in 2017, which accounted for 90% of the total biovolume (Figure 3b). *Synechococcus* sp. were dominant in lakes Rotorua (50%) and Rotoiti (30%). *Dolichospermum* sp. was dominant in Lake Rotoiti (50%) and was also a major contributor (10-30%) of cyanobacteria species in lakes Rotoehu, Okaro, Rotorua and the Kaituna River (Figure 3b).

Table 4. Total cyanobacteria species and total biovolume for each lake or river in 2016 and 2017, the sample size for each location (lake or river) and total sample size (n) and the average across all location (five lakes and one river) in 2016 (16 sites) and 2017 (10 sites).

Location Lake/river	Total cyanobacteria species (2016:2017)	Total biovolume 2016:2017 (mm ³ L ⁻¹)	n (2016:2017)
Kaituna River	16:18	4.0:0.1	13:16
Lake Okaro	12:8	20.4:69.4	16:16
Lake Rotoehu	23:12	77.7:305.7	38:33
Lake Rotoiti	27:28	32.9:11.9	63:58
Lake Rotorua	22:13	9.4:0.3	46:43
Lake Tarawera	6:7	0.3:9.9	4:13
Average across all locations (2016:2017)	17:14	24.1:66.2	180:179

2.4.2 Multivariate analysis of cyanobacteria composition

The nMDS plots of the cyanobacterial community indicated a gradient with trophic status (Figure 4). Eutrophic waters were distributed to the right side of the ordination and mesotrophic waters to the left. For sites that were categorized as mesotrophic/oligotrophic, some samples occurred on the eutrophic side of the ordination, e.g., Boat Shed Bay, Hot Water Beach and Stoney Bay (Lake Tarawera). The 2-dimensional stress values of 0.31 in 2016 (n= 180) and 0.28 in 2017 (n=179)

indicate that the nMDS has a moderate goodness of fit and the data are informative for the sample size that was analysed (Holland, 2008; Figure 4).

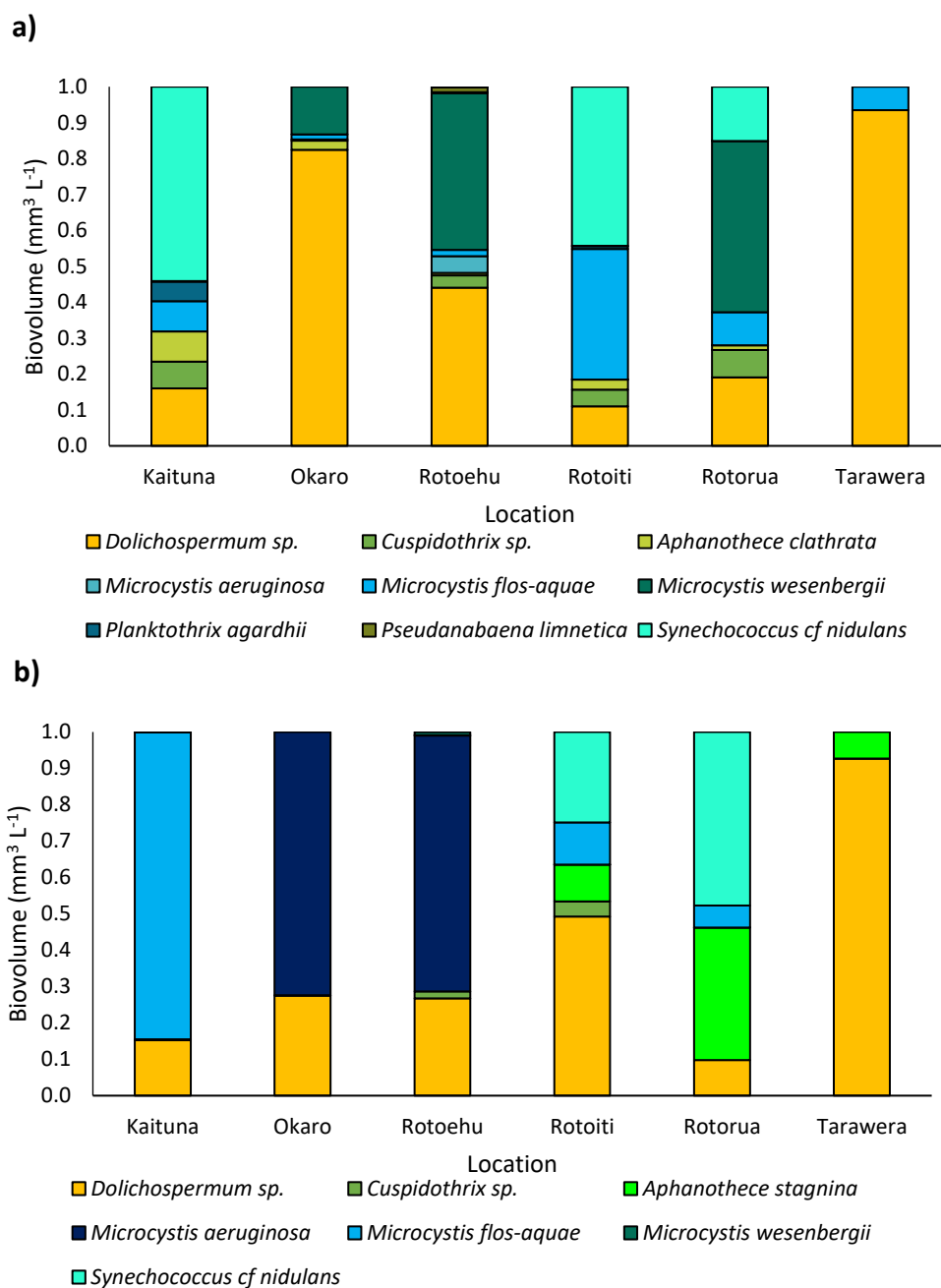


Figure 3. Proportion of biovolume for the dominant cyanobacteria species found across all locations in (a) 2016 and (b) 2017.

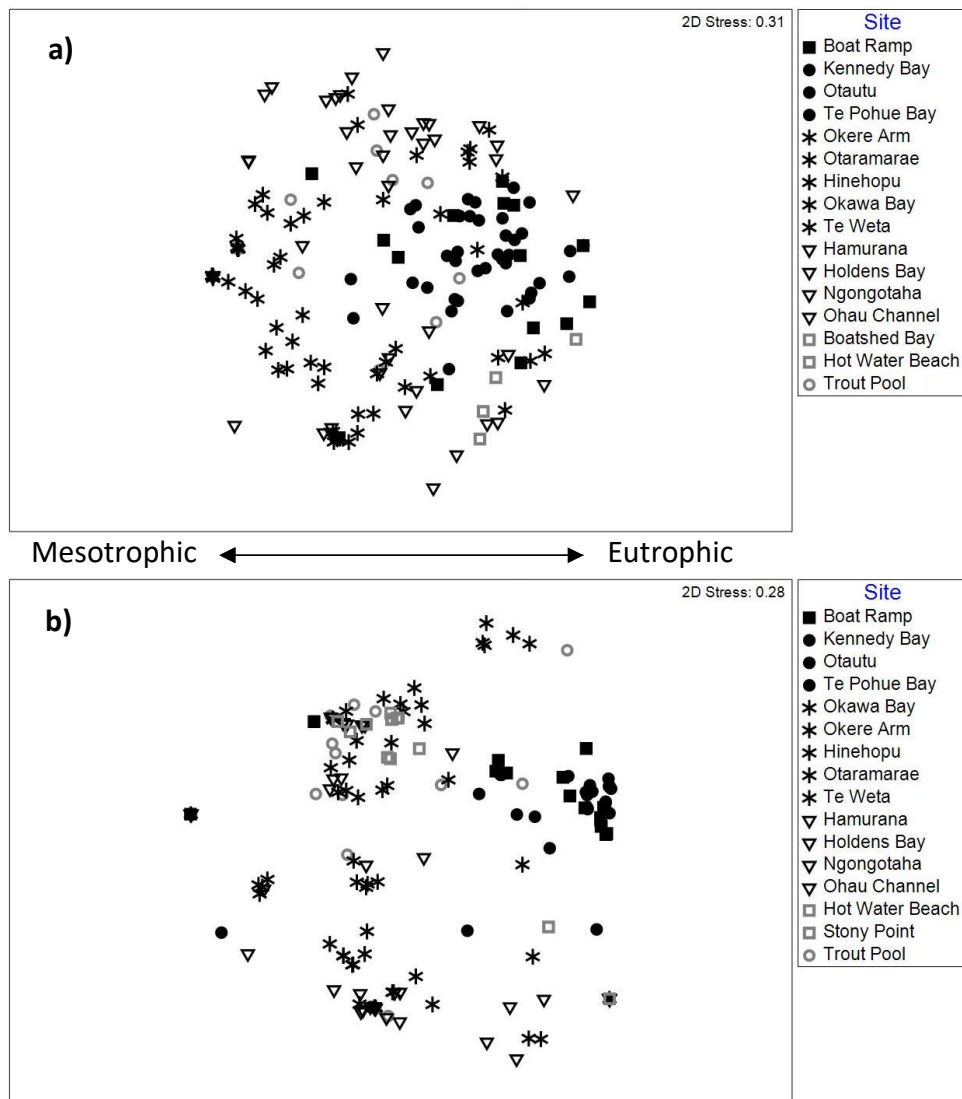


Figure 4. Non-metric Multidimensional Scaling (nMDS) plot of cyanobacterial communities on each sampling occasion at 16 sites in the five lakes and one river (Table 1) for (a) 2016 and (b) 2017. Solid square is the Lake Okaro site, solid circles are sites of Lake Rotoehu, stars are sites of Lake Rotoiti, open triangles are sites of Lake Rotorua, open squares are sites of Lake Tarawera, and the open circle is the Kaituna River site.

Multivariate analyses on cyanobacterial community composition across locations (all sites within the same lake combined) in 2016 indicated there was a significant difference between the locations (five lakes and one river) (ANOSIM; R-value=0.25, $P=0.01$). Pair-wise comparisons for 2016 showed that Lake Rotoehu was significantly different ($P<0.01$) from all other locations. Lake Okaro was significantly different ($P<0.01$) from lakes Rotoehu and Rotoiti in 2016 (Appendix

1). In 2017 there was a significant difference between locations (ANOSIM; R-value=0.24, P=0.01). Pair-wise comparisons for locations showed that Lake Rotoehu and Lake Okaro were significantly different ($P<0.01$) from all other locations in 2017 (Appendix 2).

2.4.3 Phycocyanin relationships with biovolume

There was a weak but significant relationship ($R^2=0.43$, $P<0.001$) between sensor phycocyanin (hereafter phycocyanin) and biovolume for pooled data from the 16 sites constituting five lakes and one river in 2016 (Table 5). Seventy-seven percent of field samples collected in the 2016 summer were below the amber alert threshold of $1.8 \text{ mm}^3 \text{ L}^{-1}$ (Figure 5). In 2017 there was a significant relationship ($R^2=0.63$, $P<0.001$) between phycocyanin and biovolume for pooled data from the 16 sites constituting five lakes and one river (Table 5). Sixty-seven percent of biovolume samples were above the red action threshold of $1.8 \text{ mm}^3 \text{ L}^{-1}$. Thirty-three percent of biovolume samples were below the $1.8 \text{ mm}^3 \text{ L}^{-1}$ threshold (Figure 6).

2.4.4 Relationships for phycocyanin to biovolume for different locations

In 2016, lakes Okaro ($R^2=0.33$), Rotoiti ($R^2=0.14$), and Rotorua ($R^2=0.06$) had weak, non-significant ($P>0.05$) relationships between phycocyanin and biovolume, Lake Rotoehu had a significant ($R^2=0.48$, $P<0.001$) relationship (Table 5). The Kaituna River and Lake Tarawera were data deficient ($n<10$). In 2017, Lake Okaro had a weak ($R^2=0.16$, $P=0.22$) relationship of phycocyanin to biovolume, lakes Rotoiti ($R^2=0.45$, $P<0.05$) and Rotoehu ($R^2=0.48$) had a highly significant ($P<0.001$)

relationship (Table 5). Lake Rotorua, Tarawera, and the Kaituna River were all data deficient in this year ($n < 10$). For the combined (2016 and 2017) data, Lake Okaro had a weak ($R^2 = 0.22$, $P < 0.05$) relationship of phycocyanin to biovolume, lakes Rotoiti ($R^2 = 0.24$) and Rotoehu ($R^2 = 0.66$) showed highly significant relationships ($P < 0.001$) (Table 5), and the relationship for Lake Rotorua was the weakest ($R^2 = 0.05$) and was not significant ($P > 0.05$).

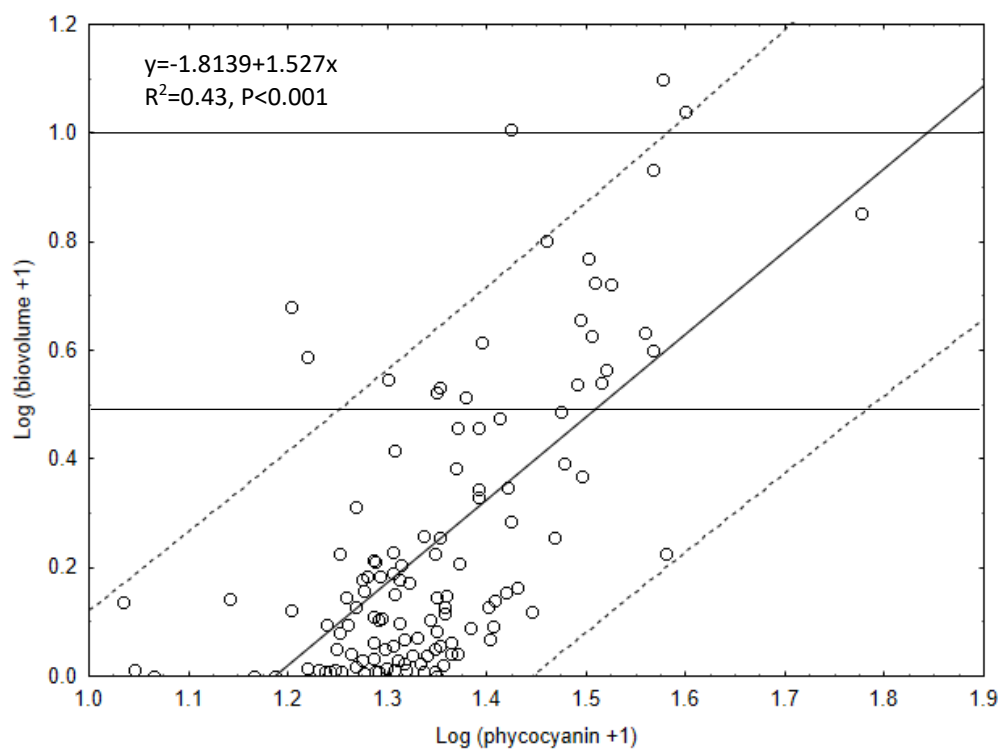


Figure 5. Relationship between log (phycocyanin +1) and log (biovolume +1) for all sites sampled from January to April 2016, $n = 121$. Phycocyanin was measured in units of $\mu\text{g L}^{-1}$ (averages \pm SD, $n = 5$) from the sensor and biovolume in $\text{mm}^3 \text{L}^{-1}$. The regression (solid line) and the 95% prediction intervals (dashed line) for the regression line are shown. Horizontal lines indicate, bottom up, the red action threshold in the New Zealand guidelines for recreational contact, with potentially toxic species $> 1.8 \text{ mm}^3 \text{L}^{-1}$ and total cyanobacteria threshold $> 10 \text{ mm}^3 \text{L}^{-1}$.

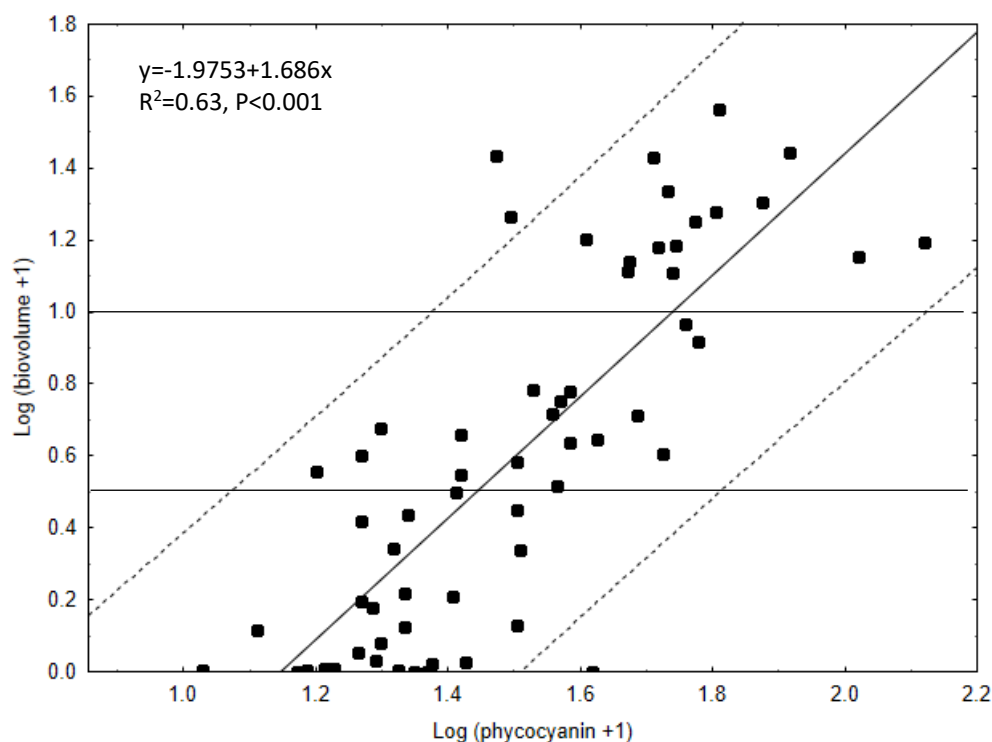


Figure 6. Relationship between log (phycocyanin +1) and log (biovolume +1) for sites sampled from January to March 2017, $n = 63$. Phycocyanin was measured in units of $\mu\text{g L}^{-1}$ (averages \pm SD, $n=5$) from the sensor and biovolume $\text{mm}^3 \text{L}^{-1}$. The regression (solid line) and the 95% prediction intervals (dashed lines) for the regression line are shown. Horizontal lines indicate, bottom up, the red action threshold in the New Zealand guidelines for recreational contact with potentially toxic species $>1.8 \text{ mm}^3 \text{L}^{-1}$ and total cyanobacteria threshold $>10 \text{ mm}^3 \text{L}^{-1}$.

2.4.5 Recreational monitoring threshold predictions for phycocyanin

The biovolume threshold values 0.5, 1.8, and $10 \text{ mm}^3 \text{L}^{-1}$ were used in the regression equations in Table 5 to predict the corresponding phycocyanin values as phycocyanin threshold values. To simplify the reporting of phycocyanin, thresholds from Table 5 for separate lakes, combined years for separate lakes, and separate years with all locations combined. The predicted phycocyanin thresholds are presented against the biovolume thresholds as green: Green surveillance mode ($<0.5 \text{ mm}^3 \text{L}^{-1}$), amber: Amber alert level ($0.5 < 1.8 \text{ mm}^3 \text{L}^{-1}$), and red: Red action mode (>1.8 or $10 \text{ mm}^3 \text{L}^{-1}$).

In 2016, predicted phycocyanin thresholds for Lake Okaro were 17, 23, and 46 $\mu\text{g L}^{-1}$ for green, amber, and red, respectively (Table 5). Lake Rotoehu had predicted phycocyanin thresholds of 18, 26, and 55 $\mu\text{g L}^{-1}$ for green, amber, and red. Lake Rotoiti had 19, 31, and 86 $\mu\text{g L}^{-1}$ for green, amber, and red. The relationship was too weak for prediction in Lake Rotorua (Table 5). In 2017, Lake Okaro had predicted phycocyanin thresholds of 6, 13, and 75 $\mu\text{g L}^{-1}$ for green, amber, and red. Lake Rotoehu had 11, 18, and 51 $\mu\text{g L}^{-1}$ and Lake Rotoiti had 21, 38, and 138 $\mu\text{g L}^{-1}$ for green, amber, and red (Table 5).

Combined data for both 2016 and 2017 produced predicted phycocyanin thresholds for green, amber, and red of 11, 19, and 68 $\mu\text{g L}^{-1}$ for Lake Okaro, 16, 24, and 54 $\mu\text{g L}^{-1}$ for Lake Rotoehu, and 20, 35, and 122 $\mu\text{g L}^{-1}$ for Lake Rotoiti. The relationship was too weak for prediction in Lake Rotorua (Table 5). Data for each year showed, for 2016, the predicted phycocyanin thresholds for green, amber, and red were 19, 29, and 73 $\mu\text{g L}^{-1}$ and for 2017, they were 18, 26, and 60 $\mu\text{g L}^{-1}$.

Table 5. Relationship between log (phycocyanin +1) and log (biovolume +1), the percentage of variation explained (R^2) value and significance value (P), sample size of for the sampling locations over two sampling years, combined years for each location and across all locations. Predicted phycocyanin ($\mu\text{g L}^{-1}$) calculated using the regression equations: a is the slope, x is the biovolume and b is the intercept at the three biovolume threshold values. Bold values are significant ($P < 0.05$). The Kaituna River and Lake Tarawera were data deficient in both years ($n < 10$) and Lake Rotorua was data deficient in 2017. NA; not applicable due to the weak relationship.

Location	n	a	b	R^2	P- value	Predicted phycocyanin ($\mu\text{g L}^{-1}$)		
						0.5 $\text{mm}^3 \text{L}^{-1}$	1.8 $\text{mm}^3 \text{L}^{-1}$	10 $\text{mm}^3 \text{L}^{-1}$
2016								
Okaro	10	2.0033	-2.3146	0.33	0.08	17	23	46
Rotoehu	22	1.8364	-2.1674	0.48	0.001	18	26	55
Rotoiti	40	1.3649	-1.6058	0.14	0.02	19	31	86
Rotorua	36	0.301	-0.2982	0.06	0.15	NA	NA	NA
2017								
Okaro	11	0.8075	-0.481	0.16	0.22	6	13	75
Rotoehu	24	1.3859	-1.3374	0.48	0.001	11	18	51
Rotoiti	11	1.0677	-1.2488	0.45	0.02	21	38	138
Combined 2016 and 2017								
Okaro	21	1.1228	-1.0227	0.22	0.03	11	19	68
Rotoehu	46	1.7359	-1.9750	0.66	0.001	16	24	54
Rotoiti	51	1.1111	-1.2805	0.24	0.001	20	35	122
Rotorua	41	0.2596	-0.2596	0.05	0.15	NA	NA	NA
Combined data across all locations								
2016	121	1.527	-1.8139	0.43	0.001	19	29	73
2017	63	1.686	-1.9753	0.63	0.001	18	26	60

2.4.6 Dilution series experiments for four species

The dilution experiments examined three different evaluations for the relationship between phycocyanin and biovolume in four cultured species. The first analysis shows the variability in phycocyanin readings for each species, the second evaluation was made from observed data and gave the minimum phycocyanin detectable from the sensor for each species, and the last result demonstrated that non-linear relationships occur between phycocyanin and low biovolumes.

Species phycocyanin variability

Sensor replicate readings (n=7) of phycocyanin were taken for each species and at each dilution (Figure 7). The standard deviation of individual readings for the colonial species *M. wesenbergii*, *D. lemmermannii*, and *C. issatschenkoi* was markedly higher than the single-celled *M. aeruginosa* (Figure 7). *Microcystis wesenbergii* had the largest average phycocyanin standard deviation across the dilutions of $240 \mu\text{g L}^{-1}$. *Dolichospermum lemmermannii* had $8.2 \mu\text{g L}^{-1}$, *C. issatschenkoi* had $2.4 \mu\text{g L}^{-1}$ and *M. aeruginosa* had $0.68 \mu\text{g L}^{-1}$ (Figure 7).

Minimum phycocyanin detection limits

Minimum phycocyanin from the last dilution in the series was defined as the point where sensor phycocyanin readings were close to but still higher than the MLA blank. The minimum (\pm S.D.) phycocyanin detection limits were $90 \pm 135 \mu\text{g L}^{-1}$ for *M. wesenbergii*, $38 \pm 0.3 \mu\text{g L}^{-1}$ for *M. aeruginosa*, $34 \pm 2.3 \mu\text{g L}^{-1}$ for *D. lemmermannii* and $30 \pm 0.3 \mu\text{g L}^{-1}$ for *C. issatschenkoi* (Table 6).

Table 6. Minimum phycocyanin detection limits ($\mu\text{g L}^{-1}$) (average \pm SD, $n=7$) and corresponding biovolume ($\text{mm}^3 \text{L}^{-1}$) using dilution series and species cell volumes (μm^3) from measured dimensions for the four-cultured species, *Microcystis wesenbergii*, *Microcystis aeruginosa*, *Dolichospermum lemmermannii*, and *Cuspidothrix issastachenkoi*.

Species	Phycocyanin \pm SD ($\mu\text{g L}^{-1}$)	Biovolume ($\text{mm}^3 \text{L}^{-1}$)	Cell volume (μm^3)
<i>Microcystis wesenbergii</i>	90 \pm 135	0.2	160
<i>Microcystis aeruginosa</i>	38 \pm 0.3	0.3	36
<i>Dolichospermum lemmermannii</i>	34 \pm 2.3	0.2	120
<i>Cuspidothrix issastachenkoi</i>	30 \pm 0.3	0.5	56

Segmented regression/Breakpoint analysis

Segmented regression showed that biovolume was significantly related to phycocyanin for all four species ($R^2=0.83-0.99$, $P<0.001$; Table 7, Figure 8). Breakpoint models for each species showed a change in the slope for each species over the dilution sequence (Figure 8). The slopes for phycocyanin to biovolume before the breakpoint ranged from 1.3 to 2.2 $\text{mm}^3 \mu\text{g}^{-1}$ at the higher concentrations, and slopes ranged from 0.1 to 1.3 $\text{mm}^3 \mu\text{g}^{-1}$ at the weakest dilutions, indicating inconsistency in sensor response between points above and below the breakpoint. The species breakpoint estimates were statistically significant (pscore test, $P<0.05$) for *M. wesenbergii*, *D. lemmermannii*, and *C. issastachenkoi* but not *M. aeruginosa* (Table 7 and Figure 8). For interpretation, the breakpoint estimates were converted back to phycocyanin ($\mu\text{g L}^{-1}$) (Table 7). The phycocyanin value corresponding to the breakpoint was 48 $\mu\text{g L}^{-1}$ for *C. issastachenkoi*, 55 $\mu\text{g L}^{-1}$ for *D. lemmermannii*, 181 $\mu\text{g L}^{-1}$ for *M. wesenbergii*, and 106 $\mu\text{g L}^{-1}$ for *M. aeruginosa*. Below the breakpoint values of phycocyanin at the biovolume threshold of 1.8 $\text{mm}^3 \text{L}^{-1}$ would not be accurately predicted from phycocyanin for both *M. aeruginosa* and *C. issastachenkoi* (Figure 8).

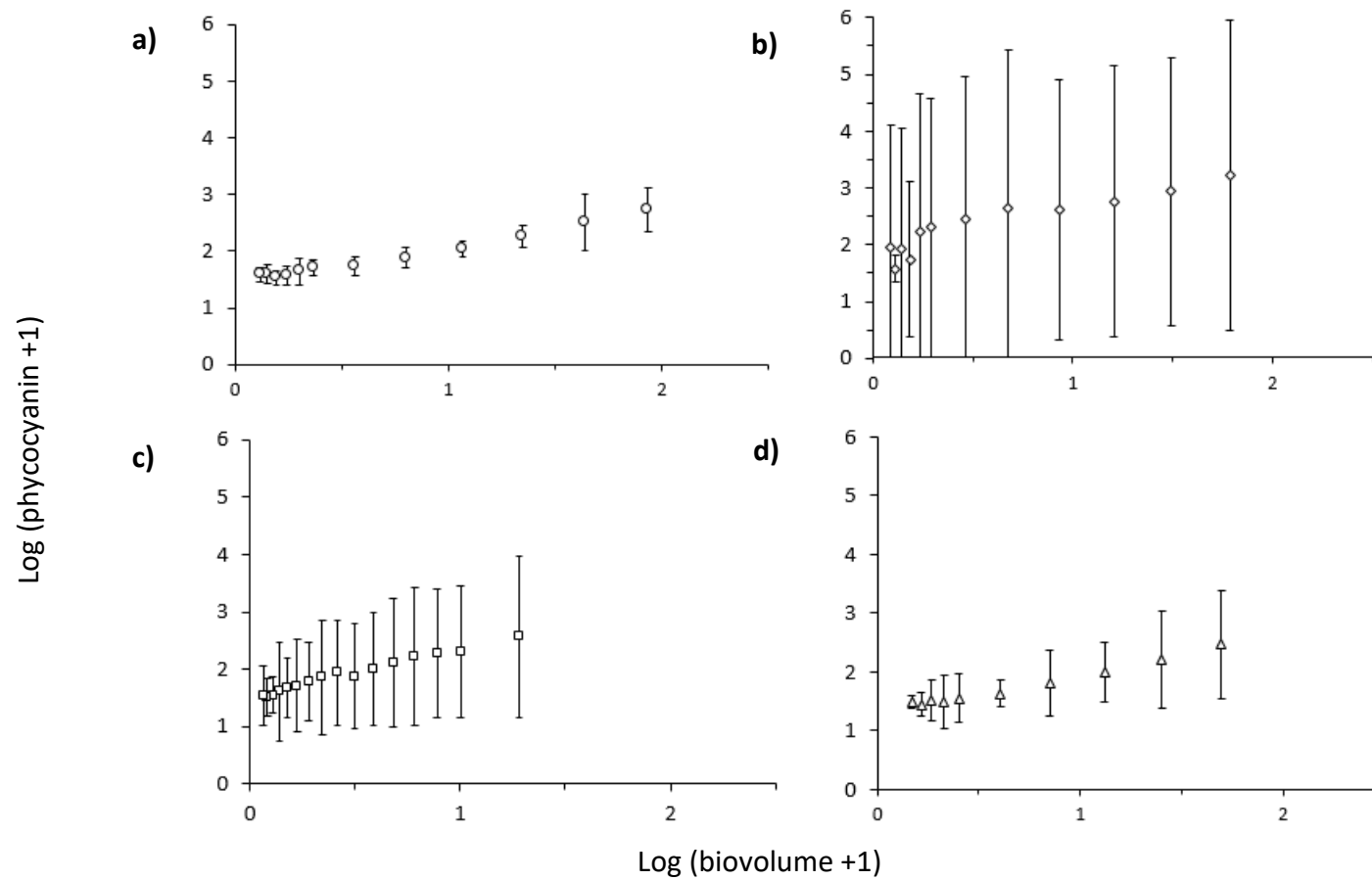


Figure 7. Log (biovolume +1) and log (phycocyanin +1) values for species dilutions. Phycocyanin was measured in $\mu\text{g L}^{-1}$ (averages $\pm\text{SD}$, $n=7$) from the sensor and biovolume in $\text{mm}^3 \text{L}^{-1}$. a) *Microcystis aeruginosa*, b) *Microcystis wesenbergii*, c) *Dolichospermum lemmermannii*, and d) *Cuspidothrix issatschenkoi*

Table 7. Segmented regression model regression coefficients and significance values, $\log(\text{phycocyanin}+1)$, breakpoint estimates (standard error), breakpoint values for phycocyanin ($\mu\text{g L}^{-1}$) and p score statistical test for significance of breakpoint.

Species	R ²	P-value	Breakpoint estimate (SE) $\log(\text{phycocyanin}+1)$	Breakpoint phycocyanin ($\mu\text{g L}^{-1}$)	p score
<i>Microcystis aeruginosa</i>	0.98	<0.001	2.03 (0.21)	106	>0.05
<i>Microcystis wesenbergii</i>	0.83	<0.001	2.26 (0.08)	181	<0.05
<i>Dolichospermum lemmermannii</i>	0.98	<0.001	1.75 (0.08)	55	<0.05
<i>Cuspidothrix issastachenkoi</i>	0.99	<0.001	1.68 (0.96)	48	<0.05

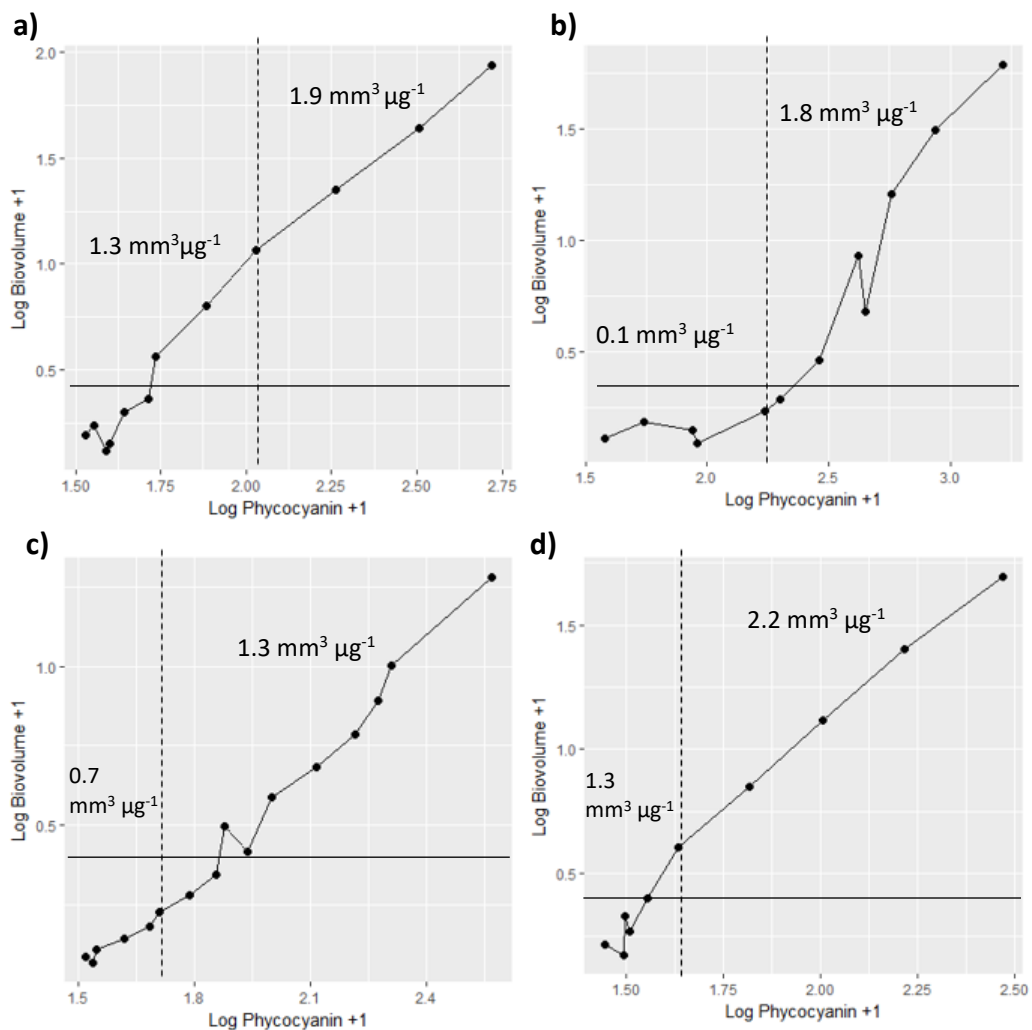


Figure 8. Breakpoint models for prediction of biovolume log (biovolume +1) from phycocyanin log (phycocyanin +1) using species dilutions for a) *Microcystis aeruginosa*, b) *Microcystis wesenbergii*, c) *Dolichospermum lemmermannii*, and d) *Cuspidothrix issastachenkoi*. Phycocyanin in units of $\mu\text{g L}^{-1}$ (averages $\pm\text{SD}$, $n=7$) from the sensor and biovolume in $\text{mm}^3 \text{L}^{-1}$. Dashed line is segmented regression breakpoint estimate for each species (see Table 6 for breakpoint estimate values). Numbers on graph are slopes ($\text{mm}^3 \mu\text{g}^{-1}$) above and below the breakpoints. Solid line is biovolume 1.8 $\text{mm}^3 \text{L}^{-1}$.

2.5 Discussion

2.5.1 Relationship of phycocyanin to biovolume in the field

In 2017, the phycocyanin relationship to biovolume across all sites ($R^2=0.63$) was stronger than in 2016 ($R^2=0.43$). Biovolumes were higher in 2017. Kong et al. (2014) found a strong relationship ($R^2=0.77$) between phycocyanin and biovolume when cyanobacterial biovolumes were high ($\geq 11 \text{ mm}^3 \text{ L}^{-1}$) and comprised of mixed species, but more so when only a single species was present ($R^2=0.89$) at high biovolumes ($9\text{-}11 \text{ mm}^3 \text{ L}^{-1}$) in the Macau Storage Reservoir in China. For three eutrophic ponds in Australia, the relationships between phycocyanin and biovolume were strongest ($R^2>0.7$) in ponds containing species with large cell volumes such as *M. wesenbergii* and *M. aeruginosa* (Bowling et al. 2016). Brient et al. (2008) also reported high R^2 values ($R^2=0.78$) for phycocyanin and biovolume in field samples containing high concentrations ($>300,000 \text{ cells mL}^{-1}$) of mixed species including *Cuspidothrix gracile*, *Pseudanabaena limnetica*, *Plankthotrix agardhii*, and *Dolichospermum spiroides*. In contrast, other studies such as McQuaid et al. (2011) have found only moderate relationships ($R^2=0.46$) between phycocyanin and biovolume in field samples dominated by *Microcystis* sp. Only three samples in the study by McQuaid et al. (2011) had biovolume $>10 \text{ mm}^3 \text{ L}^{-1}$. From these studies, it appears that samples with high biovolume ($>10 \text{ mm}^3 \text{ L}^{-1}$) and/or dominance of large-celled cyanobacteria species improve the relationship between phycocyanin and biovolume. Many studies (e.g., Ahn et al. 2007; Gregor et al. 2007; McQuaid et al. 2011; Seppälä et al. 2007) have found only moderate relationships between cyanobacteria biomass and phycocyanin sensors and

propose several variables responsible for the variability. Key factors affecting the variability that are relevant to the current dataset are discussed below.

Community composition

Community composition varied between years and lakes. In 2016, *M. wesenbergii*, and *Dolichospermum* spp. were dominant across several lakes (Rotorua, Okaro, and Rotorua). The number of species present was higher in 2016, which was likely a result of the changeable weather patterns, possibly due to strong El Niño (NIWA, 2017) which induced frequent mixing of surface waters. The effect of mixing was noted by Kong et al. (2014), who suggested that it increased diversity in their samples and reduced correlations between phycocyanin and biovolume. Such changes in the cyanobacterial community composition spatially and temporally could contribute to the variability in relationships of phycocyanin to biovolume. The two eutrophic lakes, Okaro and Rotorua, had similar community composition in 2017 compared to 2016, due to the abundance of *M. aeruginosa*. Biovolumes exceeded red action mode of $>1.8 \text{ mm}^3 \text{ L}^{-1}$ approximately seven times in Lake Okaro and 17 times in Lake Rotorua. These elevated biovolumes from Lake Rotorua may have enhanced the 2017 relationship between phycocyanin and biovolume compared with that in 2016.

Sampling errors

There can be large errors associated with taking samples from lakes (Hawkins et al. 2005). This error is due partly to the number of times the original lake water is subsampled but may also be associated with spatial variability of cyanobacteria in

the water, particularly in poorly mixed waters. In 2016 the phycocyanin was measured from a 1 L subsample of 5 L of lake water sample, from which a 100 mL subsample was taken for biovolume analysis. In 2017, the 100 mL subsample (instead of the 1 L subsample) was used for both phycocyanin measurements and biovolume assessments. This reduction in subsampling may be one factor contributing to the stronger relationships between phycocyanin and biovolume in 2017.

Counting errors

Cyanobacterial identification, enumeration, and estimates of biovolume contain a degree of error (Hawkins et al. 2005). Hawkins et al. (2005) note that there can be up to 20% error in biovolume estimates. These counting errors can be due to either low/high density coupled with high diversity (a mixture of small and large species), as well as fatigue in the observer. The non-random distribution of species in the settling chambers requires more scanning and can also contribute to observer fatigue (Hötzel & Croome, 1999). Counting errors would have influenced the relationships between phycocyanin and biovolume. The errors might have been greater in 2016 due to the high diversity when many species were identified and counted. Compared to 2017 when samples had high density of cells within large colonies of *M. aeruginosa* thus requiring high levels of concentration for counting.

Effect of pico-cyanobacteria

In this study, the contribution of pico-cyanobacteria to total biovolume across all sites was 19% in 2016 and 6% in 2017. *Synechococcus* sp. dominated in both years in Lake Rotoiti. This lake showed a poor relationship between biovolume and phycocyanin ($R^2=0.14$) in 2016 and was data deficient in 2017. Bowling et al. (2016) found a poor relationship between biovolume and phycocyanin ($R^2=0.19$) which was attributed to low phycocyanin yield per pico-cyanobacteria cell and high error in the counting of small species such as *Aphanocapsa* sp., *Cyanodictyon* sp., *Gloeotheca* sp. and *Merismopedia tenuissima*. In contrast, Kong et al. (2014), found a strong relationship ($R^2=0.89$) between phycocyanin and biovolume for high biomass ($>11 \text{ mm}^3 \text{ L}^{-1}$) of pico-cyanobacteria, which was attributed to the dominance of *Pseudanabaena* sp. and lake stability (Kong et al. 2014). The common occurrence but low overall biomass of pico-cyanobacteria in Lake Rotoiti, in 2016, may have weakened relationships between phycocyanin and biovolume.

Colonial versus filamentous species

Poor phycocyanin to biovolume relationships have been observed for both colonial and filamentous cyanobacteria (Chang et al. 2012; Hodges, 2016). Hodges (2016) found that filamentous species *Dolichospermum* and *Nodularia*, with their complex morphologies, were not well quantified by phycocyanin sensors. Large colonies have a smaller surface area to volume ratio than single cells and therefore there is a higher chance of phycocyanin not fluorescing in central areas of colonies. In 2016 there were two taxa that might have caused phycocyanin to be

underestimated. These were filamentous and coiled *Dolichospermum* species and large colonial *M. wesenbergii*, which were found in three of five lakes.

Effect of other algal groups

The study lakes contain diverse phytoplankton communities (Paul et al. 2012). In 2016, diatoms (Bacillariophyceae) were common at some sites (personal observation). Paul et al. (2012) showed that mesotrophic and oligotrophic lakes such as Tarawera and Rotoiti, and eutrophic lakes such as Rotorua, had a high abundance of diatoms. Beutler et al. (2002) demonstrated that light emitted from different algal groups could overlap with the phycocyanin signature from cyanobacteria and that high densities of non-target species could reduce the ability to detect/quantify cyanobacteria. This may have occurred during the 2016 field sampling of mesotrophic sites (lakes Rotoiti and Rotorua), where historically diatoms have been present at higher densities than cyanobacteria (Wilding, 2000; Scholes et al. 2010).

Effect of light

Cyanobacteria can adjust photosynthetic activity, pigment content, and photosynthetic energy transfer systems in response to changes in light intensity (Loftus & Seliger, 1975). At high light intensities, there is a decrease in fluorescence emission wavelengths and an increase in alternate energy transfer systems (Loftus & Seliger, 1975). Sampling times in the current study were between 10 am and 4 pm in both years. In an attempt to minimise the effect of light, phycocyanin measurements were taken in a blacked out beaker onsite in 2016. This blocked

the incident light while taking measurements, but it did not account for prior light history, with potential for high light to affect the photosynthetic energy transfer system and reduce fluorescence (Dubinsky & Stambler, 2009). Changes to this beaker method were implemented in 2017. Samples were kept in the dark until the end of sampling day. The samples were taken back to the laboratory for measurement of phycocyanin. This may have reduced the effect of high light intensity and previous light history on phycocyanin fluorescence. Contrasting to this theory, studies have been undertaken with sensors to test prior light exposure, finding no such interference in phycocyanin readings caused by prior light history (Brient et al. 2008; Zamyadi et al. 2016).

Effect of temperature

Several studies have shown that increased temperature decreases fluorescence. Kasinak et al. (2014) measured higher phycocyanin in pond samples extracted at 4°C compared to samples extracted at 21°C. Hodges (2016) also had similar findings, with phycocyanin decreasing as temperature increased above 4°C. The sampling period in this study in 2016 and 2017 spanned months from January to March/April, respectively, over which time there can be at least 3°C change in surface temperature in the Rotorua lakes (Scholes & Hamill, 2016). The changes in temperature are likely to have induced only small variations in phycocyanin and therefore not have markedly influenced the phycocyanin to biovolume relationships.

Extracellular phycocyanin

Phycocyanin readings may be affected by cell lysis, which releases pigment from cells (Zamyadi et al. 2016). Hodges (2016) found extracellular phycocyanin levels were 20% higher in field samples that contained high biomass of *Dolichospermum* sp. Brient et al. (2008) also reported a change in sensor signals due to extracellular phycocyanin. No attempt was made to quantify extracellular phycocyanin in the current study.

Bubble interference

The weaker relationships between phycocyanin and biovolume in 2016 may also have been due to bubbles on the optical face of the sensor. The photodiode that reads the emission wavelength is sensitive to air bubbles that may become trapped on the optical face when submerged in a sample (Turner Designs, 2015). This would change how the emission wavelength refracts at the photodiode interface. In the current study, when bubbles were on the optical face in blank Milli-Q water the sensor readings would indicate that there was phycocyanin present (i.e., a false positive; phycocyanin present when it is not). This was noted from repeating many blank readings in a controlled environment, but no statistical tests were carried out to quantify this error. To avoid this interference in 2017, the sensor was checked for bubbles after being submerged, but not in 2016, which may have resulted in greater variability of phycocyanin measurements in 2016.

2.5.2 Three assessments of phycocyanin for the species dilution experiments

Variability of phycocyanin in different cyanobacteria species

In the species dilution experiment, there was high variability of phycocyanin measured by the sensor from two cyanobacteria species (*D. lemmermannii* and *M. wesenbergii*). These species both have large cell volumes (120 and 160 μm^3 , respectively) and complex colonial morphology. Effect of colony morphology on phycocyanin has been investigated by Chang et al. (2012) and Hodges (2016) who found that phycocyanin derived from sensors may be underestimated for colonial species such as *Microcystis* and *Dolichospermum*. Chang et al. (2012) disaggregated *Microcystis* colonies of size up to 120 μm^3 and found a YSI 660 sonde (output in cells mL^{-1}) underestimated cell concentrations in the colonial state by up to 88%. Hodges (2016) found a 10% increase in phycocyanin when colony sizes $>250 \mu\text{m}^3$ were disaggregated. Phycocyanin may be in error by up to 40% when there are high densities of *Planktothrix rubescens* (Leboulanger et al. 2002). These studies confirm that phycocyanin detected by sensors is affected by the morphology of the cyanobacteria, with colonies or filaments leading to underestimates of phycocyanin.

Phycocyanin at low biovolumes for four species

There was a strong relationship between $\log(\text{phycocyanin}+1)$ and $\log(\text{biovolume}+1)$ in the dilution experiments for the four cultures. However, segmented regression analysis allowed a breakpoint to be established in the relationship of $\log(\text{phycocyanin}+1)$ and $\log(\text{biovolume}+1)$. The limitation of using this type of analysis is that the breakpoint must first be estimated from the

independent variable and put into the segmentation model (Muggeo, 2008). In an attempt to reduce this bias, a range of breakpoint estimates was tested between the upper and lower quartiles of phycocyanin for each species (Muggeo, 2008). Nevertheless, breakpoint values of phycocyanin showed that the biovolume threshold of $1.8 \text{ mm}^3 \text{ L}^{-1}$ may not be predictable from phycocyanin for both *M. aeruginosa* and *C. issastachenkoi* (Figure 8). This may be due to different phycocyanin quotas as a function of cell size. *Dolichospermum lemmermannii* and *M. wesenbergii* both have the largest cell sizes of the four species.

The analysis also identified that there were significant inflections in the response of the sensor phycocyanin to low biovolumes in the three colonial species, *C. issatschenkoi*, *D. lemmermannii* and *M. wesenbergii*. This suggests that below these inflection points there would be higher errors which would reduce predictive power from the relationship between phycocyanin and biovolume. Other studies have found non-linear response at saturation levels $>200 \mu\text{g L}^{-1}$ (Bastien et al. 2011; Brient et al. 2008; Kong et al. 2014). Further work needs to be carried out at lower biovolumes with mixed assemblages to add confidence to the prediction of low biovolumes from phycocyanin.

Minimum detection limits compared to biovolume thresholds

Several studies have created alert level thresholds for monitoring cyanobacteria from their sensor detection limits (Ahn et al. 2007; Bastien et al. 2011; Brient et al. 2008; Izydorczyk et al. 2009; Kong et al. 2014; McQuaid et al. 2011). Four studies (Bastien et al. 2011; Brient et al. 2008; Kong et al. 2014; McQuaid et al. 2011) indicate that the phycocyanin thresholds (often as equivalent cell concentrations)

are specific to their study site and to the sensor used. Of the four studies, the McQuaid et al. (2011) study had the highest biovolume for their minimum phycocyanin detection limit, which was comparable to the biovolume range found in the current study ($0.2\text{-}0.5\text{ mm}^3\text{ L}^{-1}$) and these are up to three times higher than most of the literature values. (Table 8). The biovolumes of $0.2\text{-}0.5\text{ mm}^3\text{ L}^{-1}$ fit within the green surveillance mode threshold ($<0.5\text{ mm}^3\text{ L}^{-1}$) for cyanobacteria monitoring for recreational purposes in New Zealand. However, the minimum phycocyanin detection limits observed for those biovolumes varied from $30\text{-}90\text{ }\mu\text{g L}^{-1}$ for the four species in the dilution experiment (Table 6). When the minimum phycocyanin detection limits of $30\text{-}90\text{ }\mu\text{g L}^{-1}$ are compared to the field studies predicted phycocyanin threshold $>40\text{ }\mu\text{g L}^{-1}$ for $1.8\text{ mm}^3\text{ L}^{-1}$, they overlap in the concentration of phycocyanin (i.e., $90\text{ }\mu\text{g L}^{-1}$ for $0.2\text{ mm}^3\text{ L}^{-1}$ is greater than $40\text{ }\mu\text{g L}^{-1}$ for $1.8\text{ mm}^3\text{ L}^{-1}$). Therefore, minimum phycocyanin detection limits from this sensor are unsuitable for implementation at the lowest biovolume threshold $<0.5\text{ mm}^3\text{ L}^{-1}$ under the recreational monitoring guidelines.

2.5.3 Recreational threshold setting for phycocyanin sensors

From the field studies, the predicted phycocyanin threshold values at the corresponding biovolume thresholds used for monitoring cyanobacteria varied between years and across different lakes. Generally, phycocyanin $>40\text{ }\mu\text{g L}^{-1}$ would exceed the red action mode biovolume threshold of $1.8\text{ mm}^3\text{ L}^{-1}$. This phycocyanin threshold is comparable to those of $40\text{ }\mu\text{g L}^{-1}$ (biovolume $>10\text{ mm}^3\text{ L}^{-1}$) found by Ahn et al. (2007) and $49.4\text{ }\mu\text{g L}^{-1}$ (biovolume $5\text{-}10\text{ mm}^3\text{ L}^{-1}$) found by Izydorczyk et al. (2009). A phycocyanin threshold $>40\text{ }\mu\text{g L}^{-1}$ could be used to prioritise samples

for enumeration, to confirm cyanobacteria biovolumes of $>1.8 \text{ mm}^3 \text{ L}^{-1}$ (i.e., the red action mode). If the organisation requires reporting at $>1.8 \text{ mm}^3 \text{ L}^{-1}$ and not $0.5 \text{ mm}^3 \text{ L}^{-1}$, this would allow more sites to be assessed with the phycocyanin sensor and fewer samples to be enumerated, saving time and cost. As the relationship between phycocyanin and biovolume is strengthened at higher biovolumes $>10 \text{ mm}^3 \text{ L}^{-1}$, this also offers the potential to issue health warnings onsite when phycocyanin exceeds $10 \text{ mm}^3 \text{ L}^{-1}$.

Table 8. Detection limits for phycocyanin (PC) from sensors, reported cell concentrations, calculated biovolumes from literature values or the source study, the sensor used and source of information. NA data not given in the study.

Species	PC ($\mu\text{g L}^{-1}$) or RFU	Cell concentration detection limit (cells mL^{-1})	Biovolume (calculated) ($\text{mm}^3 \text{ L}^{-1}$)	Phycocyanin sensor	Study
<i>Microcystis aeruginosa</i>	NA	1,500	0.06	YSI 660	Bastien et al. (2011)
<i>Microcystis aeruginosa</i>	0.69	870	0.03	TriOS micro Flu-blue	Bastien et al. (2011)
<i>Planktothrix agardhii</i>	0.53	1,700	0.1	TriOS micro Flu-blue	Brient et al. (2008)
<i>Cylindrospermopsis</i> sp.	NA	45	0.003	TriOS micro Flu-blue	Kong et al. (2014)
<i>Microcystis</i> sp.	NA	1,335	0.01	TriOS micro Flu-blue	Kong et al. (2014)
<i>Microcystis aeruginosa</i>	RFU 0.1	NA	1	YSI 6600 V2-4	McQuaid et al., (2011)

Recommendations for further study.

Three factors should be considered to ensure consistent phycocyanin readings: photoacclimation periods of samples, calibration with the dominant cyanobacteria species in the water bodies being sampled, and use of a handheld phycocyanin sensor with shade cap and auto-ranging functions. Firstly,

photoacclimation period is important as cells exposed to high irradiance show reduced fluorescence (Ibelings et al. 1994; Dubinsky & Stambler, 2009;). Secondly, the calibrations with the dominant cyanobacteria species in the water body being sampled will help to refine the phycocyanin yields and capture the specificity of a sampling site (Richardson & Lawrenz, 2011). Over time individual thresholds could be developed for each species and field microscopes could be used to confirm species and help confirm relationships specific to each sample (Richardson et al. 2010). A handheld sensor specifically designed for field applications could 1) reduce interference of light with a shade cap, and 2) have an auto ranging function or a maximum function to reduce occurrences of phycocyanin saturation of the sensor or minimum levels for specific sensor gains.

Due to the variation in the relationships found between phycocyanin and biovolume between lakes, over time in the field, with species morphology and at low concentrations of biovolume. It is recommended that caution is taken when predicting biovolumes from phycocyanin, when phycocyanin is close to the biovolume monitoring threshold of $1.8 \text{ mm}^3 \text{ L}^{-1}$. However, this is less of a concern for biovolume values of $>10 \text{ mm}^3 \text{ L}^{-1}$, which could provide onsite assessments of biomass that exceeds the red action mode for “total cyanobacteria” in the recreational monitoring framework.

2.6 References

- Ahn, C., Joung, S., Yoon, S., & Oh, H. (2007). Alternative alert system for cyanobacterial bloom, using phycocyanin as a level determinant. *Journal of Microbiology (Seoul, Korea)*, 45(2), 98–104.
- Baker, P. D., & Fabbro, L. D. (2002). *A guide to the identification of common blue-green algae (Cyanoprokaryotes) in Australian freshwaters*. Thrugoon, NSW: Cooperative Research Centre for Freshwater Ecology.
- Bastien, C., Cardin, R., Veilleux, E., Deblois, C., Warren, A., & Laurion, I. (2011). Performance evaluation of phycocyanin probes for the monitoring of cyanobacteria. *Journal of Environmental Monitoring*, 13, 110–118. <https://doi.org/10.1039/c0em00366b>.
- Bennett, A., & Bogorad, L. (1973). Complementary chromatic adaption in a filamentous blue-green alga. *The Journal of Cell Biology*, 58, 419–435. <https://doi.org/10.1083/jcb.58.2.419>.
- Bermejo, R. (2014). Phycocyanins. In *Cyanobacteria: An economic perspective* (pp. 209–225). Hoboken: John Wiley & Sons, Ltd. <https://doi.org/10.1017/CBO9781107415324.004>.
- Beutler, M., Wiltshire, K. H., Meyer, B., Moldaenke, C., Lüring, C., Meyerhöfer, M., Hansen, U. P., & Dau, H. (2002). A fluorometric method for the differentiation of algal populations *in vivo* and *in situ*. *Photosynthesis Research*, 72(1), 39–53. <https://doi.org/10.1023/A:1016026607048>.
- Bolch, C. J. S., & Blackburn, S. I. (1996). Isolation and purification of Australian isolates of the toxic cyanobacterium *Microcystis aeruginosa* Kutz. *Journal of Applied Phycology*, 8(1), 5–13. Retrieved from

<https://doi.org/10.1007/BF02186215>.

- Bowling, L. C., Zamyadi, A., & Henderson, R. K. (2016). Assessment of *in situ* fluorometry to measure cyanobacterial presence in water bodies with diverse cyanobacterial populations. *Water Research*, 105, 22–33. <https://doi.org/10.1016/j.watres.2016.08.051>.
- Brient, L., Lengronne, M., Bertrand, E., Rolland, D., Sipel, A., Steinmann, D., Baudin, I., Legeas, M., Le Rouzic, B., & Bormans, M. (2008). A phycocyanin probe as a tool for monitoring cyanobacteria in freshwater bodies. *Journal of Environmental Monitoring*, 10(2), 248–255. <https://doi.org/10.1039/B714238B>.
- Burns, N., McIntosh, J., & Scholes, P. (2005). Strategies for managing the lakes of the rotorua district, New Zealand. *Lake and Reservoir Management*, 21(1), 61–72. <https://doi.org/10.1080/07438140903083815>.
- Chang, D. W., Hobson, P., Burch, M., & Lin, T. F. (2012). Measurement of cyanobacteria using *in-vivo* fluoroscopy - Effect of cyanobacterial species, pigments, and colonies. *Water Research*, 46(16), 5037–5048. <https://doi.org/10.1016/j.watres.2012.06.050>.
- Chorus, I., & Bartram, J. (Eds.). (1999). Toxic Cyanobacteria in Water: A Guide to their Public Health Consequences, Monitoring and Management. London, U.K.: Taylor & Francis.
- Dubinsky, Z., & Stambler, N. (2009). Photoacclimation processes in phytoplankton: Mechanisms, consequences, and applications. *Aquatic Microbial Ecology*, 56(2–3), 163–176. <https://doi.org/10.3354/ame01345>.
- Glazer, A. N. (1976). Phycocyanins : Structure and Function. In *In photochemical*

and photobiological reviews (pp. 71–115). US: Springer International Publishing.

Gregor, J., Maršálek, B., & Šípková, H. (2007). Detection and estimation of potentially toxic cyanobacteria in raw water at the drinking water treatment plant by *in vivo* fluorescence method. *Water Research*, 41(1), 228–234. <https://doi.org/10.1016/j.watres.2006.08.011>.

Hamilton, D. P., Carey, C. C., Arvola, L., Arzberger, P., Brewer, C., Cole, J. J., Gaiser, E., Hanson, P. C., Ibelings, B. W., Jennings, E., Kratz, T. K., Lin, F. P., McBride, C. G., de Motta Marques, D., Muraoka, K., Nishri, A., Qin, B., Read, J. S., Rose, K. C., Ryder, E., Weathers, K. C., Zhu, G., Trolle, D., & Brookes, J. D. (2015). A Global lake ecological observatory network (GLEON) for synthesising high-frequency sensor data for validation of deterministic ecological models. *Inland Waters*, 5(1), 49–56. <https://doi.org/10.5268/IW-5.1.566>.

Harke, M. J., Steffen, M. M., Gobler, C. J., Otten, T. G., Wilhelm, S. W., Wood, S. A., & Paerl, H. W. (2016). A review of the global ecology, genomics, and biogeography of the toxic cyanobacterium, *Microcystis* spp. *Harmful Algae*, 54, 4–20. <https://doi.org/10.1016/j.hal.2015.12.007>.

Hawkins, P. R., Holliday, J., Kathuria, A., & Bowling, L. (2005). Change in cyanobacterial biovolume due to preservation by Lugol's Iodine. *Harmful Algae*, 4(6), 1033–1043. <https://doi.org/10.1016/j.hal.2005.03.001>.

Hemlata, F. T. (2009). Screening of cyanobacteria for phycobiliproteins and effect of different environmental stress on its yield. *Bulletin of Environmental Contamination and Toxicology*, 83(4), 509–515. <https://doi.org/10.1007/s00128-009-9837-y>.

- Hodges, C. (2016). *A validation study of phycocyanin sensors for monitoring cyanobacteria in cultures and field samples*. University of Waikato, Hamilton.
- Holland, S. M. (2008). Non-Metric Multidimensional Scaling (MDS). *The Journal of Cell Biology*, 8. <https://doi.org/10.1177/0272989X07302131>.
- Hötzel, G., & Croome, R. (1999). *A phytoplankton methods manual for Australian freshwaters*. Occasional Paper 22/99. Land and Water Resources Research and Development Corporation, Wodonga, Victoria, Australia. <http://npsi.gov.au/files/products/national-river-health-program/pr990300/pr990300.pdf>.
- Ibelings, B. W., Kroon, B. M. a., & Mur, L. R. (1994). Acclimation of photosystem II in a cyanobacterium and a eukaryotic green alga to high and fluctuating photosynthetic photon flux densities, simulating light regimes induced by mixing in lakes. *New Phytologist*, 128(3), 407–424. <https://doi.org/10.1111/j.1469-8137.1994.tb02987.x>.
- Izydorczyk, K., Carpentier, C., Mrówczyński, J., Wagenvoort, A., Jurczak, T., & Tarczyńska, M. (2009). Establishment of an Alert Level Framework for cyanobacteria in drinking water resources by using the Algae Online Analyser for monitoring cyanobacterial chlorophyll *a*. *Water Research*, 43(4), 989–996. <https://doi.org/10.1016/j.watres.2008.11.048>.
- Kasinak, J. M. E., Holt, B. M., Chislock, M. F., & Wilson, A. E. (2014). Benchtop fluorometry of phycocyanin as a rapid approach for estimating cyanobacterial biovolume. *Journal of Plankton Research*, 37(1), 248–257. <https://doi.org/10.1093/plankt/fbu096>.
- Komárek, J., & Komárková, J. (2002). Review of the European *Microcystis*

- morphospecies (Cyanoprokaryotes) from nature. *Czech Phycology*, 2, 1–24.
<https://doi.org/citeulike-article-id:13073212>.
- Kong, Y., Lou, I., Zhang, Y., Lou, C. U., & Mok, K. M. (2014). Using an online phycocyanin fluorescence probe for rapid monitoring of cyanobacteria in Macau freshwater reservoir. *Hydrobiologia*, 741(1), 33–49.
<https://doi.org/10.1007/s10750-013-1759-3>.
- Kusabs, I. A., & Quinn, J. M. (2009). Use of a traditional Maori harvesting method, the tau kōura, for monitoring kōura (freshwater crayfish, *Paranephrops planifrons*) in Lake Rotoiti, North Island, New Zealand. *New Zealand Journal of Marine and Freshwater Research*, 43(3), 713–722.
<https://doi.org/10.1080/00288330909510036>.
- Leboulanger, C., Dorigo, U., Jacquet, S., Le Berre, B., Paolini, G., & Humbert, J. F. (2002). Application of a submersible spectrofluorometer for rapid monitoring of freshwater cyanobacterial blooms: A case study. *Aquatic Microbial Ecology*, 30(1), 83–89. <https://doi.org/10.3354/ame030083>.
- Loftus, M. E., & Seliger, H. H. (1975). Some limitations of the *in vivo* fluorescence technique. *Chesapeake Science*, 16(2), 79–92.
- McQuaid, N., Zamyadi, A., Prévost, M., Bird, D. F., & Dorner, S. (2011). Use of *in vivo* phycocyanin fluorescence to monitor potential microcystin-producing cyanobacterial biovolume in a drinking water source. *Journal of Environmental Monitoring*, 13(2), 455–463.
<https://doi.org/10.1039/C0EM00163E>.
- Muggeo, V. M. (2008). Segmented: an R package to fit regression models with broken-line relationships. *R News*, 8(May), 20–25.

<https://doi.org/10.1159/000323281>.

Muggeo, V. M. R. (2016). Testing with a nuisance parameter present only under the alternative: a score-based approach with application to segmented modelling. *Journal of Statistical Computation and Simulation*, 9655, 1–9. <https://doi.org/10.1080/00949655.2016.1149855>.

Muggeo, V. M. R. (2017). Package “segmented.” *Biometrika*, 58, 525–534.

NIWA. (2017). *Annual Climate Summary 2016*. NIWA (National Institute of Water and Atmospheric Research, New Zealand. Retrieved March 4, 2017, from <https://www.niwa.co.nz/climate/summaries/annual-climate-summary-2016>.

Özkundakci, D., Hamilton, D. P., McDowell, R., & Hill, S. (2014). Phosphorus dynamics in sediments of a eutrophic lake derived from ³¹P nuclear magnetic resonance spectroscopy. *Marine and Freshwater Research*, 65(1), 70–80. <https://doi.org/10.1071/MF13033>.

Özkundakci, D., Hamilton, D. P., & Scholes, P. (2010). Effect of intensive catchment and in-lake restoration procedures on phosphorus concentrations in a eutrophic lake. *Ecological Engineering*, 36(4), 396–405. <https://doi.org/10.1016/j.ecoleng.2009.11.006>.

Paerl, H. W., Gardner, W. S., Havens, K. E., Joyner, A. R., McCarthy, M. J., Newell, S. E., Qin, B., & Scott, J. T. (2016). Mitigating cyanobacterial harmful algal blooms in aquatic ecosystems impacted by climate change and anthropogenic nutrients. *Harmful Algae*. <https://doi.org/10.1016/j.hal.2015.09.009>.

Paul, W. J., Hamilton, D. P., Ostrovsky, I., Miller, S. D., Zhang, A., & Muraoka, K.

- (2012). Catchment land use and trophic state impacts on phytoplankton composition: a case study from the Rotorua lakes' district, New Zealand. *Hydrobiologia*, 698(1), 133–146. <https://doi.org/10.1007/s10750-012-1147-4>.
- R Development Core Team. (2016). R: A language and environment for statistical computing. *R Foundation for Statistical Computing*, Vienna, Austria. URL <https://www.R-project.org/>.
- Reynolds, C. S. (2006). *The Ecology of Phytoplankton*. Cambridge, UK: Cambridge University Press. 551p. <https://doi.org/10.1177/0309133310367548>.
- Rhodes, L., Smith, K., MacKenzie, L., Wood, S., Ponikla, K., Harwood, D., Packer, M., & Munday, R. (2016). The Cawthron Institute Culture Collection of Microalgae: a significant national collection. *New Zealand Journal of Marine and Freshwater Research*, 8330, 1–26. <https://doi.org/10.1080/00288330.2015.1116450>.
- Ribeiro, R., & Torgo, L. (2008). A comparative study on predicting algae blooms in Douro River, Portugal. *Ecological Modelling*. <https://doi.org/10.1016/j.ecolmodel.2007.10.018>.
- Richardson, T. L., & Lawrenz, E. (2011). How does the species used for calibration affect chlorophyll *a* measurements by in situ fluorometry? *Estuaries and Coasts*, 34(4), 872–883. <https://doi.org/10.1007/s12237-010-9346-6>.
- Richardson, T. L., Lawrenz, E., Pinckney, J. L., Guajardo, R. C., Walker, E. A., Paerl, H. W., & MacIntyre, H. L. (2010). Spectral fluorometric characterization of phytoplankton community composition using the Algae Online Analyser. *Water Research*, 44(8), 2461–2472.

<https://doi.org/10.1016/j.watres.2010.01.012>.

Scholes, P. (2011). *2010/2011 Rotorua Lakes Trophic Level Index Update*.

Environmental Publication 2011/17. Bay of Plenty Regional Council,
Whakatane, New Zealand. 37p.

https://www.boprc.govt.nz/media/213116/2011_17_2010-2011_rotorua_lakes_trophic_level_index_update_final.pdf.

Scholes, P., Dorrington, P., & Bruere, A. (2010). *Lake Rotorua Ohau Channel Algae*

Harvest Project. Environmental Publication 2010/20. Bay of Plenty Regional
Council, Whakatane, New Zealand. 72p.

https://www.boprc.govt.nz/media/99806/2010_20_lake_rotorua_ohau_channel_algae_harvest_project.pdf.

Scholes, P., & Hamill, K. (2016). *Rotorua Lakes Water Quality Report 2014/2015*.

Environmental Publication 2016/06. Bay of Plenty Regional Council,
Whakatane, New Zealand. 130p.

https://www.boprc.govt.nz/media/566926/rotorua-lakes-report-2014_2015.pdf.

Seppälä, J., Ylöstalo, P., Kaitala, S., Hällfors, S., Raateoja, M., & Maunula, P. (2007).

Ship-of-opportunity based phycocyanin fluorescence monitoring of the
filamentous cyanobacteria bloom dynamics in the Baltic Sea. *Estuarine,
Coastal and Shelf Science*, 73(3–4), 489–500.

<https://doi.org/10.1016/j.ecss.2007.02.015>.

Smith, V. H., Wood, S. A., McBride, C. G., Atalah, J., Hamilton, D. P., & Abell, J.

(2016). Phosphorus and nitrogen loading restraints are essential for
successful eutrophication control of Lake Rotorua, New Zealand. *Inland*

- Waters*, 6(2), 273–283. <https://doi.org/10.5268/IW-6.2.909>.
- Turner Designs. (2015). Technical Note: *An Introduction to Fluorescence Measurements*. Retrieved January 10 2016, from <http://www.turnerdesigns.com/customer-care/fluorometer-technical-notes>.
- Utermöhl, H. (1958). Zur Vervollkommung der quantitativen Phytoplankton Methodik (Towards a perfection of quantitative phytoplankton methodology). *Mitteilungen Der Internationale Vereinigung Für Theoretische Und Angewandte Limnologie*, 9, 1–38.
- Von Westernhagen, N., Hamilton, D. P., & Pilditch, C. (2010). Temporal and spatial variations in phytoplankton productivity in surface waters of a warm-temperate, monomictic lake in New Zealand. *Hydrobiologia*, 652(1), 57–70. <https://doi.org/10.1007/s10750-010-0318-4>.
- Wilding, T. K. (2000). *Rotorua Lakes Algae Report*. Environmental Report 2000/06. Environment BOP, Whakatane, New Zealand. 105p. <http://docs.niwa.co.nz/library/public/EBOPer2000-06.pdf>.
- Wood, S., Goodwin, E., & Hamilton, D. (2014). *National Objectives Framework for Freshwater: An Assessment of Banding Statistics for Planktonic Cyanobacteria*. Cawthron Report No. 2493, prepared for the Ministry for the Environment. Cawthron Institute, Nelson, New Zealand. 55p. http://www.mfe.govt.nz/sites/default/files/media/Fresh%20water/nof-for-fw-an-assessment_0.pdf.
- Wood, S. A., Hamilton, D. P., Paul, W. J., Safi, K. A., & Williamson, W. M. (2009). *New Zealand Guidelines for Cyanobacteria in Recreational Fresh Waters –*

Interim Guidelines. Publication number ME 981, prepared for the Ministry for the Environment and the Ministry of Health. Ministry for the Environment, Wellington, New Zealand. 88p.
<http://www.mfe.govt.nz/sites/default/files/nz-guidelines-cyanobacteria-recreational-fresh-waters.pdf>.

Wood, S. A., Paul, W. J., & Hamilton, D. P. (2008). *Cyanobacterial Biovolumes for the Rotorua Lakes*. Cawthron Report No. 1504, prepared for Environment Bay of Plenty. 27p. <https://www.boprc.govt.nz/media/32233/Cawthron-090803-CyanobacterialbiovolumesforRotorualakes.pdf>.

Zamyadi, A., Choo, F., Newcombe, G., Stuetz, R., & Henderson, R. K. (2016). A review of monitoring technologies for real-time management of cyanobacteria: Recent advances and future direction. *TrAC - Trends in Analytical Chemistry*, 85, 83–96. <https://doi.org/10.1016/j.trac.2016.06.023>.

Zamyadi, A., McQuaid, N., Dorner, S., Bird, D. F., Burch, M., Baker, P., Hobson, P., & Prévost, M. (2012). Cyanobacterial detection using *in vivo* fluorescence probes: Managing interferences for improved decision-making. *Journal - American Water Works Association*.
<https://doi.org/10.5942/jawwa.2012.104.0114>.

Chapter 3

Effects of nutrients and light intensity on phycocyanin quota and growth rates in *Microcystis aeruginosa*

3.1 Abstract

Cyanobacterial blooms are increasing in abundance and severity, and there is a need for new methods to effectively quantify biomass. Phycocyanin sensors can provide rapid assessments of cyanobacterial biomass, however, the amount of phycocyanin within a cell can be influenced by the growth phase of cyanobacteria and environmental factors, including nutrients and light intensity. Sensors may therefore lack the ability to accurately measure cyanobacterial biomass. In this study, an experiment using a Central Composite design involving 20 treatments was used to examine the effect of nitrogen, phosphorus and light intensity on the growth rate and phycocyanin quota of *Microcystis aeruginosa*. Phycocyanin content of each treatment was measured every 4-5 days for 22 or 26 days (depending on treatment) using a sensor and microscopy, to assess phycocyanin and cell concentrations, respectively. Phycocyanin quota was significantly ($P<0.05$) higher in four of the 20 treatments at day 18 compared to the day 22. Response Surface Methodology demonstrated that light had a significant ($P<0.01$) effect on both growth rate and phycocyanin quota. Light and phosphorus had a significant ($P<0.05$) interaction effect on phycocyanin at day 18, while low light and nitrogen was important for phycocyanin quota at day 22. Growth rates were similar across

treatments, they increased with the effect of low light intensity and high nutrient concentrations. This study provides new data on the effect of these variables on phycocyanin quota in *M. aeruginosa*. It also points to the importance of phycocyanin measurements for natural cyanobacterial populations which will consist of a mixture of growth stages with different nutritional and physiological states.

3.2 Introduction

Microcystis is a planktonic bloom-forming cyanobacterium that is known globally to produce toxins (Paerl & Otten, 2013). Global warming and increasing eutrophication are predicted to result in an increase in the distribution and intensity of *Microcystis* blooms (Carey et al. 2012; Wood et al. 2017). Some *Microcystis* strains produce hepatotoxins known as microcystins, and ingestion of water contaminated by these can cause harm to humans and animals (Chorus & Bartram, 1999). Because of the risk posed by cyanobacteria, many countries have developed guidelines and standards which use thresholds based on specific cell concentrations (Chorus & Bartram, 1999) or biovolumes to estimate the risk from cyanobacteria (Wood et al. 2009). Biovolumes have traditionally been assessed using grab samples that are then analysed by microscopy (Wood et al. 2008). The biovolume method is time-consuming, expensive, and requires taxonomic expertise. This limits the frequency with which samples can be collected and analysed. For example, many recreational cyanobacterial monitoring programs in New Zealand rely on samples collected weekly at one location within a lake, and results are not available for several days (NIWA, 2017).

Cyanobacteria have accessory pigments, including phycocyanin and allophycocyanin, to aid in light harvesting in the red and orange part of the light spectrum (Glazer, 1976). Phycocyanin has a characteristic fluorescence signature which is derived from absorption at wavelengths between 610 and 640 nm, with a maximum absorption peak at 620 nm. Phycocyanin fluorescence emission is concentrated between 640 and 660 nm, with a maximum at 645-655 nm, which corresponds to where allophycocyanin absorption is maximal (Shevela et al. 2013).

In freshwater bodies, phycocyanin is primarily associated with cyanobacteria, which enables their biomass to be estimated in water bodies containing mixed phytoplankton communities. Phycocyanin content can be determined in laboratories using fluorometry or spectrophotometry, and recent advances in compact optical sensor technology have led to the development of phycocyanin sensors which enable concentrations to be assessed *in situ* (Izydorczyk et al. 2009). The sensors excite the pigment and detect the corresponding wavelength, which is then used to estimate phycocyanin concentration. Phycocyanin sensors are now used for a suite of applications including real-time assessments of bloom formation (Kong et al. 2014); *in-situ* monitoring of drinking water reservoirs (Izydorczyk et al. 2009); and in the development of predictive water quality models (Hamilton et al. 2015).

While the rapid *in situ* assessment of cyanobacterial biomass may be advantageous for water management, there are several limitations that must be considered. Because phycocyanin sensors are optical and rely on fluorescence, they are subject to interferences. The presence of other algal pigments such as

chlorophyll *a* (Zamyadi et al. 2012) or turbidity (Chang et al. 2012) can interfere with the fluorescence signal from phycocyanin. In addition to factors that directly affect the sensor readings, phycocyanin content is not constant in cyanobacteria, during growth cycles and differs among species (Campbell et al. 1998; Ibelings et al. 1994). Chang et al. (2012) found cultures of *M. aeruginosa* had the highest phycocyanin content in the exponential phase of growth. Hemlata (2009) screened multiple species of cyanobacteria and found different phycocyanin yields. Several studies have screened a number of cyanobacteria species to find the maximum phycocyanin for production purposes (Khattar et al. 2015; Singh et al. 2009). Little is known, however, about the effect of growth phase and the interactive influence of nitrogen, phosphorus and light intensity on phycocyanin content in *M. aeruginosa* for fluorescence monitoring purposes.

Photosynthetically available radiation (PAR) is affected by the incoming light, which varies seasonally, diurnally and at high frequency (e.g., with clouds), as well as with reflection at the water surface and underwater attenuation. Talbot et al. (1991) found higher growth rates for *Phormidium* sp. and *Oscillatoria* sp. at a higher temperature and light intensity. Chaneva et al. (2007) found higher growth rates for *Arthronema africanum* at light intensity $>300 \mu\text{mol m}^{-2} \text{s}^{-1}$. In addition, they found phycocyanin content was 20% higher at a light intensity of $150 \mu\text{mol m}^{-2} \text{s}^{-1}$ compared with $300 \mu\text{mol m}^{-2} \text{s}^{-1}$. Similarly, Raps et al. (1983) found that as light intensity increased, phycocyanin decreased due to chromatic adaptation in *M. aeruginosa*, and growth rates increased. Ibelings et al. (1994) simulated diurnal light fluctuations to show that the phycocyanin fluorescence in *M. aeruginosa* was diminished at midday. While these studies show that the effect of high light

intensity can increase growth rates in a variety of species, they also show a decrease in phycocyanin cell quota.

There is limited understanding of whether phycocyanin quotas respond to the interactive effects of light intensity, nitrogen, and phosphorus. Some studies have investigated the effect of nutrients on the growth of *Microcystis* sp. and some have investigated the effect of nutrients on phycocyanin quota. Vézie et al. (2002) tested several *Microcystis* strains and reported that growth was increased in toxin producing strains with the addition of nitrogen and phosphorus. Chaneva et al. (2007) showed that biomass increased in *Arthronema africanum* with the addition of nitrate. Nitrogen and sucrose stimulated phycocyanin production in *Anabaena fertilissima* (Khattar et al. 2015). Hemlata (2009) experimented on a *Dolichospermum* species and showed that the highest phycocyanin quota was at the lowest nitrogen conditions. In contrast, Singh et al. (2009) found that nitrogen increased phycocyanin quotas in *Phormidium ceylanicum*. Differences in phycocyanin quotas in response to rapidly changing environmental conditions could be an important consideration for monitoring toxic cyanobacteria with phycocyanin sensors. Underestimates of phycocyanin due to low quota could lead to ill-informed management decisions for health warnings and higher risk for water users.

The aim of this study was to investigate the effects of nitrogen, phosphorus and light intensity on growth rates and phycocyanin content over the growth cycle of *M. aeruginosa* using a batch culture experiment. A Central Composite design was used to select 20 treatments of nitrogen and phosphorus concentrations, and light

intensity used for experimental purposes. The CCD is a statistical method to derive different treatments within a determined range of values. The intention of CCD is to explore an optimal treatment combination for the response variables. The data were analysed using Response Surface Methodology, (RSM is an extension to linear regression suited to analysis of optimisation designs such as CCD) to assess the significance of any individual or interactive effects amongst experimental factors on the response variables; maximum growth rate and phycocyanin content. It was hypothesised that: 1) that potential growth-limiting factors of light, nitrogen, and phosphorus affect phycocyanin in *M. aeruginosa* independently of changes in biomass, and 2) there may be specific nutrient concentrations and light intensities that would produce high growth rates and/or high phycocyanin quotas.

3.3 Methodology

3.3.1 Stock cyanobacteria culture

A culture of *M. aeruginosa* (CAWBG617) was sourced from the Cawthron Institute Culture Collection of Micro-algae (www.cultures.cawthron.org.nz; Rhodes et al. 2016). The culture was maintained in a stationary phase in MLA medium (Bolch & Blackburn, 1996) under a light regime of $90 \mu\text{mol m}^{-2} \text{s}^{-1}$ with a 12 h: 12 h light: dark cycle at 18°C ($\pm 1^{\circ}\text{C}$). In batch culture, *M. aeruginosa* is present as single cells or small colonies, creating a relatively homogenous culture mixture.

3.3.2 Nitrate and phosphate stock solutions and treatment preparation

Central Composite design (CCD) was used as a statistical design method to derive the 20 treatments from the lowest and highest value of each experimental factor

(nitrogen, phosphorus, and light intensity). The stock concentrations of each analyte were analytical grade sodium nitrate (NaNO_3 , nitrate-N 84 mg L^{-1}) and monopotassium phosphate (KH_2PO_4 , phosphate-P 5.47 mg L^{-1}) in sterile Milli-Q water. To make the working solutions for each treatment, 1 L bottles (Schott, DURAN®), containing MLA media (Bolch & Blackburn, 1996) were spiked with the stock concentrations (Table 1). Aliquots (55 mL, pH 7, $n=60$) were subsequently transferred to gamma-sterilised polystyrene culturing containers (ThermoFisher Scientific, New Zealand). A subsample (1 mL) of *M. aeruginosa* (CAWBG617; ca. $500 \text{ cells mL}^{-1}$) culture was pipetted separately into each replicate. Triplicates for each treatment and control were randomly placed within designated light treatments (Table 1) and rotated on sampling days to reduce the effect of minor variations in light intensity.

3.3.3 Sampling

Treatments 2-20 were sampled on days 0, 6, 14, 18, and 22, whereas treatment 1 was sampled on days 0, 6, 16, 21, and 26. Treatment 1 was the $10 \mu\text{mol m}^{-2} \text{ s}^{-1}$ light treatment (Table 1). These sampling days were selected to capture the growth curve of *M. aeruginosa*. Treatment controls (for nutrients) were sampled at day 0. Treatment controls (for species) ran in parallel with the experiment.

Light intensity for each treatment (Table 1) was measured on sampling days 0, 6, 14, 18, and 22 using a light meter with a quantum sensor (Li-250A Light Meter, LI-COR® Biosciences, NE, USA). Temperature was monitored for the duration of the experiment (26 days) using temperature loggers (HOBO pendant®

Temperature/light 8K data loggers, Onset, MA, USA) (Table 1). Treatment controls (for species) were measured on day 22 or 26 (treatment 1) for pH, using a pH probe, (Thermo Scientific Orion Star A211 with Orion 8107BNUMD Ross Ultra pH/ATC Triode).

Nutrient controls were sampled at day 0 for nitrate (NO₃-N) and dissolved reactive phosphorus (DRP). Nutrient controls were subsampled (15 mL), filtered (GF/C, Whatman, Buckinghamshire, UK), and stored at -20°C. The subsamples were analysed using a Lachat Quickchem® flow injection analyser (FIA+8000 Series, Zellweger Analytics, Inc.) using APHA (2005) 4500 methods for NO₃-N and DRP.

Table 1. Experimental design matrix for concentrations of nitrate-N (N), phosphate-P (P) and light intensity (I) for each treatment from the Central Composite design, ratios of nitrogen to phosphorus and the average temperature for the 12 h light: 12 h dark periods.

Treatment	N	P	I	N:P	Temperature 12 h light: 12 h dark (°C)
(n=3)	(mg L ⁻¹)	(mg L ⁻¹)	(μmol m ⁻² s ⁻¹)	(ratio)	
1	55	0.52	10	97	20±1 : 17±1
2	37.8	3.47	128.5	10	21±3 : 18±1
3	72.3	3.47	128.5	19	21±3 : 18±1
4	72.3	0.24	128.5	277	21±3 : 18±1
5	37.8	0.24	128.5	145	21±3 : 18±1
6	55	0.52	302.4	97	24±2 : 18±1
7	55	0.52	302.4	97	24±2 : 18±1
8	55	0.52	302.4	97	24±2 : 18±1
9	26	0.52	302.4	46	24±2 : 18±1
10	84	0.52	302.4	148	24±2 : 18±1
11	55	0.05	302.4	1011	24±2 : 18±1
12	55	0.52	302.4	97	24±2 : 18±1
13	55	0.52	302.4	97	24±2 : 18±1
14	55	0.52	302.4	97	24±2 : 18±1
15	55	5.47	302.4	9	24±2 : 18±1
16	37.8	3.47	360.7	10	24±2 : 18±1
17	37.8	0.24	360.7	145	24±2 : 18±1
18	72.3	3.47	360.7	19	24±2 : 18±1
19	72.3	0.24	360.7	277	24±2 : 18±1
20	55	0.52	400.5	97	24±2 : 18±1

Samples for *M. aeruginosa* cell counts were collected on days 0, 6, 14, 18, and 22 (treatments 2-20) and days 0, 6, 16, 21, and 26 (treatment 1). Samples of either 0.5 or 1 mL were preserved with Lugol's iodine and stored in the dark until enumeration. *Microcystis aeruginosa* samples (0.5-1 mL) were pipetted into 12-well plates (Costar, Corning, NY, USA), and allowed to settle for a least 72 h. *Microcystis aeruginosa* was enumerated by scanning 1-2 transects or 10 fields (selected by density) at 400-800x magnification using an inverted microscope (Olympus CKX41 or IX70) and converted to cells mL⁻¹ using calculations in Lawton et al., (1999).

Phycocyanin measurements were undertaken by two different methods; sensor and spectrophotometry. Sensor readings in volts were taken on days 0, 6, 14, 18, and 22 (treatments 2-20) and days 0, 6, 16, 21, and 26, (treatment 1) using a phycocyanin sensor (Cyclops 7, Turner Designs, CA, USA). Sensor readings for each sample were conducted under low light conditions (ca. 5 $\mu\text{mol m}^{-2} \text{s}^{-1}$) and constant temperature ($18 \pm 1^\circ\text{C}$). During the measurements, the sensor was submerged 1 cm beneath the surface of the sample and the sample was placed on a non-reflective black surface (Cinefoil™, Rosco, CT, USA). Three sensor readings were taken over a 20-second duration and values were averaged. Measurements for background sensor noise were taken on each sampling day using Milli-Q water. Average sensor values that were three times the background noise were considered reliable (i.e., higher than the background noise). Average sensor values on days 18, 21, 22, and 26, were considered reliable, with the exception of one replicate from treatment 17 on day 18, which was removed from further analysis.

3.3.4 Phycocyanin determination for sensor phycocyanin and extracted phycocyanin samples

Sensor phycocyanin measurements from samples were converted from volts to sensor phycocyanin ($\mu\text{g L}^{-1}$) using a calibration curve. The calibration curve was an eleven-point standard curve ($0.5\text{--}1,000 \mu\text{g L}^{-1}$) prepared using phycocyanin standard (10 mg: Spirulina-P2172; Sigma-Aldrich, USA). The phycocyanin standard was dissolved in sodium phosphate buffer (30 mL; 50 mM, pH 7), and diluted to 300 mL with Milli-Q water. The phycocyanin standard concentrations were determined using spectrophotometry. The sensor had an acceptable linear fit ($R^2=0.99$) and all sensor readings were converted using:

$$\text{Sensor phycocyanin } (\mu\text{g L}^{-1}) = \text{Sensor reading (V)} / 0.00202 \quad (3-1)$$

Spectrophotometry phycocyanin was measured on day 22 and day 26 (treatment 1), the experiment endpoint, using a spectrophotometer (Eppendorf BioSpectrometer® fluorescence, Eppendorf, Hamburg, Germany). Spectrophotometer phycocyanin samples (ca. 40 mL) were filtered (GF/C, Whatman, Buckinghamshire, UK) and stored frozen (-20°C). Filters were extracted for analysis in sodium phosphate buffer (1 mL, 50 mM, pH 7) and subject to three cycles of freeze-thaw, using sonication (30 min, 70 kHz) followed by freezing (-20°C , 1.5 hr). The samples were clarified by centrifugation (7 min, $3,200\times g$) and the supernatant was pipetted into 1 cm disposable cuvettes. Spectrophotometer phycocyanin measurements were determined using spectrophotometry at wavelengths 615 nm and 652 nm using:

$$\text{Phycocyanin } (\mu\text{g L}^{-1}) = \left[\frac{A_{615} - (0.474 \times A_{652})}{5.34 \times VF} \right] \times 1,000,000 \quad (3-2)$$

where A_{615} is the maximum absorbance of phycocyanin and A_{652} is the maximum absorbance of allophycocyanin at the path length of 1 cm, VF is the volume filtered in L, and 1,000,000 is used to convert the data from mg mL^{-1} to $\mu\text{g L}^{-1}$ (Bennett & Bogorad, 1973).

3.3.5 Response variable calculations for maximum growth rates and phycocyanin quotas

The response variables, maximum growth rate, and phycocyanin quota, were calculated for each treatment replicate from the cell concentration data and sensor phycocyanin measurements taken over the experiment. Cell concentration data from sampling days 6, 14, 18, and 22 (treatments 2 to 20), and days 6, 16, 21, and 26 (treatment 1) were used to calculate the maximum growth rate for each treatment replicate. The maximum growth rate was determined from the maximum change in cell density between sampling days and was calculated using:

$$\text{Growth rate } (\text{day}^{-1}) = \text{Ln} \left(\frac{C2}{C1} \right) / (T2 - T1) \quad (3-3)$$

where $C1$ is the cells concentration at time $T1$, $C2$ is the cells concentration at time $T2$ as per Lüring et al. (2017).

For the calculation of phycocyanin quota, the sensor phycocyanin measurements and cell concentration data were used from days 18 and 22 (treatments 2-20), and days 21, and 26, (treatment 1). The phycocyanin quota (pg cell^{-1}) for both days was calculated as:

$$\text{Phycocyanin quota (pg cell}^{-1}\text{)} = \frac{\text{sensor PC (}\mu\text{g L}^{-1}\text{)}}{\text{cell count (cells mL}^{-1}\text{)}} \times 1,000 \quad (3-4)$$

where phycocyanin quota was derived from the sensor phycocyanin (PC) ($\mu\text{g L}^{-1}$) divided by the replicate cell count (cells mL^{-1}).

The response variable calculations were dependent on the cell concentration data. Some replicates contained highly variable cell concentrations and were considered outliers. Outliers were removed in treatments 8, 12, 13 and 20 for maximum growth rate ($n=1$), and treatments 1, 12, 15, 16, 17 and 20, for phycocyanin quota ($n=1$).

3.3.6 Data analysis

Linear regression (Excel, Microsoft®) was used to compare the relationship between phycocyanin concentration measured by the sensor and by spectrophotometry. A Levene's test for equality of variance (Excel, Microsoft®) was used to assess the variability between the sensor and spectrophotometry data. These results were used to determine which phycocyanin values were used for calculating phycocyanin quota, which were then used in the Response Surface Methodology.

Averages for cell concentration, sensor phycocyanin, biovolume, pH and average phycocyanin quota for the 20 treatments were calculated for days 18 and 22. Students t-tests (Excel, Microsoft®) were used to test for significant differences between the phycocyanin quota on day 18 with day 22.

Response variables and factors from the CCD experiment were transformed to ensure the data was normally distributed. Maximum growth rate and day 18 phycocyanin quota were square-rooted, and day 22 phycocyanin quota was transformed using an inverse of square-root. Phosphorus and light were log and square-root transformed, respectively.

Analysis of the CCD experiment was undertaken with Response Surface Methodology (RSM) using the RSM package in R (Lenth, 2012, 2016; R Core Team, 2017). RSM is an extension to linear regression, suited to the analysis of multi-variable optimisation experiments. A linear model including the first order, second order, and interactions terms, was fitted, followed by an Analysis of Variance (ANOVA) and a lack-of-fit test. This means that each factor was modelled against the response to find the best predictors of the response (the optimum), including non-linear relationships. Non-linear relationships exist for yield optimums when there are lower values on either side of the optimum, thus creating a mound shaped curve in the relationship (Anderson & Whitcomb, 2005).

The first analysis of the CCD experiment is generally a preliminary exploration to find the significant factors whose ranges are refined before rerunning experiments and the model to find a final optimum set of factors. The model response variable is presented as a 3D-surface approximation within the ranges of the relevant experimental factors. This visualization allows for an interpretation to be made for further optimisation with regard to which factors may be of the greatest relative importance.

The optimum allows the experimental conditions to be predicted from the optimum response variable (Anderson & Whitcomb, 2005). To test the predictive power of the model, the lack of fit is calculated from pure error (F value) in the ANOVA sums of squares. In RSM models when the lack of fit is significant this means the data may not be reliable for prediction from the model. The data is better fitted to the model when the significance value for the lack of fit assessment is non-significant ($P > 0.05$) (Lenth, 2016). If the relationship is well explained from the R^2 value, then the weight of the significance of the lack of fit may be less important in predicting an optimum (Anderson & Whitcomb (2005).

3.3.7 Normalisation

Coding is a normalisation technique used in RSM analysis (Lenth, 2016). Coding ensures that all experimental factors are evaluated on the same scale (-1 to 1). This is a way of giving each experimental factor (i.e., predictor) an equal share in determining the steepest ascent (linear increase) towards the maximum response (optimum yield). Coded variables were calculated as:

$$x_{\text{coded}} = \frac{x_{\text{real}} - x_{\text{mean}}}{\Delta} \quad (3-5)$$

where x_{coded} is the coded value of the factor, x_{real} is the original value of the factor, x_{mean} is the mean value of x_{min} (the minimum original values of the factor), x_{max} is the maximum original values of the factor and Δ is the centre point, i.e., $\frac{1}{2} \times (x_{\text{max}} - x_{\text{min}})$ (range of original values of the factor).

3.4 Results

The experiment ran for 22 days for treatments 2-20 and 26 days for treatment 1 (due to slow growth). There was an initial lag phase in growth from day 0-6 where cell concentration did not increase (Appendix 4). Hereafter the treatments grew, and some cells immediately went into exponential phase between days 6-14 in the low and high light treatments (treatments 2-5 and 16-19, respectively; Table 2, Appendix 4). Mid-light treatments (6-15) showed exponential growth between days 14 and 18. From the growth curves, there is no evidence that any treatments were entering the stationary phase by day 22. Day 22 or day 26 (treatment 1) was the endpoint of the experiment, hereafter referred to as day 22. Maximum growth rate was specific to each treatment and for different time points (Table 2).

The results presented for phycocyanin are focused around day 18 and day 22 (Table 2). Based on the sensor background noise measurements for the experiment, the sensor could not accurately detect phycocyanin in the 20 treatments until day 18 (i.e., treatment < blank MLA \times 3). This was when the biomass had reached a minimum of ca. 40,000 cells mL⁻¹, equal to a biovolume of ca. 1.5 mm³ L⁻¹ (Appendix 3).

Treatment conditions as concentrations of nitrate-N (N) (mg L⁻¹), phosphate-P (P) (mg L⁻¹), and light intensity (I) (μ mol m⁻² s⁻¹) are reported as (N concentration: P concentration: light intensity) for simplicity when reporting multiple treatment comparisons.

Table 2. Experimental results of the phycocyanin (PC) quota, (pg cell^{-1}) at day 18 and day 22 and the maximum growth rate and day interval for maximum growth rate calculation between days 6-22. Experimental results are averages ($n=3$). Bold values represent results of Students t-test ($P<0.05$ significance level) for PC quota between two growth phases, (*) could not conduct Students t-test due to reduced sample size.

Response variables				
Treatment	Day 18 PC quota	Day 22 PC quota	Maximum growth rate	Day interval corresponding to max. growth rate
(n=3)	(pg cell^{-1})	(pg cell^{-1})	(day^{-1})	(day)
1	1.38*	0.33	0.63	21-26
2	0.45	0.24	0.68	6-14
3	0.34	0.10	0.75	6-14
4	0.55	0.15	0.78	6-14
5	0.47	0.12	0.63	14-18
6	0.63	0.18	0.55	18-22
7	0.32	0.16	0.68	6-14
8	0.26	0.17	0.49	14-18
9	0.37	0.35	0.73	14-18
10	0.35	0.16	0.67	14-18
11	0.32	0.11	0.62	14-18
12	1.23*	0.20	0.66	14-18
13	0.28	0.26	0.63	14-18
14	0.36	0.29	0.67	14-18
15	0.37*	0.34	0.65	6-14
16	1.48*	0.53	0.48	6-14
17	0.50*	0.53	0.53	6-14
18	0.60	0.43	0.69	14-18
19	0.51	0.27	0.73	6-14
20	0.59-	0.28	0.58	18-22

3.4.1 Comparison of phycocyanin determination from two methods (spectrophotometry and sensor) at experiment endpoint

To determine which phycocyanin concentrations would be used in the RSM models, the sensor and spectrophotometry phycocyanin concentrations on day 22 were compared. Linear regression showed there was a weak but significant relationship ($R^2<0.18$, $P<0.001$) between the phycocyanin concentrations determined by spectrophotometry and the sensor (Figure 1). The slope was 0.29 indicating that for every increase of $1 \mu\text{g L}^{-1}$ of phycocyanin from

spectrophotometry there was $0.29 \mu\text{g L}^{-1}$ increase in the sensor phycocyanin. Levene's tests showed that there was a significantly ($P < 0.05$) higher variance in phycocyanin measured by spectrophotometry compared to that obtained from the sensor (also see error bars Figure 2). Based on these assessments the phycocyanin measurements from the sensor were used for all further analysis and is referred to as sensor phycocyanin hereafter.

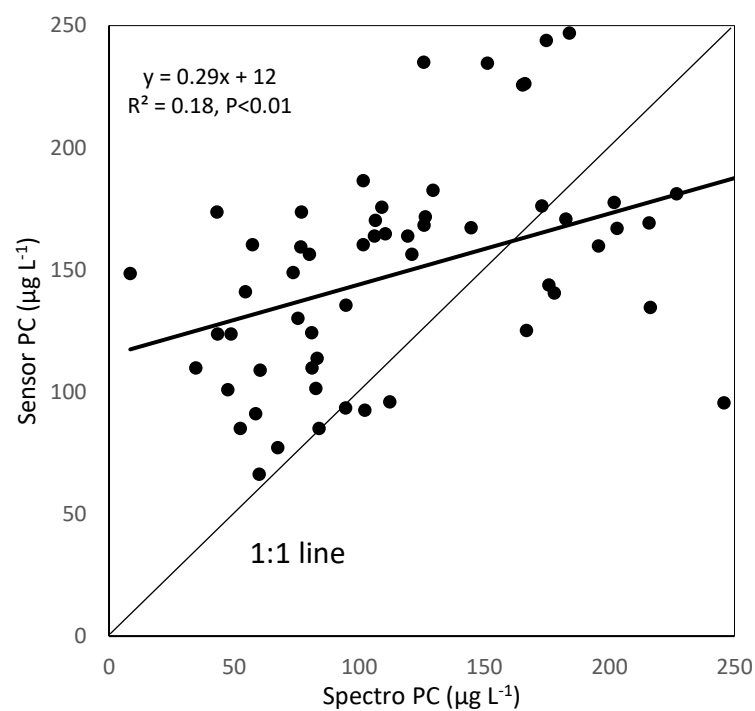


Figure 1. Phycocyanin (PC) measured by spectrophotometry (Spectro PC) and a sensor (Sensor PC) at day 22.

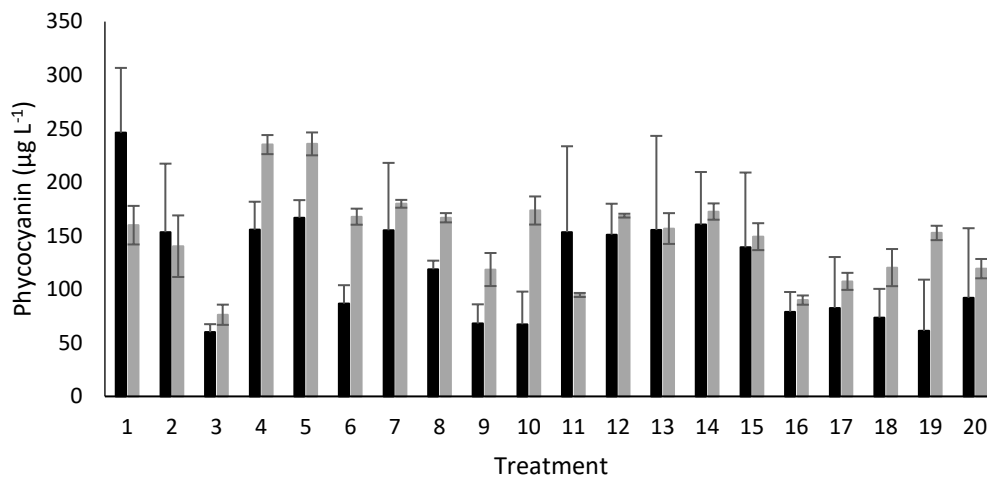


Figure 2. Average phycocyanin (n=3) on day 22 for each treatment measured by spectrophotometry (black) and the sensor (grey). Error bars are \pm one standard deviation. See Table 1 for individual treatment nutrient concentrations and light intensity used in each treatment.

3.4.2 Comparing Phycocyanin quota at day 18 and day 22

3.4.2.1 Phycocyanin quotas

Phycocyanin quotas for *M. aeruginosa* were calculated from sensor phycocyanin and cell concentrations on day 18 and day 22 across the 20 treatments (Figure 3). On day 18 the phycocyanin quota was highest in treatment 1 (N:55, P:0.52, I:10), 12 (N:55, P:0.52, I:302.4), and 16 (N:37.8, P:3.47, I:360.7) (Table 2 and Figure 3). Quotas for these treatments were 1.38, 1.23 and 1.48 pg cell⁻¹, respectively. The lowest phycocyanin quotas on day 18 were in treatments 8 (N:55, P:0.52, I:302.4), 11 (N:55, P:0.05, I:302.4), and 13 (N:55, P:0.52, I:360.7).

On day 22, treatment 16 (N:37.8, P:3.47, I:360.7) had the highest phycocyanin quota, followed by treatment 17 (N:37.8, P:0.24, I:360.7) and treatment 18 (N:72.3, P:3.47, I:360.7). On day 22, the lowest phycocyanin quotas were in treatments 3 (N:72.3, P:3.47, I:128.5), 5 (N:37.8, P:0.24, I:128.5), and 11 (N:55,

P:0.05, I:302.4). Treatment 5 had the highest cell concentrations (ca. 2 million cells mL⁻¹) and sensor phycocyanin (236 µg L⁻¹). When there were high cell counts, there was generally low phycocyanin quota and this was observed across both days (18 and 22), however, this result was not consistent across all 20 treatments (Appendix 3).

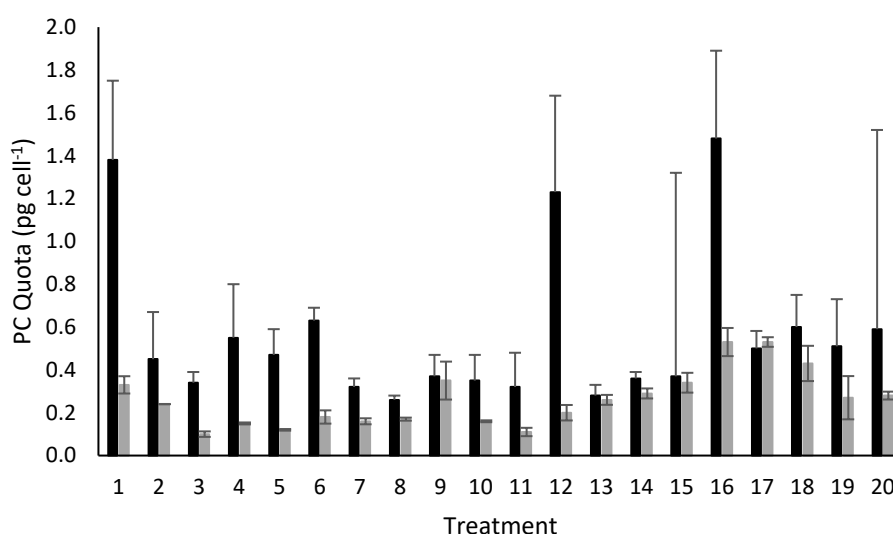


Figure 3. Average (n=3) phycocyanin quota (pg cell⁻¹) (PC quota) for the 20 treatments on days 18 (black) and 22 (grey). Error bars show one standard deviation. See Table 1 for nutrients concentrations and light intensity used for each treatment.

Phycocyanin quotas in *M. aeruginosa* were generally higher at day 18 compared to day 22 across the 20 treatments. Students t-tests showed there was a significantly (P<0.05) higher phycocyanin quota on day 18 compared to day 22 for treatments 3, 6, 7, and 8. These treatments had similar N:P ratios (Table 2). Treatments 6, 7 and 8 all had a ratio of N:P of 97 (N: 55 mg L⁻¹, P: 0.52 mg L⁻¹) whereas, treatment 3 had a ratio of 19 (N: 72.3 mg L⁻¹, P: 3.47 mg L⁻¹). The light in treatments 3 (128.5 µmol m⁻² s⁻¹) differed from 6, 7 and 8 (302.4 µmol m⁻² s⁻¹).

3.4.3 Effects of nutrients and light on phycocyanin quotas and maximum growth rate

Response Surface Methodology analysis of the CCD results was used to run three separate RSM models for the response variables, phycocyanin quota on day 18 and day 22 and maximum growth rate across 20 treatments. Phycocyanin quota at day 18 had a significant ($P<0.001$) dependence on light and on second-order light (Table 3). There was also a significant interactive effect ($P<0.05$) of phosphate-P and light on phycocyanin quota (Table 3). On day 22, nitrate-N ($P<0.05$), and second-order light ($P<0.001$) had a significant effect on phycocyanin quota (Table 3). There were significant interaction effects of nitrate-N and phosphate-P ($P<0.01$), and phosphate-P and light ($P<0.05$) on phycocyanin quota. Maximum growth rates had a second order dependence on light ($P<0.01$) (Table 3). There were no interactive effects of the three experimental factors on maximum growth rates.

RSM model and surface plots for phycocyanin at day 18

The RSM model for the response of phycocyanin quota on day 18 as a function of nutrients and light was significant ($P<0.001$) with an adjusted R^2 value of 0.33 (Table 3). The model was well fitted to the data (lack of fit >0.05) (Table 3 and Appendix 6). The RSM model output (Appendix 5) provides estimates for the approximated response and these are presented as 3D-surface plots to aid the interpretation of the significant effects of nutrients and light (Figure 4). Phycocyanin quota increased with concentrations of phosphate-P $>1 \text{ mg L}^{-1}$ (Figure 4a) and light ca. $300 \text{ } \mu\text{mol m}^{-2} \text{ s}^{-1}$, (Figure 4b), and when nitrate-N concentrations

were relatively low ca. $<50 \text{ mg L}^{-1}$ (Figure 4a, b). There was an interactive effect of both high phosphate-P and light, on phycocyanin quota (Figure 4c).

Table 3. Summary of relationship, significance values and ANOVA lack of fit values generated from the Response Surface Methodology analysis of maximum growth rates (day^{-1}) and phycocyanin quota (pg cell^{-1}) at day 18 and day 22. Variables are first order N: Nitrate-N, P: log-transformed phosphate-P, I: light, I^2 : light squared; and their interaction N&P, N&I, P&I. NS: not significant. There were no significant terms for N^2 and P^2 .

	Day 18	Day 22	Maximum growth
	phycocyanin quota	phycocyanin quota	rate
R²	0.33	0.73	0.27
P-values	<0.001	<0.001	<0.001
ANOVA-Lack of fit	>0.05	<0.001	<0.05
First order effects			
N	NS	<0.05	NS
P	NS	NS	NS
I	<0.001	NS	NS
Second order effects			
I^2	<0.001	<0.001	<0.01
Interaction effects			
N & P	NS	<0.01	NS
N & I	NS	NS	NS
P & I	<0.05	<0.05	NS

RSM model and surface plots for phycocyanin quota at day 22

The RSM model for the response of phycocyanin quota at day 22 as a function of nutrient and light showed there was a significant ($P<0.001$) and strong relationship (adjusted $R^2=0.73$; Table 3). However, the model did not fit the data well (lack of fit <0.001 ; Appendix 8). The approximated response of phycocyanin at day 22 showed that phycocyanin quota increased with decreasing nitrate-N $<40 \text{ mg L}^{-1}$ and increasing phosphate-P $>0.52 \text{ mg L}^{-1}$ with a notable interaction between the

two experimental variables (Table 3, Figure 5a). There was increased phycocyanin quota when the light was $<200 \mu\text{mol m}^{-2} \text{s}^{-1}$ and nitrate-N was $>50 \text{ mg L}^{-1}$ (Figure 5b). There was an interactive effect on phycocyanin quota when the light was $<200 \mu\text{mol m}^{-2} \text{s}^{-1}$ and when phosphate-P concentrations $>0.50 \text{ mg L}^{-1}$ (Table 3, Figure 5c).

Maximum growth rates across treatments

Maximum growth rates for *M. aeruginosa* were calculated from changes in cell counts between days 6 to 22. Growth rates ranged from 0.48 to 0.78 day^{-1} across all treatments. Growth rates were highest in treatment 4 (N:72.3, P:0.24, I:128.5) and lowest in treatment 16 (N:37.8, P:3.47, I:360.7; Table 2).

RSM model and surface plots for maximum growth rates

Maximum growth rate had a significant ($P<0.01$) dependence on second order light, although the adjusted R^2 of 0.27 suggests a large amount of unexplained variation (Table 3) and with a significant lack of fit (<0.05) the data was not well fitted to the model (Appendix 10). The approximated maximum growth rates increased as nitrate-N concentration increased with a decrease in phosphate-P, although this change was not significant (Figure 6a). Maximum growth rates appeared highest at the lower end of the tested light range (ca. $100 \mu\text{mol m}^{-2} \text{s}^{-1}$; Figure 6b and c), and there was a slight increase in growth rate with maximum ranges of nitrate-N or phosphate-P (Figure 6b and c).

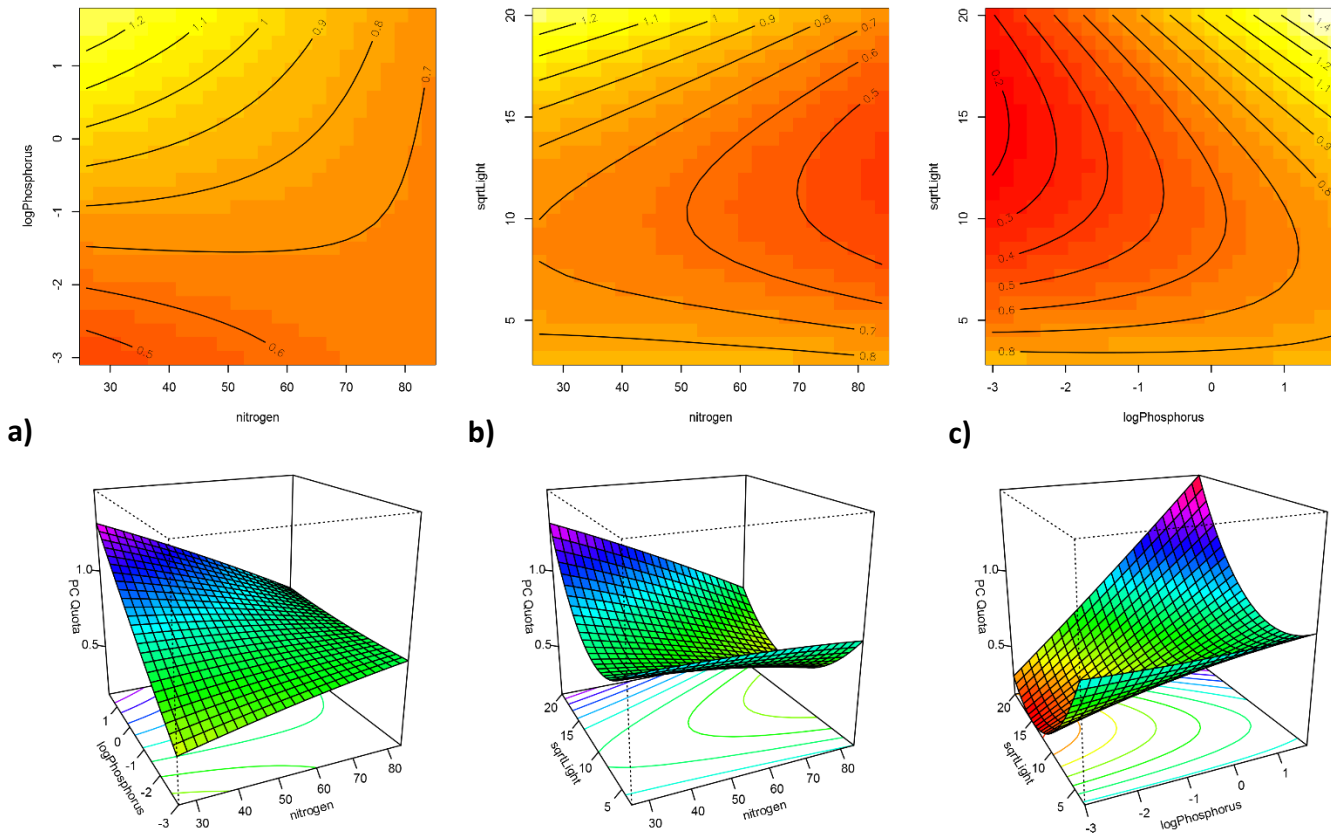


Figure 4. Contour plots (upper pane) and response surface plots (lower pane) showing phycocyanin quota (PC Quota) at day 18 in response to combinations of: (a) nitrogen (nitrate-N) and log-transformed phosphorus (phosphate-P) (b) square root-transformed light and nitrogen (nitrate-N) (c) square root-transformed light and log-transformed phosphorus (phosphate-P). Contour lines show phycocyanin quota values.

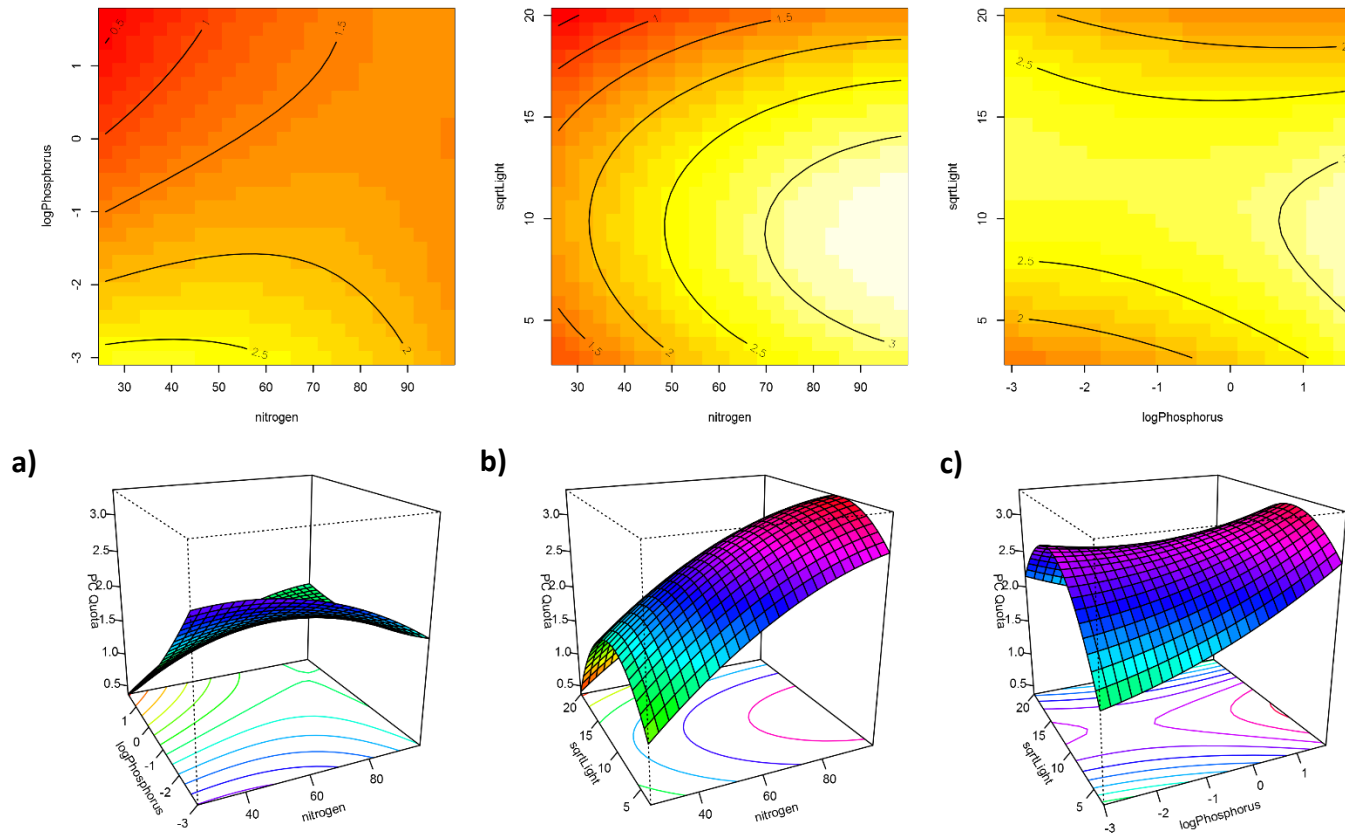


Figure 5. Contour plots (upper pane) and response surface plots (lower pane) showing phycocyanin quota (PC Quota) at day 22 in response to combinations of: (a) nitrogen (nitrate-N) and log-transformed phosphorus (phosphate-P) (b) square root-transformed light and nitrogen (nitrate-N) (c) square root-transformed light and log-transformed phosphorus (phosphate-P). Contour lines show phycocyanin quota value

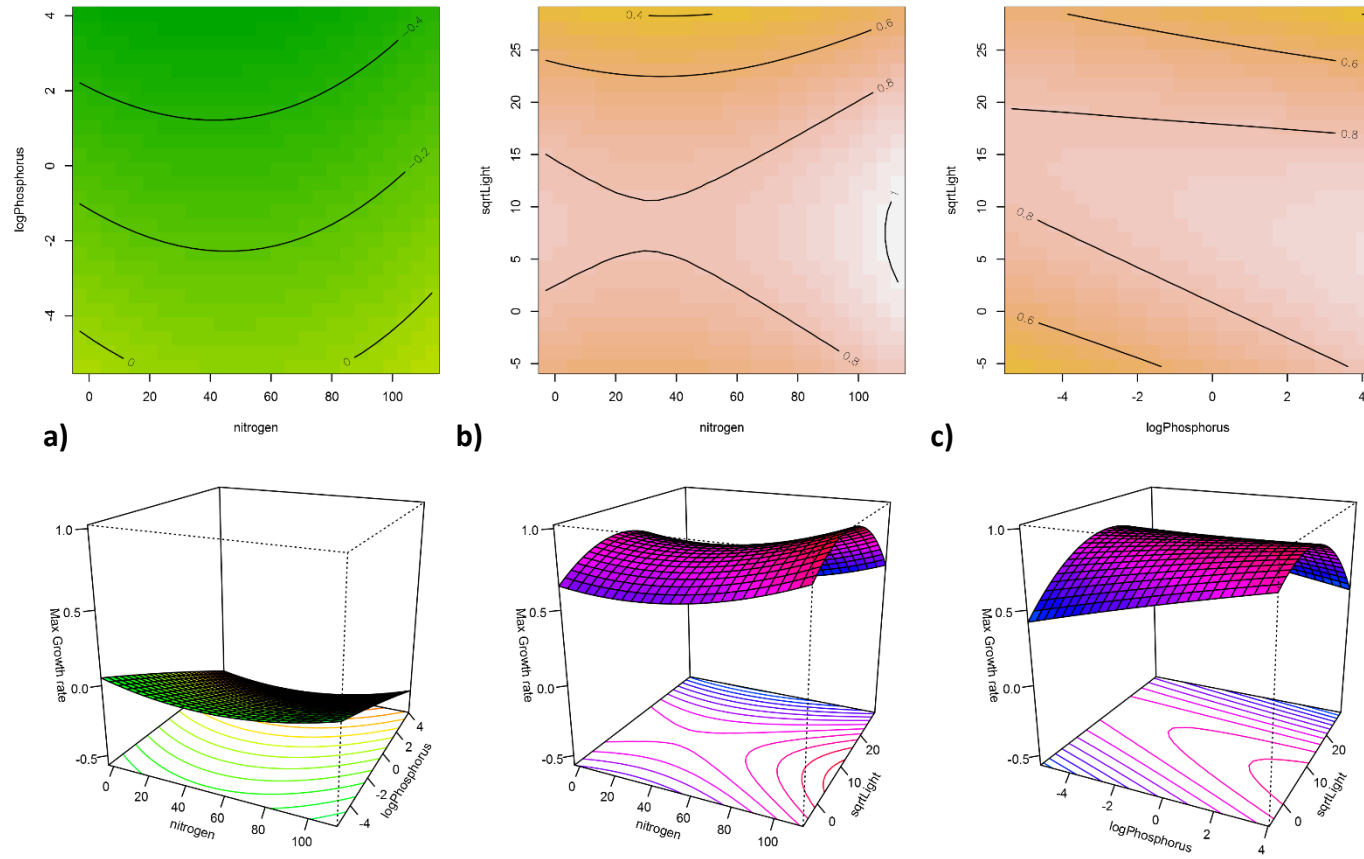


Figure 6. Contour plots (upper pane) and response surface plots (lower pane) showing maximum growth rates in response to combinations: (a) nitrogen (nitrate-N) and log-transformed phosphorus (phosphate-P) (b) square root-transformed light and nitrogen (nitrate-N) (c) square root-transformed light and log-transformed phosphorus (phosphate-P). Contour lines show maximum growth rates (day⁻¹).

3.5 Discussion

3.5.1 Comparison of phycocyanin measurements undertaken by sensor and spectrophotometry

Phycocyanin measurements of *M. aeruginosa* were compared using two methods; spectrophotometry and a phycocyanin sensor. There was only a weak relationship between the two methods ($R^2=0.18$), in contrast to other studies such as Hodges (2016), who found a strong relationship ($R^2=0.63$). The most likely reason for this difference is that the phycocyanin concentrations measured in this study ranged from 76-236 $\mu\text{g L}^{-1}$, which is much lower than those used in Hodges (2016; 195-1,594 $\mu\text{g L}^{-1}$). The results in Chapter 2 of this research suggest that the linear working range for the sensor for *M. aeruginosa* is 100 to 500 $\mu\text{g L}^{-1}$. The sensor results are within the expected linear range for the most part, yet may have been skewed by the readings that were not within this range. Similarly, it is likely that low concentrations limited the accuracy of the measurements taken with spectrophotometry, although a full assessment of this was not undertaken.

An alternative explanation may be the influence of extracellular phycocyanin. The sensor may have detected extracellular phycocyanin (Bastien et al. 2011) in the treatment samples, whereas spectrophotometry can only determine the phycocyanin extracted from the cells that were collected on filter paper (Hagerthey et al. 2006). If extracellular phycocyanin was present in the treatments of this study, the spectrophotometry may have underestimated the phycocyanin content compared to the sensor. Hodges (2016) measured phycocyanin with sensors in the field and found that in samples containing high biomass (17-27 mm^3

L⁻¹), 20% of the phycocyanin was extracellular. Most of the treatments in this study had biovolumes around 20 mm³ L⁻¹ at day 22. This could explain why the sensor measured higher phycocyanin values for many of the treatments on day 22.

3.5.2 Comparing phycocyanin quotas at day 18 to day 22

Phycocyanin quotas for *M. aeruginosa* were generally higher at day 18 than at day 22. For many treatments, this aligned to the period of exponential growth. Yamamoto & Shiah (2010) found the highest growth rate between 0 and 14 days for *M. aeruginosa* grown in flasks. A limited number of studies have examined the changes in phycocyanin over the growth phase. Peng et al. (2016) found the highest phycocyanin concentrations of 8 mg L⁻¹ in *M. aeruginosa* on day 12 at the end of the exponential growth phase. Chang et al. (2012) found phycocyanin quotas started to decrease after exponential growth at day 10 of the growth phase for *M. aeruginosa*. This study has yielded similar results and added to the knowledge of changes in phycocyanin quota over the growth cycle.

3.5.3 Effects of nutrients and light on phycocyanin quotas

Phycocyanin quotas in *M. aeruginosa* were affected differently by nutrients and light on day 18 compared to day 22. On day 18 the RSM indicated that high light, low nitrate-N and high phosphate-P (N<60: P>1: I>300) would result in the highest phycocyanin quotas. On day 22, high nitrate-N, high phosphate-P and low light intensity (N>50: P>0.52: I<200) yielded high phycocyanin quotas across the 20 treatments. Chaneva et al. (2007) found that light of around 150 $\mu\text{mol m}^{-2} \text{s}^{-1}$ produced the highest phycocyanin quota in *Arthronema africanum* in an

optimisation study. Raps et al. (1983) had higher phycocyanin to chlorophyll ratios at higher light intensities, up to $565 \mu\text{mol m}^{-2} \text{s}^{-1}$, and found adaptation responses to low light of $20 \mu\text{mol m}^{-2} \text{s}^{-1}$ for *M. aeruginosa*. Hesse et al. (2001) reported changes in photosystems one and two (PSI/PSII) ratio at lower light levels and increased phycocyanin content. This enhanced response to both high and low light was observed in the current study as phycocyanin quotas were dependent on second order light. On day 18 phycocyanin quotas had a greater response to high light than day 22 where phycocyanin quotas had a greater response to low light (i.e., the response went from high to low from day 18 to day 22). This may be due to *M. aeruginosa* having photoacclimation adaptations to both high and low light (Ibelings et al. 1994).

Optimisation studies have used nitrogen to generate large quantities of phycocyanin for industrial production purposes. Khattar et al. (2015) found high nitrogen of ca. 140 mg L^{-1} produced the highest phycocyanin content of $696 \mu\text{g mg}^{-1}$ dry weight in *Dolichospermum/Anabaena fertilissima*. Hemlata (2009) reported a species of *Dolichospermum* to have the highest phycobiliprotein content of 91.54 mg g^{-1} dry weight at nitrogen concentrations of 71.4 mg L^{-1} . Singh et al. (2009) optimised the phycocyanin content of 0.73 mg mL^{-1} in *P. ceylanicum* using nitrate-N of 450 mg L^{-1} . Chang et al. (2012) tested three species and found that all had different phycocyanin quotas under batch culture concentrations of nitrate-N 1500 mg L^{-1} . These studies show how various species under high nutrients and low light conditions can optimise phycocyanin quotas.

Three factors that can also contribute to low phycocyanin quotas are discussed here. Rastogi et al. (2015) reported a decrease in phycobiliproteins over a range of acid and alkaline pH values. Liu et al. (2009) found that a high pH of 12 decreased phycobiliproteins in *Polysiphonia urceolata*. Hemlata (2009) found a pH of 8 favored phycobiliprotein production in a *Dolichospermum* species. The treatments in this study had an initial pH value of 7 in each treatment and increased to pH of 12 at the end of the experimental period. Xing et al. (2007) found iron limitation reduced phycocyanin content in *M. aeruginosa*, while iron replete increased phycocyanin concentrations. Chaneva et al. (2007) optimised phycocyanin dry weight of *A. africanum* at a temperature of 36°C, the light of 150 $\mu\text{mol m}^{-2} \text{s}^{-1}$ and 420 mg L^{-1} of nitrogen. The factors listed above may have resulted in differences in phycocyanin across treatments and over time.

3.5.4 Effects of nutrients and light intensity on growth rates

In the current study, the surface response approximation showed that growth rates were higher when the light was around 100 $\mu\text{mol m}^{-2} \text{s}^{-1}$, nitrate-N was above 60 mg L^{-1} , and phosphate-P was above 0.52 mg L^{-1} . Talbot et al. (1991) found *Phormidium bohneri* and *Planktothrix agardhii* growth rates of 0.6 and 1.5 day^{-1} , respectively with light <255 $\mu\text{mol m}^{-2} \text{s}^{-1}$. Hesse et al. (2001) found two strains of *M. aeruginosa* both had growth rates of ca.0.21 day^{-1} at low light 38 $\mu\text{mol m}^{-2} \text{s}^{-1}$. In addition, Yamamoto & Shiah (2010) had growth rates of 0.26 and 0.31 day^{-1} for two strains of *M. aeruginosa* at a light intensity of 100 $\mu\text{mol m}^{-2} \text{s}^{-1}$. High growth rates from these studies compare to a growth rate of 0.78 day^{-1} at a light intensity

of $100 \mu\text{mol m}^{-2} \text{s}^{-1}$ in the current study, likely around the optimum light intensity for *M. aeruginosa*.

The estimates for nutrients for increased growth rate response from the RSM in this study were similar to a study by Jiang et al. (2008), who demonstrated that increasing nitrogen to 357 mg L^{-1} and phosphorus to 6 mg L^{-1} increased the growth rate (dry weight) of *M. aeruginosa*, with no significant interaction effects. The RSM model of Jiang et al. (2008) gave lower bounds for growth with the nitrogen of 91 mg L^{-1} , phosphorus of 3.3 mg L^{-1} , and light of $81 \mu\text{mol m}^{-2} \text{s}^{-1}$. Lürting et al. (2017) found growth rates of $0.46\text{-}0.59 \text{ day}^{-1}$ over a 6-day period for two strains of *M. aeruginosa* when pond water was spiked with nitrogen at 14 mg L^{-1} and phosphorus at 1.4 mg L^{-1} . Growth rates were tested by Vézie et al. (2002) using similar phosphorus ranges to this study. Vézie et al. (2002) had the highest growth (dry weight) in four strains of *Microcystis* sp. with nitrogen $>40 \text{ mg L}^{-1}$ and phosphorus from 0.28 to 0.55 mg L^{-1} . They state that high nitrogen was more important for growth than phosphorus, with all strains not growing under high phosphorus (5.5 mg L^{-1}) and low nitrogen (0.84 mg L^{-1}). This did not align with the current study, where the RSM gave slight increases in growth rates with increases in phosphorus $>0.52 \text{ mg L}^{-1}$ and light of $100 \mu\text{mol m}^{-2} \text{s}^{-1}$.

The differences in growth responses to nutrients between Vézie et al. (2002) and this study may be due to cell starvation prior to the commencement of the experiment in the study by Vézie et al. (2002). Nutrient starvation may have increased the growth response of all four strains to nutrients. The current study

did not undertake a nutrient starvation prior to inoculation. This may have led to cells having large intracellular nutrient stores (Singh et al. 2009) and might explain the lack of response in growth rates across the range of nutrients and light.

Neither phycocyanin quotas nor growth rates were fully optimised with the ranges of nutrients and light used in the current study. Phycocyanin quotas varied between nitrogen, phosphorus and light treatments. These are all factors that change temporally and spatially in a lake environment and could help explain the variable (and often weak) relationships between phycocyanin and biovolume observed in the field studies. To advance the use of sensors as a monitoring tool for cyanobacteria there would ideally need to be multi-sensor sampling in lakes which would include nitrate, phosphate, irradiance and phycocyanin sensors as an integrated platform. This could help provide identify variables generating variability between phycocyanin and biovolume. Further studies with different sensors are needed to explore the universality of phycocyanin responses in *M. aeruginosa*. In future work, considerations could be given to the use of Pulse Amplitude Modulated Fluorometry (PAM) as a measurement of photosynthetic health (Marinho et al. 2013; Lüring et al. 2017). PAM measures the photosynthetic pigment fluorescence as an indicator of photosynthetic energy conversion. This measurement could help compare different pigment ratios from different treatments of nutrients, and light. This may help to better the optimum nutrient concentrations for growth rate and phycocyanin quota responses in *M. aeruginosa*.

3.6 References

- Anderson, M., & Whitcomb, P. (2005). *RSM simplified : Optimizing processes using response surface methods for design of experiments*. New York, New York: Productivity Press.
- Bastien, C., Cardin, R., Veilleux, E., Deblois, C., Warren, A., & Laurion, I. (2011). Performance evaluation of phycocyanin probes for the monitoring of cyanobacteria. *Journal of Environmental Monitoring*, 13, 110–118. <https://doi.org/10.1039/c0em00366b>.
- Bennett, A., & Bogorad, L. (1973). Complementary chromatic adaption in a filamentous blue-green alga. *The Journal of Cell Biology*, 58, 419–435. <https://doi.org/10.1083/jcb.58.2.419>.
- Bolch, C. J. S., & Blackburn, S. I. (1996). Isolation and purification of Australian isolates of the toxic cyanobacterium *Microcystis aeruginosa* Kutz. *Journal of Applied Phycology*, 8(1), 5–13. Retrieved from <https://doi.org/10.1007/BF02186215>.
- Campbell, D. A., Hurry, V., Clarke, K., Gustafsson, P., & Oquist, G. (1998). Chlorophyll fluorescence analysis of cyanobacterial photosynthesis and acclimation. *Microbiology and Molecular Biology Reviews : MMBR*, 62(3), 667–683. <https://doi.org/10.1093/mmb/62.3.667>.
- Carey, C. C., Ibelings, B. W., Hoffmann, E. P., Hamilton, D. P., & Brookes, J. D. (2012). Eco-physiological adaptations that favour freshwater cyanobacteria in a changing climate. *Water Research*, 46(5), 1394–1407. <https://doi.org/10.1016/j.watres.2011.12.016>.

- Chaneva, G., Furnadzhieva, S., Minkova, K., & Lukavsky, J. (2007). Effect of light and temperature on the cyanobacterium *Arthronema africanum* - A prospective phycobiliprotein-producing strain. *Journal of Applied Phycology*, 19(5), 537–544. <https://doi.org/10.1007/s10811-007-9167-6>.
- Chang, D. W., Hobson, P., Burch, M., & Lin, T. F. (2012). Measurement of cyanobacteria using *in-vivo* fluoroscopy - Effect of cyanobacterial species, pigments, and colonies. *Water Research*, 46(16), 5037–5048. <https://doi.org/10.1016/j.watres.2012.06.050>.
- Chorus, I., & Bartram, J. (Eds.). (1999). Toxic Cyanobacteria in Water: A Guide to their Public Health Consequences, Monitoring and Management. London, U.K.: Taylor & Francis.
- Glazer, A. N. (1976). Phycocyanins : Structure and Function. In *In photochemical and photobiological reviews* (pp. 71–115). US: Springer International Publishing.
- Hagerthey, S. E., William Louda, J., & Mongkronsri, P. (2006). Evaluation of pigment extraction methods and a recommended protocol for periphyton chlorophyll *a* determination and chemotaxonomic assessment. *Journal of Phycology*, 42(5), 1125–1136. <https://doi.org/10.1111/j.1529-8817.2006.00257.x>.
- Hamilton, D. P., Carey, C. C., Arvola, L., Arzberger, P., Brewer, C., Cole, J. J., Gaiser, E., Hanson, P. C., Ibelings, B. W., Jennings, E., Kratz, T K., Lin, F. P., McBride, C. G., de Motta Marques, D., Muraoka, K., Nishri, A., Qin, B., Read, J. S., Rose, K. C., Ryder, E., Weathers, K. C., Zhu, G., Trolle, D., & Brookes, J. D. (2015). A Global lake ecological observatory network (GLEON) for synthesising high-

frequency sensor data for validation of deterministic ecological models.

Inland Waters, 5(1), 49–56. <https://doi.org/10.5268/IW-5.1.566>.

Hemlata, F. T. (2009). Screening of cyanobacteria for phycobiliproteins and effect of different environmental stress on its yield. *Bulletin of Environmental Contamination and Toxicology*, 83(4), 509–515. <https://doi.org/10.1007/s00128-009-9837-y>.

Hesse, K., Dittmann, E., & Börner, T. (2001). Consequences of impaired microcystin production for light-dependent growth and pigmentation of *Microcystis aeruginosa* PCC 7806. *FEMS Microbiology Ecology*, 37(1), 39–43. [https://doi.org/10.1016/S0168-6496\(01\)00142-8](https://doi.org/10.1016/S0168-6496(01)00142-8).

Hodges, C. (2016). *A validation study of phycocyanin sensors for monitoring cyanobacteria in cultures and field samples*. University of Waikato, Hamilton.

Ibelings, B. W., Kroon, B. M. a., & Mur, L. R. (1994). Acclimation of photosystem II in a cyanobacterium and a eukaryotic green alga to high and fluctuating photosynthetic photon flux densities, simulating light regimes induced by mixing in lakes. *New Phytologist*, 128(3), 407–424. <https://doi.org/10.1111/j.1469-8137.1994.tb02987.x>.

Izydorczyk, K., Carpentier, C., Mrówczyński, J., Wagenvoort, A., Jurczak, T., & Tarczyńska, M. (2009). Establishment of an Alert Level Framework for cyanobacteria in drinking water resources by using the Algae Online Analyser for monitoring cyanobacterial chlorophyll *a*. *Water Research*, 43(4), 989–996. <https://doi.org/10.1016/j.watres.2008.11.048>.

Jiang, Y., Ji, B., Wong, R. N. S., & Wong, M. H. (2008). Statistical study on the effects

- of environmental factors on the growth and microcystins production of bloom-forming cyanobacterium-*Microcystis aeruginosa*. *Harmful Algae*, 7(2), 127–136. <https://doi.org/10.1016/j.hal.2007.05.012>.
- Khattar, J. I. S., Kaur, S., Kaushal, S., Singh, Y., Singh, D. P., Rana, S., & Gulati, A. (2015). Hyperproduction of phycobiliproteins by the cyanobacterium *Anabaena fertilissima* PUPCCC 410.5 under optimized culture conditions. *Algal Research*, 12, 463–469. <https://doi.org/10.1016/j.algal.2015.10.007>.
- Kong, Y., Lou, I., Zhang, Y., Lou, C. U., & Mok, K. M. (2014). Using an online phycocyanin fluorescence probe for rapid monitoring of cyanobacteria in Macau freshwater reservoir. *Hydrobiologia*, 741(1), 33–49. <https://doi.org/10.1007/s10750-013-1759-3>.
- Lawton, L., Marsalek, B., Padisák, J., & Chorus, I. (1999). Determination of cyanobacteria in the laboratory. In I. Chorus & J. Bartram (Eds.), *Toxic Cyanobacteria in Water: A Guide to their Public Health Consequences, Monitoring and Management* (pp. 203-216). London, U.K.: Taylor & Francis.
- Lenth, R. (2016). Response-Surface Analysis. CRAN. [computer software]. Retrieved January 10 2017, from <https://cran.r-project.org/web/packages/rsm/rsm.pdf>.
- Lenth, R. V. (2012). Surface plots in the rsm package, 7. Retrieved January 17, 2017, from <https://cran.r-project.org/web/packages/rsm/vignettes/rsm-plots.pdf>.
- Liu, L. N., Su, H. N., Yan, S. G., Shao, S. M., Xie, B. Bin, Chen, X. L., Zhang, X. Y., Zhou, B. C., Zhang, Y. Z. (2009). Probing the pH sensitivity of R-phycoerythrin: Investigations of active conformational and functional variation. *Biochimica*

et Biophysica Acta - Bioenergetics, 1787(7), 939–946.

<https://doi.org/10.1016/j.bbabbio.2009.02.018>.

Lürling, M., van Oosterhout, F., & Faassen, E. (2017). Eutrophication and warming boost cyanobacterial biomass and microcystins. *Toxins*, 9(2), 64. <https://doi.org/10.3390/toxins9020064>.

Marinho, M. M., Souza, M. B. G., & Lürling, M. (2013). Light and Phosphate Competition Between *Cylindrospermopsis raciborskii* and *Microcystis aeruginosa* is Strain Dependent. *Microbial Ecology*, 66(3), 479–488. <https://doi.org/10.1007/s00248-013-0232-1>.

NIWA. (n.d.). Algal monitoring service. NIWA (National Institute of Water and Atmospheric Research, New Zealand. Retrieved May 1, 2017, from www.niwa.co.nz/our-science/freshwater/our-services/specialist-analytical-services/algae-monitoring-service.

Paerl, H. W., & Otten, T. G. (2013). Harmful cyanobacterial blooms: causes, consequences, and controls. *Microbial Ecology*, 65(4), 995–1010. <https://doi.org/10.1007/s00248-012-0159-y>.

Peng, G., Fan, Z., Wang, X., & Chen, C. (2016). Photosynthetic response to nitrogen source and different ratios of nitrogen and phosphorus in toxic cyanobacteria, *Microcystis aeruginosa* FACHB-905. *Journal of Limnology*, 75(3), 560–570. <https://doi.org/10.4081/jlimnol.2016.1458>.

R Core Team. (2017). R: A language and environment for statistical computing. *R Foundation for Statistical Computing*, Vienna, Austria. URL <https://www.R-project.org/>.

- Raps, S., Wyman, K., Siegelman, H. W., & Falkowski, P. G. (1983). Adaptation of the cyanobacterium *Microcystis aeruginosa* to light intensity. *Plant Physiology*, 72(3), 829–832. <https://doi.org/10.1104/pp.72.3.829>.
- Rastogi, R. P., Sonani, R. R., & Madamwar, D. (2015). Physico-chemical factors affecting the in vitro stability of phycobiliproteins from *Phormidium rubidum* A09DM. *Bioresource Technology*, 190, 219–226. <https://doi.org/10.1016/j.biortech.2015.04.090>.
- Shevela, D., Pishchalnikov, R. Y., Eichacker, L. A., & Govindjee. (2013). Oxygenic Photosynthesis in Cyanobacteria. In *Stress Biology of Cyanobacteria* (pp. 3–40). <https://doi.org/10.1201/b13853-3>.
- Singh, N. K., Parmar, A., & Madamwar, D. (2009). Optimization of medium components for increased production of C-phycocyanin from *Phormidium* *ceylanicum* and its purification by single step process. *Bioresource Technology*, 100(4), 1663–1669. <https://doi.org/10.1016/j.biortech.2008.09.021>.
- Talbot, P., Thébault, J., Dauta, A., & De la Noüe, J. (1991). A comparative study and mathematical modeling of temperature, light and growth of three microalgae potentially useful for wastewater treatment. *Water Research*, 25(4), 465–472. [https://doi.org/10.1016/0043-1354\(91\)90083-3](https://doi.org/10.1016/0043-1354(91)90083-3).
- Vézie, C., Rapala, J., Vaitomaa, J., Seitsonen, J., & Sivonen, K. (2002). Effect of nitrogen and phosphorus on growth of toxic and nontoxic *Microcystis* strains and on intracellular microcystin concentrations. *Microbial Ecology*, 43(4), 443–454. <https://doi.org/10.1007/s00248-001-0041-9>.

Wood, S. A., Borges, H., Puddick, J., Biessy, L., Atalah, J., Hawes, I., Dietrich, D. R., & Hamilton, D. P. (2017). Contrasting cyanobacterial communities and microcystin concentrations in summers with extreme weather events: insights into potential effects of climate change. *Hydrobiologia*, 785(1), 71–89. <https://doi.org/10.1007/s10750-016-2904-6>.

Wood, S. A., Hamilton, D. P., Paul, W. J., Safi, K. A., & Williamson, W. M. (2009). *New Zealand Guidelines for Cyanobacteria in Recreational Fresh Waters – Interim Guidelines*. Publication number ME 981, prepared for the Ministry for the Environment and the Ministry of Health. Ministry for the Environment, Wellington, New Zealand. 88p. <http://www.mfe.govt.nz/sites/default/files/nz-guidelines-cyanobacteria-recreational-fresh-waters.pdf>.

Wood, S. A., Paul, W. J., & Hamilton, D. P. (2008). *Cyanobacterial Biovolumes for the Rotorua Lakes*. Cawthron Report No. 1504, prepared for Environment Bay of Plenty. 27p. <https://www.boprc.govt.nz/media/32233/Cawthron-090803-CyanobacterialbiovolumesforRotorualakes.pdf>.

Xing, W., Huang, W. M., Li, D. H., & Liu, Y. D. (2007). Effects of iron on growth, pigment content, photosystem II efficiency, and siderophores production of *Microcystis aeruginosa* and *Microcystis wesenbergii*. *Current Microbiology*, 55(2), 94–98. <https://doi.org/10.1007/s00284-006-0470-2>.

Yamamoto, Y., & Shiah, F. K. (2010). Variation in the growth of *Microcystis aeruginosa* depending on colony size and position in colonies. *Annales de Limnologie - International Journal of Limnology*, 46(1), 47–52. <https://doi.org/10.1051/limn/2010006>.

Zamyadi, A., McQuaid, N., Dorner, S., Bird, D. F., Burch, M., Baker, P., Hobson, P.,
& Prévost, M. (2012). Cyanobacterial detection using *in vivo* fluorescence
probes: Managing interferences for improved decision-making. *Journal -
American Water Works Association.*
<https://doi.org/10.5942/jawwa.2012.104.0114>.

Chapter 4

Conclusion

This study demonstrated that a phycocyanin sensor could be used to increase efficiency for cyanobacteria monitoring programs provided considerations are made for the factors that can contribute to interference in the field and factors that may weaken the phycocyanin to biovolume relationship.

In the field studies, there were moderate to strong relationships between phycocyanin and biovolume, but relationships varied amongst individual lakes and years. The most obvious causes for the variability in this relationship were changes in cyanobacterial abundance and the species present. Eutrophic lakes with high biovolumes ($>1.8 \text{ mm}^3 \text{ L}^{-1}$) which were mostly dominated by a single species had stronger relationships between phycocyanin and biovolume than lakes with lower biovolumes ($<1.8 \text{ mm}^3 \text{ L}^{-1}$) and a mixed species composition.

Regression equations from the field studies were used to predict a phycocyanin threshold suited for recreational monitoring of cyanobacteria. Using the green ($<0.5 \text{ mm}^3 \text{ L}^{-1}$), amber ($0.5 < 1.8 \text{ mm}^3 \text{ L}^{-1}$), and red (>1.8 or $10 \text{ mm}^3 \text{ L}^{-1}$) biovolume thresholds to predict phycocyanin thresholds, a value of $>40 \text{ } \mu\text{g L}^{-1}$ approximated a health warning exceeding a biovolume of $1.8 \text{ mm}^3 \text{ L}^{-1}$. The phycocyanin threshold of $>40 \text{ } \mu\text{g L}^{-1}$ for biovolume of $1.8 \text{ mm}^3 \text{ L}^{-1}$ was consistent across lakes with strong relationships between phycocyanin and biovolume (Lake Rotoehu). This phycocyanin threshold could be used to prioritise high-risk samples for

enumeration of cyanobacteria. The phycocyanin sensor allows more sites to be assessed and fewer low-biovolume ($<0.5 \text{ mm}^3 \text{ L}^{-1}$) samples to be enumerated.

Consideration, however, needs to be given to factors which contribute to variation in relationships between phycocyanin and biovolume in the field, such as community composition, bubble interferences, physical factors (e.g., light and temperature), and extracellular phycocyanin. These factors may potentially interact synergistically to increase error in the relationship. Sensor shade caps can reduce effects of high light to cells during readings and auto-ranging functions reduce the occurrence of non-detection or saturation levels. These two considerations could increase the reliability of a phycocyanin sensor for cyanobacterial biomass assessment.

In the dilution experiments of the four cultured species (one single cell, one coiled filamentous colonial, one bunched filamentous colonial, and one large globular colonial) an in-depth assessment of the phycocyanin to biovolume relationship was investigated in a controlled laboratory environment. Three different assessments were carried out on the data produced by the dilution series of each species to, 1) gain insight into variation in phycocyanin readings based on morphological differences, 2) find the minimum phycocyanin detection limits of each species observed at the end of the dilution series, and 3) to assess if there were non-linear relationships between phycocyanin and biovolume at lower concentrations of biovolume using a segmented regression and breakpoint analysis.

The experiment indicated that low densities and colonial morphology resulted in inaccuracies in phycocyanin measurements relative to the biovolume present. There was high variability in sensor phycocyanin readings for large colonial *Microcystis wesenbergii*. At the end of the dilution series, each species had a minimum phycocyanin detection limit. These were between 30-90 $\mu\text{g L}^{-1}$. The minimum phycocyanin detection limits corresponded to biovolumes of 0.2-0.5 $\text{mm}^3 \text{L}^{-1}$. The ability of the minimum phycocyanin detection limits to provide a consistent biovolume threshold ($<0.5 \text{ mm}^3 \text{L}^{-1}$) was unreliable for recreational guideline values. This led to the further assessment of the phycocyanin to biovolume relationship using breakpoint analysis.

From breakpoint analysis, there was evidence of change in phycocyanin responses from above and below the breakpoint which was significant for the three colonial species. This provided a quantitative evaluation of the previously observed minimum phycocyanin detection limits by the sensor. The breakpoint phycocyanin values were considerably higher than the minimum phycocyanin detection limits. The non-linear relationships illustrate that biovolume predicted from phycocyanin for the $1.8 \text{ mm}^3 \text{L}^{-1}$ threshold could not be obtained for two of the four species. This may be due to different phycocyanin quotas in different species (*M. wesenbergii* and *D. lemmermannii*). The large cell size has possibly strengthened the relationship. This research offers new data on the use of a phycocyanin sensor for recreational monitoring. The minimum phycocyanin detection limits and the breakpoint phycocyanin values are contrasting to many literature values, where

sensor detection limits gave biovolumes three times lower than those found in this study.

A Central Composite design experiment was used to investigate the effects of nitrogen, phosphorus, and light on growth and phycocyanin quotas in the common bloom-forming species of cyanobacterium, *Microcystis aeruginosa*. Twenty treatments with varying combinations of nitrogen, phosphorus, and light were set up in replicate (n=3) trials which examined phycocyanin quotas and biomass of *M. aeruginosa* over 22 (treatment 2-20) or 26 days (treatment 1). The sensor was able to detect phycocyanin at the minimum biomass of 40,000 cells mL⁻¹. Phycocyanin quotas varied across treatment and different days over the experiment. Maximum growth rates were gained by different treatments between different days and were therefore in different growth phases over the course of the experiment.

At the endpoint of the experiment, the sensor phycocyanin was compared to spectrophotometry extracted phycocyanin. A weak relationship was obtained contrasting other studies that have found a strong relationship between these methods. This was attributed to some samples falling outside of the linear range (100-500 µg L⁻¹) of the sensor for *M. aeruginosa* phycocyanin (previously established from the segmented regression in Chapter 2). In addition, the presence of extracellular phycocyanin in samples could have increased the sensor phycocyanin while the spectrophotometry could only detect the extracted phycocyanin from the samples.

Students t-tests showed that four treatments had significantly higher phycocyanin quotas on day 18 compared to day 22. While the RSM indicated that phycocyanin quotas on day 18 responded to high irradiance ($>300 \mu\text{mol m}^{-2} \text{s}^{-1}$), relatively low nitrogen ($<50 \text{ mg L}^{-1}$) and relatively high phosphorus ($>1 \text{ mg L}^{-1}$) compared to day 22 where low light ($< \text{ca. } 100 \mu\text{mol m}^{-2} \text{s}^{-1}$), high nitrogen ($>50 \text{ mg L}^{-1}$) and high phosphorus ($>1 \text{ mg L}^{-1}$) produced higher phycocyanin quotas. RSM indicated moderate light ($<300 \mu\text{mol m}^{-2} \text{s}^{-1}$), high nitrogen ($>60 \text{ mg L}^{-1}$) and high phosphorus ($>0.52 \text{ mg L}^{-1}$) elevated growth rates. These results demonstrate that there is a need for further research to assess changes in phycocyanin quota over the growth cycle, under different nutrient and light conditions, and for different cyanobacteria species. Differences in phycocyanin quotas at different growth stages will contribute to variation in the phycocyanin to biovolume relationship.

This research has helped to assess changes in phycocyanin quotas in response to changing nutrient and light levels that can occur in lake environments. It could help to use phycocyanin sensors coupled with multi-sensor applications for detecting an array of variables (nutrients, light, and phycocyanin) which may provide information on the effects of environmental variables on phycocyanin quotas. Collectively, the data presented from this research offer insight into the opportunities and challenges of using a phycocyanin sensor as a field monitoring tool for cyanobacteria biomass. Phycocyanin quotas vary with time, location and species, however, when biovolumes exceed the $>10 \text{ mm}^3 \text{ L}^{-1}$ threshold a sensor may be more reliable. This can greatly increase sampling frequency and spatial extent and may lead to improved protection of human health from the toxicity associated with cyanobacteria blooms.

Appendices

Appendix 1. Analysis of Similarity (ANOSIM) statistics for tests of cyanobacteria (cell counts) composition with location in 2016. Similarity R-value and significance level (%) of similarity (0-100) values in bold were significantly different $p < 0.1\%$ ($P < 0.01$).

Comparison		R-	Significance
Location 1	Location 2	value	Level %
Kaituna	Okaro	0.28	0.2
Kaituna	Rotoehu	0.74	0.1
Kaituna	Rotoiti	0.00	46
Kaituna	Rotorua	-0.11	99.7
Kaituna	Tarawera	0.41	0.2
Okaro	Rotoehu	0.63	0.1
Okaro	Rotoiti	0.30	0.1
Okaro	Rotorua	0.06	6.2
Okaro	Tarawera	0.23	9.2
Rotoehu	Rotoiti	0.43	0.1
Rotoehu	Rotorua	0.30	0.1
Rotoehu	Tarawera	0.94	0.1
Rotoiti	Rotorua	0.14	0.1
Rotoiti	Tarawera	0.34	0.1
Rotorua	Tarawera	0.10	10.9

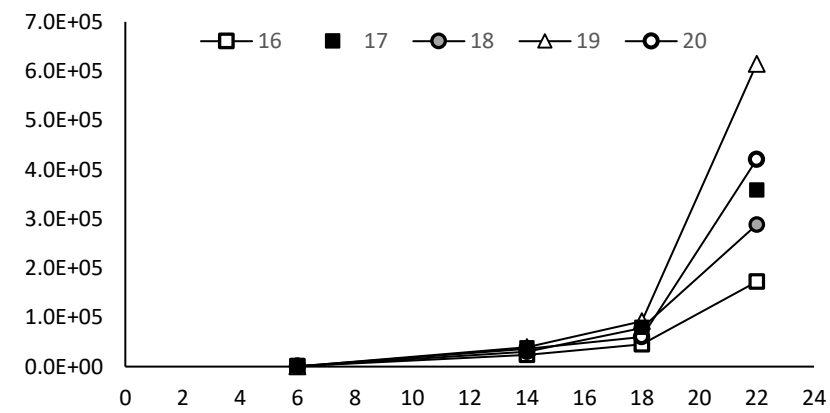
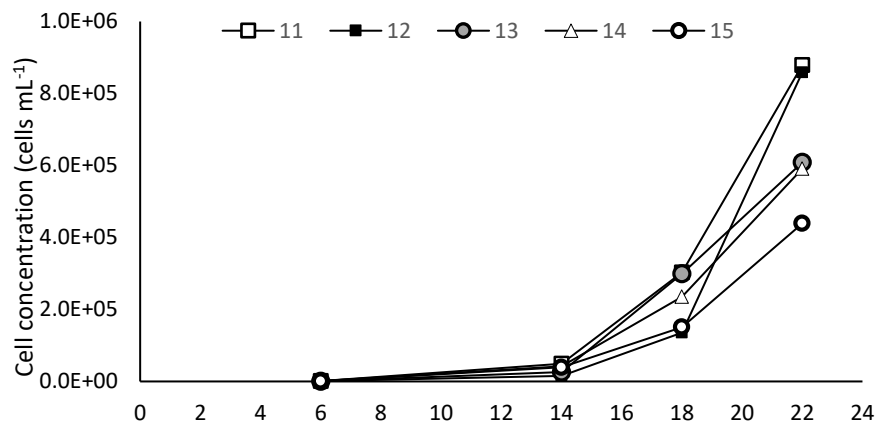
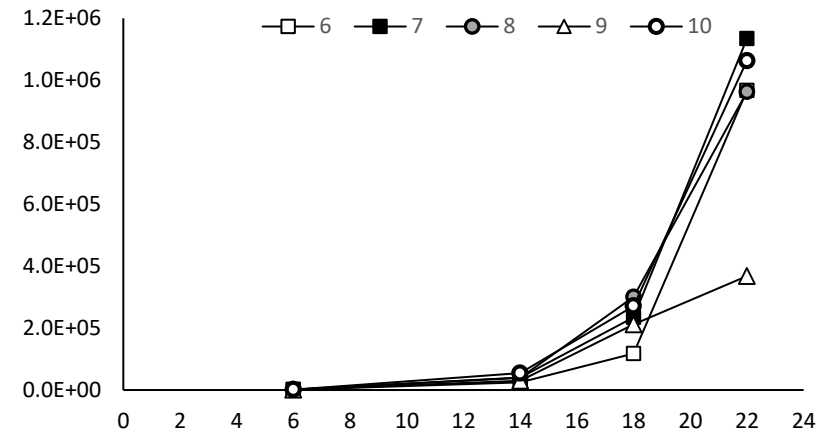
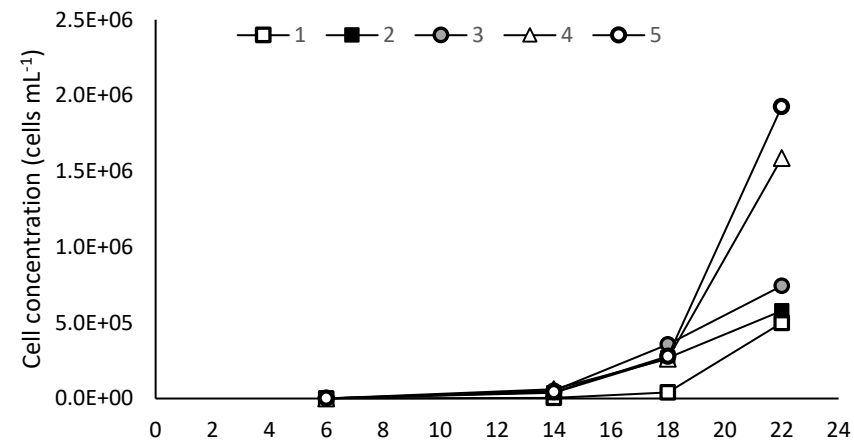
Appendix 2. Analysis of Similarity (ANOSIM) statistics for tests of cyanobacteria (cell counts) composition with location in 2017. Similarity R-value and significance level (%) of similarity (0-100) values in bold were significantly different $p < 0.1\%$ ($P < 0.01$).

Comparison		R	Significance
Location 1	Location 2	Statistic	Level %
Kaituna	Okaro	0.47	0.1
Kaituna	Rotoehu	0.69	0.1
Kaituna	Rotoiti	0.00	45.6
Kaituna	Rotorua	-0.04	83.2
Kaituna	Tarawera	0.21	0.2
Okaro	Rotoehu	0.03	28.5
Okaro	Rotoiti	0.34	0.1
Okaro	Rotorua	0.22	0.1
Okaro	Tarawera	0.65	0.1
Rotoehu	Rotoiti	0.43	0.1
Rotoehu	Rotorua	0.41	0.1
Rotoehu	Tarawera	0.78	0.1
Rotoiti	Rotorua	0.05	1.2
Rotoiti	Tarawera	0.09	7.9
Rotorua	Tarawera	0.02	33

Appendix 3. Average (n=3) for twenty treatments with the average (n=3) biomass (cells mL⁻¹), sensor phycocyanin (µg L⁻¹), and biovolume (mm³ L⁻¹) all measured at day 18 and 22, and the pH measured from treatments controls (species) on day 22.

Treatment (n=3)	Day 18 biomass (cells mL ⁻¹)	Day 22 biomass (cells mL ⁻¹)	Day 18 Sensor phycocyanin (µg L ⁻¹)	Day 22 Sensor phycocyanin (µg L ⁻¹)	Day 18 Biovolume (mm ³ L ⁻¹)	Day 22 Biovolume (mm ³ L ⁻¹)	Day 22 pH
1	39,423	499,188	61	160	1.44	18.22	9.91
2	268,209	578,436	100	140	9.79	21.11	11.51
3	357,702	742,826	117	76	13.05	27.11	11.34
4	261,047	1,585,657	118	235	9.53	57.86	12.33
5	278,031	1,926,060	121	236	10.15	70.28	12.07
6	117,573	966,836	74	168	4.29	35.28	10.77
7	234,376	1,134,320	74	180	8.55	41.39	10.76
8	300,677	962,486	78	167	10.97	35.12	9.18
9	211,264	367,728	70	118	7.71	13.42	9.21
10	271,093	1,063,085	84	174	9.89	38.79	11.22
11	302,435	878,744	75	95	11.04	32.07	10.79
12	135,171	858,625	82	169	4.93	31.33	10.72
13	299,313	608,176	81	157	10.92	22.19	10.8
14	235,194	590,850	85	173	8.58	21.56	10.74
15	150,617	438,738	79	149	5.50	16.01	10.13
16	44,954	172,303	48	90	1.64	6.29	9.73
17	79,855	358,794	43	107	2.91	13.09	10.53
18	107,542	287,990	59	120	3.92	10.51	9.95
19	135,960	614,451	57	153	4.96	22.42	9.95
20	60,295	420,457	52	119	2.20	15.34	9.73

Appendix 4. Average cell concentrations (n=3) for *Microcystis aeruginosa* in 20 treatments from day 6 to 22.



Appendix 5. Outputs of Response Surface Methodology analysis for phycocyanin quotas at day 18. Response estimates for nitrate-N; N, log-transformed phosphate-P; P, square root light; I, second order terms for these variables. x^2 is shown in the “estimate” column followed by standard error, T values and probability. Significant values are in bold.

	Estimate	Std Error	T value	Probability (> t)
Intercept	0.65	0.059	10.97	0.000
N	0.05	0.082	0.59	0.561
P	-0.08	0.087	-0.90	0.375
I	-0.21	0.059	-3.62	0.001
I ²	0.35	0.093	3.73	0.001
P ²	0.02	0.075	0.24	0.812
N ²	-0.02	0.077	-0.23	0.823
N:P	-0.21	0.105	-1.98	0.054
P:I	0.30	0.131	2.29	0.027
N:I	-0.13	0.125	-1.06	0.296
Multiple R-squared: 0.44 Adjusted R-squared: 0.33				
F-statistic: 3.899 on 9 and 44 DF, p-value: 0.0011				

Appendix 6 Analysis of Variance for Response Surface Methodology analysis for Appendix 5 (phycocyanin quota at day 18).

Analysis of Variance table for day 18 PC quotas					
	Degrees of Freedom	Sum of Sq	Mean of sq	F value	Probability (> t)
First order (N, P, I)	3	0.16	0.053	1.84	0.154
Quadratic (P, N, I)	3	0.59	0.198	6.79	<0.001
Two-way interaction (P, I, N)	3	0.27	0.090	3.08	0.037
Residuals	44	1.28	0.029		
Lack of fit	5	0.23	0.045	1.65	0.169
Pure error	39	1.06	0.027		

Appendix 7. Outputs of Response Surface Methodology analysis for phycocyanin (PC) quotas at day 22. Response estimates for nitrate-N; N, log-transformed phosphate-P; P, square root light; I, second order terms for these variables. x^2 is shown in the “estimate” column followed by standard error, T values and probability. Significant values are in bold.

	Estimate	Std Error	T value	Probability (> t)
Intercept	2.71	0.087	31.02	0.000
N	0.29	0.123	2.33	0.024
P	-0.26	0.131	-1.95	0.057
Li	-0.03	0.076	-0.40	0.692
Li ²	-0.99	0.127	-7.75	0.000
P ²	0.16	0.109	1.45	0.154
N ²	-0.18	0.115	-1.57	0.123
N:P	0.42	0.152	2.75	0.008
P:Li	-0.45	0.190	-2.37	0.022
N:Li	-0.10	0.184	-0.55	0.587
Multiple R-squared: 0.77 Adjusted R-squared: 0.73				
F-statistic: 18.87 on 9 and 50 DF, p-value: <0.001				

Appendix 8. Analysis of Variance for Response Surface Methodology analysis for Appendix 7 (phycocyanin quota at day 22).

Analysis of Variance table for day 22 PC quotas					
	Degrees of Freedom	Sum of Sq	Mean of sq	F value	Probability (> t)
First order (N, P, Li)	3	4.72	1.574	23.36	<0.001
Quadratic (P, N, Li)	3	5.79	1.931	28.66	<0.001
Two-way interaction (P, Li, N)	3	0.93	0.310	4.60	0.006
Residuals	50	3.37	0.067		
Lack of fit	5	1.39	0.278	6.34	0.0001
Pure error	45	1.98	0.044		

Appendix 9. Outputs of Response Surface Methodology analysis for maximum growth rate. Response estimates for nitrate-N; N, log-transformed phosphate-P; P, square root light; I, second order terms for these variables. x^2 is shown in the “estimate” column followed by standard error, T values and probability. Significant values are in bold.

	Estimate	Std Error	T value	Probability (> t)
Intercept	0.80	0.018	44.82	0.000
N	0.04	0.024	1.53	0.132
P	0.01	0.026	0.56	0.580
Li	-0.02	0.015	-1.44	0.157
N ²	0.00	0.022	-0.12	0.908
P ²	0.03	0.023	1.15	0.256
Li ²	-0.07	0.026	-2.79	0.008
N:P	-0.04	0.038	-1.04	0.306
P:Li	0.01	0.030	0.18	0.856
N:Li	0.00	0.036	-0.12	0.906

Multiple R-squared: 0.39 Adjusted R-squared: 0.27

F-statistic: 3.263 on 9 and 46 DF, p-value: 0.004

Appendix 10. Analysis of Variance for Response Surface Methodology analysis for Appendix 9 (maximum growth rate).

Analysis of Variance table for maximum growth rate					
	Degrees of Freedom	Sum of Sq	Mean of sq	F value	Probability (> t)
First order (N, P, Li)	3	0.038	0.013	4.842	0.005
Quadratic (P, N, Li)	3	0.036	0.012	4.572	0.007
Two-way interaction (P, Li, N)	3	0.003	0.001	0.375	0.772
Residuals	46	0.121	0.003		
Lack of fit	5	0.030	0.006	2.764	0.031
Pure error	41	0.090	0.002		